UNDERSTANDING THE LYTIC FUNCTION OF A_2:

THE MATURATION PROTEIN OF ssRNA BACTERIOPHAGE Qβ

A Dissertation

by

CARRIE-LYNN LANGLAIS

Submitted to the Office of Graduate Studies of
Texas A&M University
in partial fulfillment of the requirements for degree of

DOCTOR OF PHILOSOPHY

May 2007

Major Subject: Biochemistry

UNDERSTANDING THE LYTIC FUNCTION OF A_2:

THE MATURATION PROTEIN OF ssRNA BACTERIOPHAGE Qβ

A Dissertation

by

CARRIE-LYNN LANGLAIS

Submitted to the Office of Graduate Studies of
Texas A&M University
in partial fulfillment of the requirements for the degree of

DOCTOR OF PHILOSOPHY

Approved by:

Chair of Committee,	Ryland F. Young
Committee Members	Susan S. Golden
	Andy LiWang
	Michael Kladde
Head of Department,	Gregory D. Reinhart

May 2007

Major Subject: Biochemistry

ABSTRACT

Understanding the Lytic Function of A_2:

the Maturation Protein of ssRNA Bacteriophage Qβ. (May 2007)

Carrie-Lynn Langlais, B.S., University of Great Falls

Chair of Advisory Committee: Dr. Ryland F. Young, III

Most bacteriophage escape the confines of the host bacterium by compromising the integrity of its cell wall, an event that results in rupture (lysis) of the cell. The lysis strategy of bacteriophage Qβ is inhibition of cell wall biosynthesis while the cell is growing. To elicit lysis, the maturation protein (A_2) of Qβ inhibits the catalytic activity of MurA, an essential, induced fit enzyme in the cell wall biosynthetic pathway. Consequent lysis releases progeny phage into the environment.

The research in this dissertation addresses how lysis timing is integrated into Qβ's life cycle and discerns the molecular basis of the lytic event. Working off the notion that, as displayed by the mature virion, A_2 inhibits MurA, we developed an *in vivo* bioassay to resolve the amount of inhibitory A_2 during infection. We found that the amount of free A_2 is vastly greater than the amount of virion-associated A_2 and that both forms inhibit MurA. Additionally, the amount of A_2 correlates to lysis time and the burst size, as mutant Qβ with upregulated expression of A_2 ($Q\beta^{por}$) elicit host cell lysis faster and release fewer mature virions than with the wildtype level of A_2. This further suggests that protection from Qβ lysis afforded by $MurA^{L138Q}$ is due to perturbed affinity

between A_2 and MurA. Yeast two-hybrid analysis supports that A_2 and MurA^{L138Q} interact with weaker affinity by rendering small colonies compared to yeast containing interacting A_2-MurA^{wt}. Scanning mutagenesis of MurA's surface near L138 identified residues that may be important for A_2 contact in the inhibitory complex. Potentially important residues map to a contiguous area on the surface of MurA that spans both lobes on the flexible loop face of the enzyme, suggesting that A_2 prevents the induced fit mechanism of MurA in an uncompetitive manner. Subsequent truncation analysis reveals that the amino-terminal half of A_2 is sufficient to mediate host cell lysis. Together, these findings insinuate a model in which the amino-terminus of free A_2 interacts with, and inhibits MurA. Then, when the infected cell initiates division, septal catastrophe ensues causing the cell to lyse and liberate progeny bacteriophage Qβ.

ACKNOWLEDGMENTS

I would like to thank my committee chair, Dr. Ryland Young, III, and my committee members, Dr. Susan Golden, Dr. Andy LiWang, and Dr. Michael Kladde, for their guidance and support throughout the duration of this research. I would like to thank Dr. Vlad Panin for sitting in on the defense. Additionally I would like to acknowledge and extend sincere gratitude to Dr. Douglas K. Struck, for his invaluable advice, dedication to science, and assistance in the preparation of this dissertation. Thank you to fellow Young lab members, past and present for understanding the excitement and importance of phage biology, constructive criticism and emotional support.

Thanks also to the faculty and staff in the Department of Biochemistry & Biophysics for making me feel welcome, even before I arrived at Texas A&M University. Your genuine smiles have made my time here wonderful. To my colleagues, thank you for talking science and smiling in passing.

Thank you to my family and friends for constant encouragement, motivation to “do what I’ve got to do”, and reminding me that it is okay to bake the cake and eat it, too. To all of the people that passed through my life in College Station and Bryan, thank you for your true friendship, good food, great wine, long runs, disc golf, and the generous supply of laughter. Finally, I cannot forget to thank Superman, the invisible jet, red rocket and the leaning blue house for adding plenty of color and strength to this journey.

TABLE OF CONTENTS

Page

LIST OF FIGURES

FIGURE Page

LIST OF TABLES

CHAPTER I

INTRODUCTION

INTRODUCTION

The vegetative growth cycle of lytic bacteriophage ends with the abrupt rupture (lysis) of the bacterial host and release of progeny virions into the environment. In order for lysis to occur, the structural integrity of the host's peptidoglycan cell wall must be compromised to the point that it no longer protects the cytoplasmic membrane against osmotic rupture. One can imagine two distinct mechanisms by which this might be accomplished. First, enzymes (lysins) which break specific bonds in peptidoglycan could be encoded by the bacteriophage genome. In this case, lysis of the host would result from the exposure of its cell wall to the phage-encoded lysin. Alternatively, lysis could occur due to the inhibition of peptidoglycan synthesis in growing, phage-infected cells. Here, the phage would encode some function to block a step in the peptidoglycan biosynthetic pathway. Lysis by this mechanism would be similar to that which occurs when growing bacterial cells are exposed to antibiotics that inhibit peptidoglycan synthesis, for example penicillin (27). As it happens, both of these lytic strategies have been adopted by bacteriophage in order to escape from the host cell at the end of their growth cycle (107, 108).

This dissertation follows the style of Journal of Bacteriology.

Interestingly, the lytic strategies of bacteriophage with large and small genomes are strikingly different. The former encode a multi-component system that is capable of precisely controlling the time of host lysis. The hallmark components of these systems are their holin and endolysin proteins. Holins are small proteins that oligomerize to form a lesion(s) in the inner membrane. Holin-mediated lesion formation is used to control the function of the endolysin, an enzyme with the ability to degrade peptidoglycan (29). By contrast, phage with small, single-stranded RNA or DNA genomes encode a single lysis protein. In the cases of bacteriophage ΦX174, a single-stranded DNA phage, and Qβ, a single-stranded RNA phage, these lysis proteins have been shown to inhibit a specific step in the peptidoglycan biosynthetic pathway. As a further economy, these single component lysis systems are encoded by genes that either lie within other genes or encode proteins with multiple functions including host lysis.

Multi-component lysis systems

Bacteriophage λ has long served as the prototype for phage employing a multicomponent lysis sytsem. The λ lysis cassette, consisting of the *SRRzRz1* genes, is expressed from the late promoter, pR', beginning at approximately 8 minutes after infection. The protein products of the *S* and *R* genes are essential for host lysis under all culture conditions while those of *Rz* and *Rz1* are only required when millimolar concentrations of divalent cations are present in the

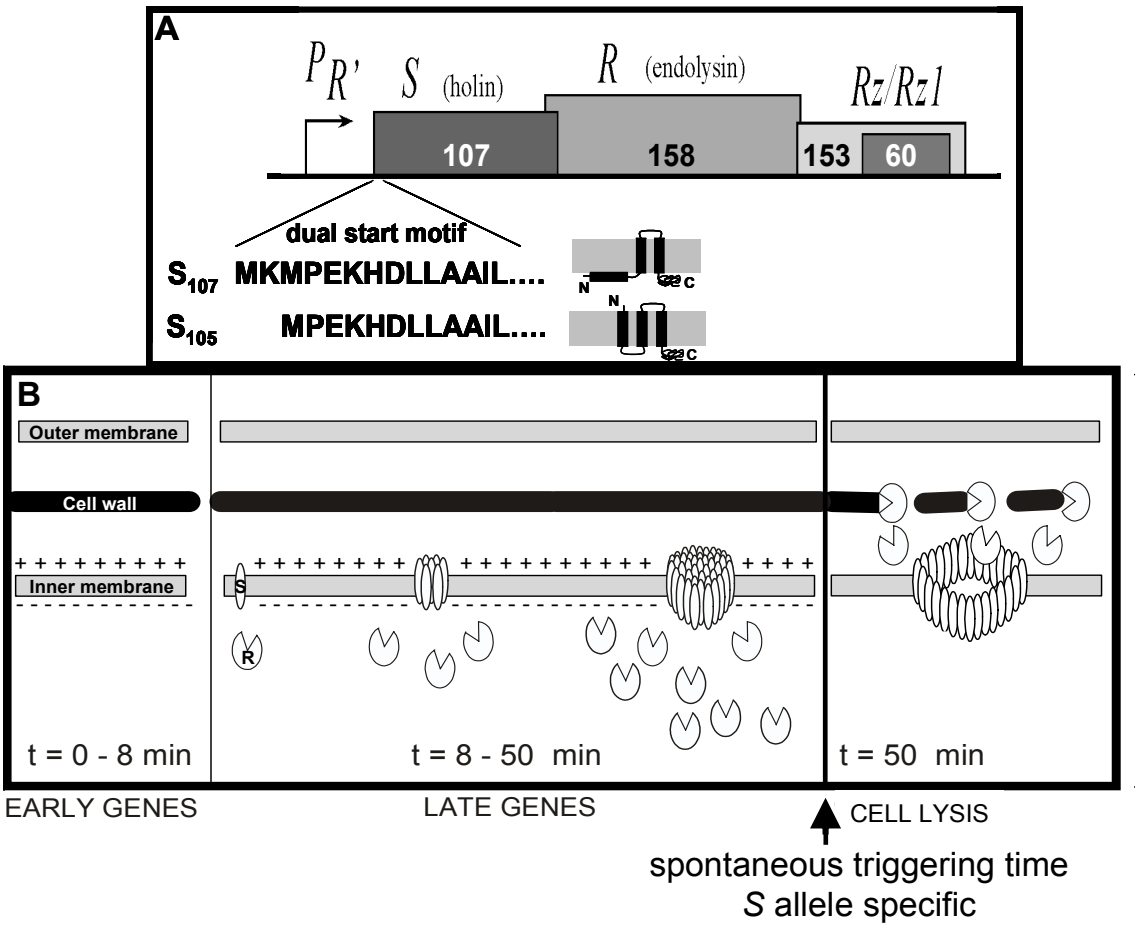

Figure 1.1. The lysis strategy of bacteriophage λ.
(A) The lysis cassette of bacteriophage λ includes the *S, R, Rz and Rz1* genes under the control of the late promoter, P_R'. Each gene is represented by a box with the number of codons within the box. The dual start motif of *S* encodes two proteins, S107 and S105 that differ at the amino-terminus (N) by two amino acids. The predicted topology of S107 is N-in, C-in with two transmembrane domains. S105 is predicted to have three transmembrane domains with N-out, C-in topology. The gray rectangle represents the inner membrane. (B) Lysis is preceded by accumulation of the holin (S) in the inner membrane. Prior to lysis, the holin (S) oligomerizes in the membrane due to interactions between its transmembrane helices. Upon dissipation of the proton motive force (represented by the +/- symbols along the membrane) S oligomers rearrange to form lesions large enough to allow the passage of the cytosolic endolysin (R) into the periplasm. Rupture of the cell occurs immediately following cell wall degradation.

growth medium (105). By virtue of two translational starts, the *S* gene encodes two small membrane proteins (Figure 1.1). These proteins form membrane lesions large enough to allow the passage of the R protein, an endolysin with transglycosylase activity, from the cytosol to the periplasm (Figure 1.1). Thus, within seconds of lesion formation, the cell wall is degraded and the cell is subject to osmotic rupture, liberating the progeny bacteriophages (30).

The two products of the *S* gene, S105 (a holin; 105 amino acids) and S107 (an antiholin; 107 amino acids) differ only by an additional Met-Lys dipeptide at the N-terminus of S107. This subtle difference results in two proteins with different topologies and opposing functions. S105 has three tramsmembrane domains (TMDs) and adopts an N-out, C-in topology in the cytoplasmic membrane. The Lys_2 residue of S107 contributes an extra positive charge to its N-terminus when compared to S105 and prevents the insertion of TMD1 of nascent S107 into the membrane. Thus, S107 has only two TMDs with an N-in, C-in topology; the sequence that is equivalent to TMD1 of S105 is retained in the cytosolic compartment (Figure 1.1). While S105 is capable of forming lethal membrane lesions, S107 inhibits this process and, for this reason, is called an antiholin. Altering the ratio of the two proteins has been shown to alter the timing of membrane disruption (13).

The process of membrane disruption has been studied using a modified form of the λ *S* gene, *S105*, which encodes only the S105 protein. Crosslinking studies have shown that S105 oligomerizes in the membrane and that lysis-

defective alleles of *S* encode S105 proteins that are blocked at defined points along the oligomerization pathway (29). Moreover, the inhibitiory character of S107 is due to its ability to dimerize with S105, presumably interfering with the process of oligomerization. Finally, studies with both *S107* and *S105* have, somewhat surprisingly, shown that single missense changes in *S/S105* allow λ to explore an almost infinite number of lysis times (72, 29). Thus, in addition to their role in disrupting the cytoplasmic membrane, holins are also instrumental in controlling the time at which lysis occurs. The ability to adjust lysis times rapidly may be important from an evolutionary standpoint and may be the reason why holin-endolysin based lytic systems have been universally adopted by phage with genomes having sufficient coding capacity.

An important property of holin proteins is their ability to accumulate in the membrane until, at a time dictated by their primary structure, a triggering event occurs leading to the formation of the lethal membrane lesions. A clue to the nature of this triggering event comes from early studies of phage-mediated host lysis where it was observed that the addition of energy poisons to infected cultures resulted in their premature lysis (73). In more recent studies, it has been found that each allele of *S* has its own lysis time, and all functional alleles appear to be sensitive to premature triggering by agents such as cyanide or dinitrophenol (108).

In fact, even S107, which, unlike S105, does not undergo spontaneous triggering, can be artificially triggered to disrupt the membrane by the addition of

energy poisons. This can be explained if triggering results in the movement of the N-terminus of S107 across the membrane. In its new topological state, S107 would become equivalent to S105 and would acquire holin activity.

A recent model for holin function holds that S molecules form large two-dimensional aggregates in the cytoplasmic membrane. Allowing all surfaces of all three TMDs to participate in this process would account for the fact that mutations in positions all the way around all three TMDs have dramatic and unpredictable effects on lysis timing. The model is that at some point, a small defect occurs in the aggregate, resulting in a local depolarization of the cytoplasmic membrane. This event causes the immediate reorganization of the S molecules in the patch (including topological changes for S107) into a large hole sufficient for the passage of the endolysin. This model would explain the sensitivity of S105/S107 to artificial triggering. Moreover, it would explain why holins accumulate in membranes without affecting the proton motive force across the cytoplasmic membrane until the time of lysis.

Single component lysis systems

Due to limitations imposed by their genome size, the *Microviridae* (e.g., ΦX174), the *Allolevivirida*e (e.g., Qβ), and *Leviviridae* (e.g., MS2) do not encode multi-component lysis systems. Instead, they encode a single protein that is both necessary and sufficient for host lysis. Moreover, during infections with

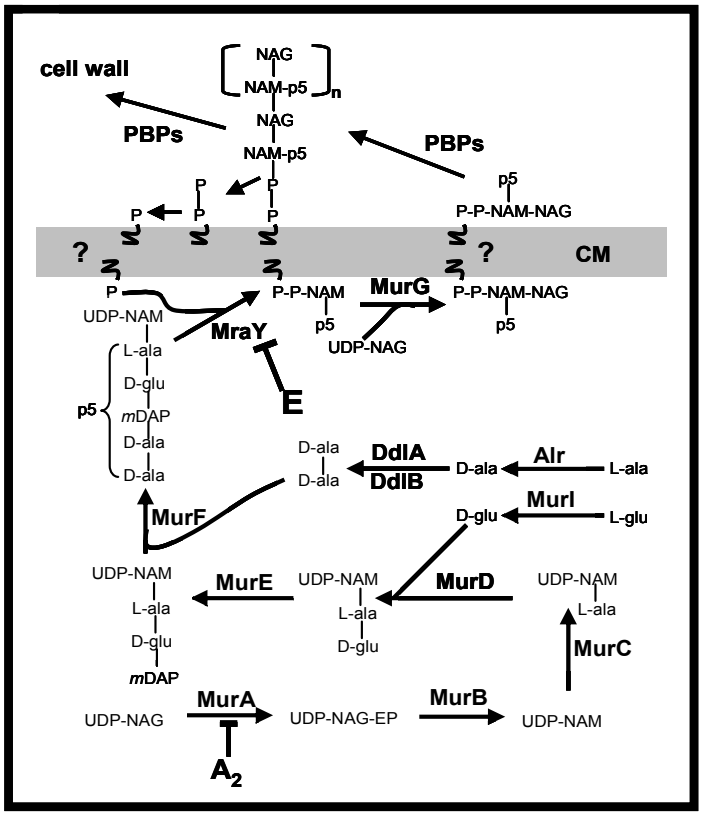

Figure 1.2. The lysis strategy of small bacteriophages.
The cell wall biosynthetic pathway of eubacteria generates the basic cell wall unit, a disaccharide decorated with a pentapeptide chain (NAG-NAMp5). Enzymes catalyzing each step are in bold. Biosynthesis begins with modification of the sugar nucleotide UDP-NAG (UDP-*N*-acetyl glucosamine) into UDP-NAM (UDP-*N*-acetyl muramic acid). The wavy line in the cytoplasmic membrane (CM) represents the lipid undecaprenol. The lipid-linked NAG-NAMp5 is translocated through the CM by an unknown mechanism. In the periplasm, penicillin binding proteins (PBPs) incorporate NAG-NAMp5 into the existing cell wall. The sites of inhibition by the lysis proteins E of ØX174 and A_2 of Qβ are indicated.

these phage, no phage-encoded enzyme capable of degrading peptidoglycan is produced. Using a combined genetic and biochemical approach, Bernhardt, *et al.* (7-10) demonstrated that the lysis proteins of ΦX174 (E) and Qβ (A_2) inhibit the essential enzymes MraY and MurA, respectively. Because both of these enzymes catalyze steps in peptidoglycan synthesis, both E and A_2 have a mode of action that is reminiscent of antibiotics such as penicillin.

The pathway for peptidoglycan synthesis is depicted in Figure 1.2. In *E. coli*, the monomeric units of peptidoglycan is the disaccharide pentapeptide, *N*-acetyl-glucosamine-*N*-acetyl-muramic acid-L-Ala-γ-D-Glu-DAP-D-Ala-D-Ala (NAG-NAMp5). Biosynthesis of peptidoglycan, or murein, is a three-stage process: synthesis of the repeating unit in the cytosol, transport of the repeating unit across the membrane, and polymerization into the pre-existing murein sacculus (Figure 1.2). Both E and A_2 inhibit enzymes that participate in the assembly of the repeating subunit. The mechanism by which the L protein of MS2 causes host lysis is still unknown. Unlike E and A_2, the L protein of bacteriophage MS2 does not block the incorporation of diaminopimelic acid (DAP) into hot SDS-insoluble material (crosslinked peptidoglycan chains). Thus, L must either act at a later step in peptidoglycan maturation or interfere with some other aspect of peptidoglycan maintenance and turnover.

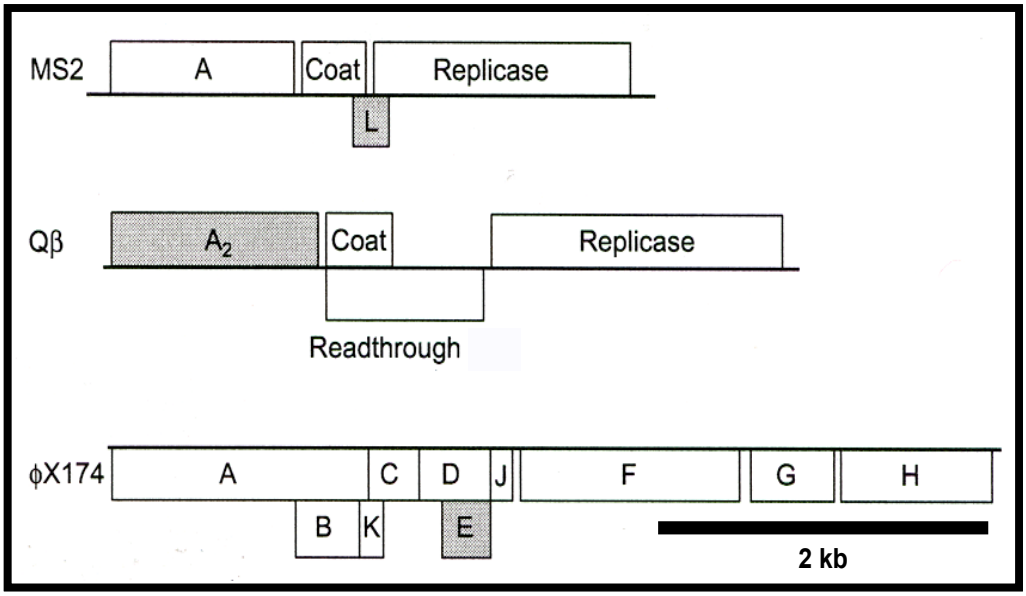

Figure 1.3. Small bacteriophage genomes.
Shown are the genomes of ssRNA bacteriophages MS2 and Qβ, and ssDNA bacteriophage ΦX174. MS2 and Qβ genomes are linear and for convenience, the circular, ssDNA genome of ΦX174 is represented linearly. The boxed regions identify the genes and the shaded boxes indicate genes that encode lysis proteins. Note that MS2 and ΦX174 lysis genes reside within other genes, while lysis function is intrinsic to the Qβ maturation protein, A_2.

A_2 is a multifunctional protein

The small, ssRNA bacteriophage Qβ has a 4,217 nucleotide genome, containing three cistrons, but encoding four proteins: maturation (A_2), coat, readthrough coat (99) and replicase (Figure 1.3) (112). Infective Qβ virions are composed of one genomic ssRNA molecule encapsulated by 180 copies of a combination of the coat protein and readthrough protein (99) and a single copy of A_2 (111). Replicase associates with host proteins S1, Ef-Ts and Ef-Tu to form the RNA-dependent RNA polymerase holoenzyme, and is essential for replication of the viral genome but is not part of the virion (98). Originally, A_2 was thought to solely function as a classic phage maturation protein; as assembled into the phage particle, maturation protein protects the ssRNA genome from RNase degradation and is required for adsorption to the host F pilus (55). However, the search for a separate lysis polypeptide of Qβ was unsuccessful until Winter and Gold (101) discovered that expression of a cloned A_2 gene was necessary and sufficient to elicit host-cell lysis in 1983. Nearly 20 years later, Bernhardt, *et al.* (9) discovered that A_2 inhibits of the catalytic activity of MurA.

Properties of MurA and the related enoylpyruvyl transferase, EPSPS

The committed step in peptidoglycan synthesis is catalyzed by MurA. This enzyme transfers a enolpyruvyl moiety from phosphoenolpyruvate to UDP-N-acetyl glucosamine (UDP-NAG), releasing phosphate in the process (Figure

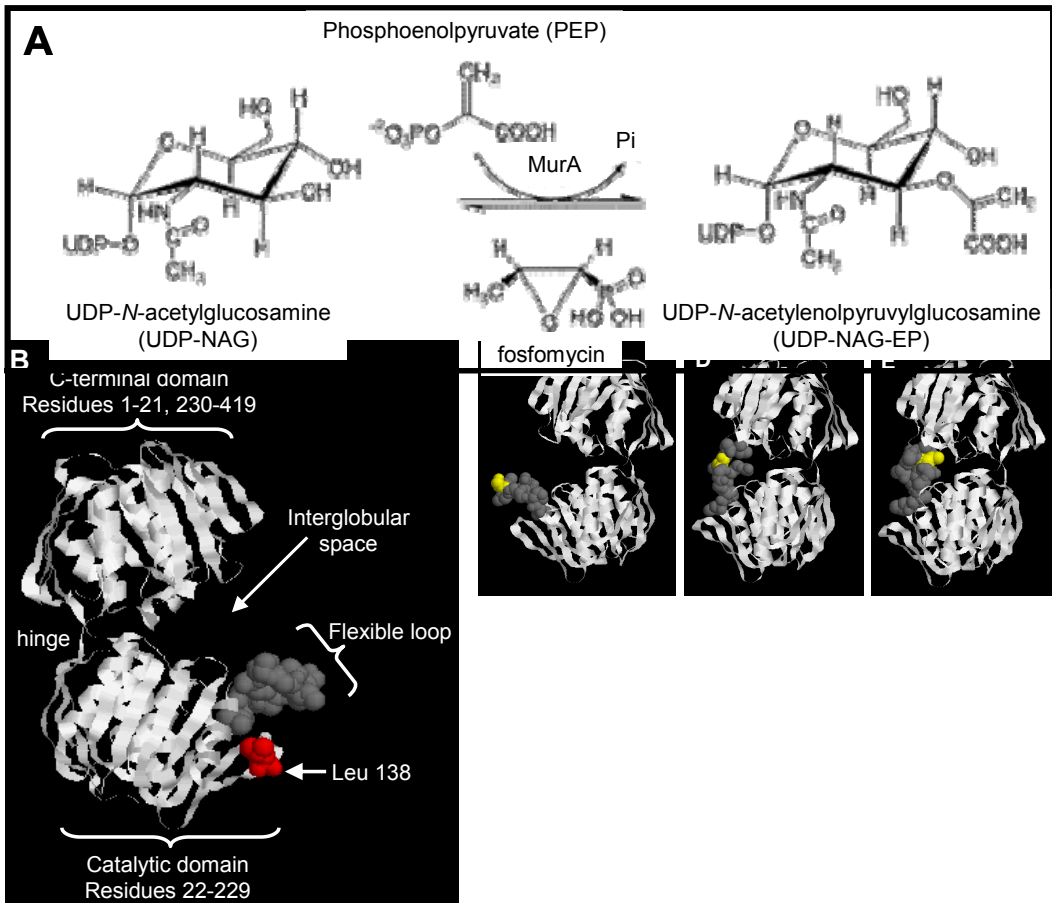

Figure 1.4. The enzymatic mechanism and induced fit structure of MurA. (A) MurA catalyzes the transfer of enolpyruvate (EP) from phosphoenolpyruvate (PEP) to UDP-*N*-acetylglucosamine (UDP-NAG) (23). Inorganic phosphate (Pi) is a byproduct of the reaction. Fosfomycin is the natural, competitive inhibitor of MurA. (B) A ribbon diagram of the open conformation of *Enterobacter cloacae* MurA (PDB accession no. 1DLG) (78). Highlighted are the two globular domains connected by a double stranded hinge. The flexible loop is represented as gray spacefill model. The red spacefill is Leu 138. The interglobular space is also identified. (C) A view of (B) from the left with residue 115 of the flexible loop labelled yellow. (D) *Escherichia coli* MurA (PDB accession no. 1UAE) (81) with UDP-NAG bound (not shown) shows the flexible loop in the interglobular space. (E) The structure of *Escherichia coli* MurA (PDB accession no. 1A2N) (82) in the fluoro-tetrahedral intermediate state shows the flexible loop changes conformation upon transition from the singly-liganded state (D) to the tetrahedral intermediate. The flexible loop, residues 111-120 are spacefilled gray with amino acid 115 highlighted yellow (Panels C-E). All ribbon diagrams were generated using the RasMol molecular graphics visualization tool (version 2.7.3).

1.4A). MurA is a 45,000 Dalton (419 amino acids) enzyme composed of two globular domains connected by a double stranded hinge (Figure 1.4B). The catalytic domain houses a flexible loop. Upon binding of the sugar nucleotide (UDP-NAG), the loop moves closer to the interdomain region (Figure 1.4B). Isothermal calorimetry (ITC) reveals that binding of PEP does not significantly alter the conformation of MurA (74). In a tetrahedral intermediate (THI) state (MurA:UDP-NAG:fosfomycin), the crystal structure of MurA corroborates with ITC data, showing only a slight movement of the apex of the flexible loop into the active site cleft (81).

Crystallography studies and ITC studies reveal that MurA liganded with a fungal inhibitor, fosfomycin, bound is in an open conformation (74, 81). Addition of UDP-NAG to MurA:fosfomycin locks MurA in a closed conformation (82). Addition of PEP to MurA:fosfomycin or MurA:fosfomycin:UDP-NAG does not change the conformation state or reinstate catalytic activity because fosfomycin is an irreversible inhibitor. Fosfomycin covalently binds to C115, a residue at the apex of the flexible loop, while occupying the PEP binding pocket of the active site of MurA. Once a common drug to treat bacterial infections (46), therapeutic use of fosfomycin has lost its effectiveness because mutant MurA alleles emerged that protect the bacterium from the antibiotic. For example, *Mycobacterium tuberculosis* has evolved to be resistant to fosfomycin by replacing the active site cysteine with aspartate (C117D allele of MurA) (22).

Interestingly, the other known bacterial enolpyruvyl transferase, EPSPS (5'-enolpyruvyl-shikimate-3-phosphate) is also an essential enzyme. EPSPS catalyzes the sixth step of the shikimate pathway in plants, fungus and microbes yielding chorismate (14). Chorismate can then be modified into aromatic compounds including tryptophan, tyrosine and phenylalanine. Like MurA, EPSPS exhibits an induced fit mechanism and is composed of two inside-out α/β barrel domains connected by a double-stranded hinge (77, 81, 85). Binding of the enolpyruvyl-accepting substrate induces the closed conformation of both enzymes, which precedes catalysis.

EPSPS and MurA are structurally and mechanistically very similar (50, 24), but are found in different essential biosynthetic pathways. Fosfomycin irreversibly inhibits MurA by covalently modifying the active cysteine residue (46) while occupying the PEP binding pocket, and similarly, glyphosate (the active ingredient of Roundup®) reversibly inhibits EPSPS by competing with PEP binding (86). Isolation of the lytic A_2 domain may provide the information necessary for rational design of a novel antibiotic with dual inhibitory action on the enolpyruvyl transferases.

Proteins as enzyme inhibitors: overview

Enzymes that are inhibited by another protein are rare in nature. In most cases, such enzymes are hydrolases involved in the cleavage/degradation of macromolecules, usually other proteins or RNA. Often these enzymes are

destined for secretion from the cell and once in the extracellular environment their hydrolytic function serves a beneficial purpose. In some cases, the binding of the enzyme to its protein inhibitor must be tight enough to prevent its function prior to secretion, but after secretion the enzyme:inhibitor complex must be able to dissociate. This situation is often encountered with digestive enzymes in both eukaryotic and prokaryotic systems. In other cases, the inhibitor controls the activity of the hydrolytic enzyme after its secretion, as is the case for the myriad of proteolytic enzymes found in the circulation of higher eukaryotes.

Recognition sites between enzymes and their protein inhibitors exhibit characteristic structural properties. Three strategies to block proteolysis exist: (1) a peptide loop of the protein inhibitor binds to the catalytic site of the protease, mimicking either the substrate or the product, (2) the inhibitor binds to the surface of the enzyme adjacent to the catalytic residues, (3) the protease is translated as an inactive enzyme (zymogen) and must itself undergo proteolytic cleavage to remove a covalently attached inactivation peptide. Regardless of how inhibition is achieved, the result is inhibition of the protease and immunity for the cell that encodes it. In another example, the bacteriophage T7 RNA polymerase is regulated by the binding of the T7 Lysozyme far away from its catalytic center. As a result, the polymerase is blocked from undergoing conformational changes that enable transcriptional processivity. In other words, T7 Lysozyme exhibits an indirect mode of inhibition, in contrast to the type of

inhibition imposed on proteases. It is possible that additional modes of enzyme-protein inhibition exist but await discovery and characterization.

Zymogens: Self inhibition with a covalently attached inactivation peptide

As noted above, some proteases are synthesized in an inactive, or zymogen, state (93). Zymogens contain an inactivation peptide that must be cleaved from the proenzyme as a prerequisite for activation (Figure 1.5). Trypsinogen and chymotrypsinogen are two well studied examples of zymogens. In the inactivated state, the proteases are secreted into the small intestines where their digestive function is needed. In the small intestine, the zymogens undergo proteolysis to remove the inactivation peptide sequence. Trypsinogen is cleaved by enteropeptidase at the peptide bond between K^{23} and I^{24} of the proenzyme to become an enzymatically competent protease (trypsin) (89). Similarly, chymotrypsinogen is cleaved at the peptide bond between R^{15} and I^{16} by trypsin. Finally an autolytic cleavage occurs between residues 147-148 to complete the maturation process. Two cleavage events occur to yield chymotrypsin in three segments covalently linked together by disulfide bonds. Once their digestive services are no longer needed, the proteases are inhibited by serine protease inhibitors.

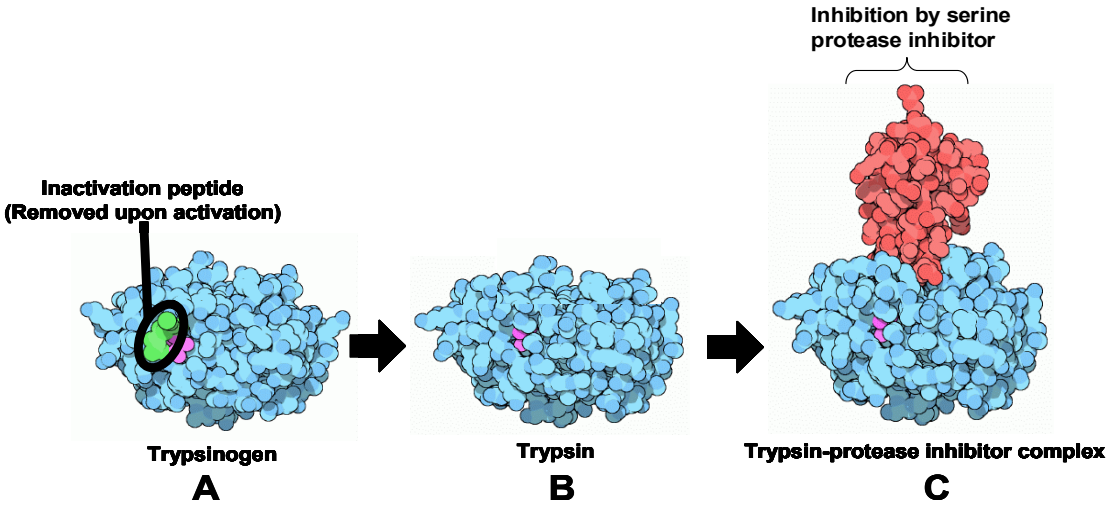

Figure 1.5. Activation and inhibition of Trypsin.
(A) The inactivating peptide (green) inhibits the activation of the proenzyme Trypsinogen (blue). (B) Proteolytic cleavage of the inactivating peptide activates Trypsin. (C) Trypsin activity is inhibited by a serine protease inhibitor (red) (93).

Serpins: Inhibiting proteases by mimicking the protein substrate

Serine protein inhibitors are members of a family of structurally related proteins known as the serpins. The serpins are composed of a similar arrangement of 8-9 alpha-helices, 3 beta-pleated sheets and a reactive center loop. The serpins are divided into two functional classes: protease inhibitors such as α 1-antitrypsin, and non-inhibitors including ovalbumin (58). Antitrypsin is the major antiprotease circulated in the blood, and although it inhibits trypsin, its primary target is elastase. Antitrypsin binds to, and irreversibly inhibits elastase and the binary complex is cleared from circulation (58). Antitrypsin deficiency results in hyperaccumulation of elastase. The uncontrolled proteolytic activity causes tissue damage, most notably manifesting in the symptoms of emphysema. Ovalbumin is the major protein found in the white of a chicken egg and has no inhibitory function. The major structural difference between the two functional classes is the orientation of the reactive center loop (58). Inhibition of proteases is mediated by the reactive center loop, which acts as a pseudosubstrate for the target protease. The pseudosubstrate region of the loop occupies the catalytic cavity of the protease upon binary complex formation and the protease catalyzes the hydrolysis of the pseudosubstrate peptide bond (41). The serpin immediately responds to the cleavage event by a dramatic, spring-loaded change in conformation (Figure 1.6) (41), locking the inhibitor to the protease and preventing future substrate binding.

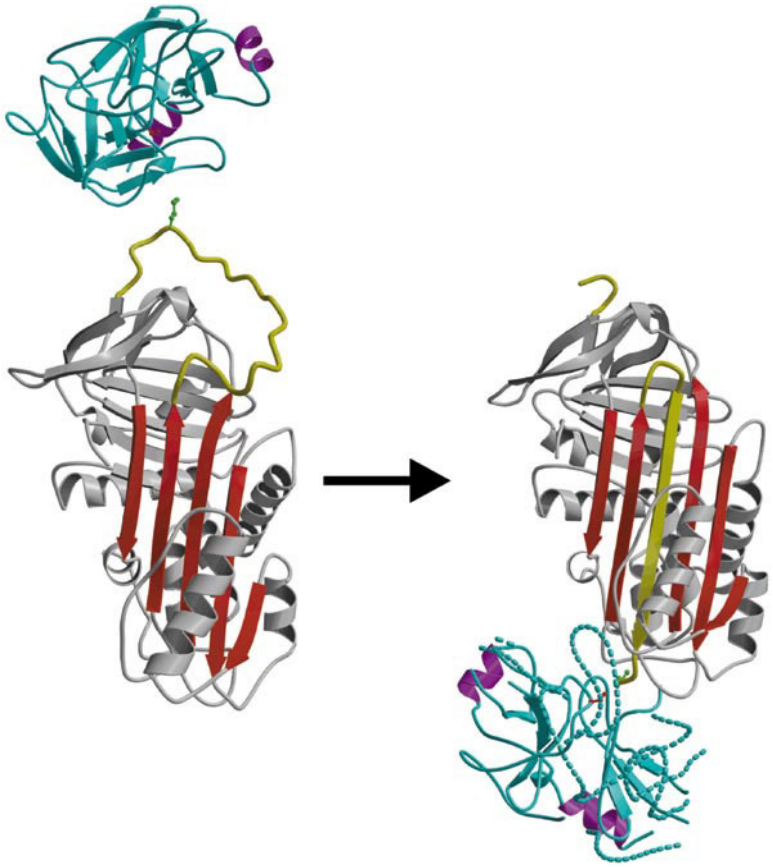

Figure 1.6. Protease cleavage engages irreversible serpin inhibition. The reactive center loop (yellow) of serpins binds to the active site of its cognate target serine protease (blue and purple). The protease recognizes the loop as a pseudosubstrate, and hydrolyzes a peptide bond. Cleavage of the loop changes the state of the serpin from the stressed (S) conformation (left) to the relaxed (R) conformation (right), stabilizing the protein inhibitor-protease complex. Following protease cleavage, the reactive center loop inserts into a β-sheet (red) as a β strand as shown on the right (41).

The crystal structure of ovalbumin reveals that the reactive center loop is ordered into a helical conformation protruding from the protein (58). The structure of antitrypsin is comparable to ovalbumin when it has been proteolytically cleaved and rearranged into the relaxed (R) state, whereas the active inhibitor is in a more compact, or stressed (S) conformation. The dramatic conformational change that occurs during the transition from S to R state is unique to inhibitory serpins; the noninhibitory serpins exhibit an R state only.

α_2-Macroglobulin: Inhibiting proteases by physical trapping

In stark contrast, one of the many functions of the α–Macroglobulin class of serum proteins is to inhibit proteases by trapping them, rather than binding to the protease active site (Figure 1.7) (71). As a homotetramer of 750,000 Daltons, α_2-Macroglobulin displays an exposed bait region composed of a 25 amino acid stretch (15). Upon protease-cleavage, a dramatic conformational change traps the protease (16). The physical capture of the protease prevents access of large substrates, thereby inhibiting the protease. The conformational change exhibited immediately after hydrolysis in the bait region is linked with the cleavage of a unique, and very labile, cyclic thiol-ester bond. The cyclic thiol ester bond is the characteristic feature of the α-Macroglobulin protein family (15). The labile cyclic thiol ester linkage is formed between a cysteine and a glutamine and upon breaking, the reactive glutamyl can covalently react with a

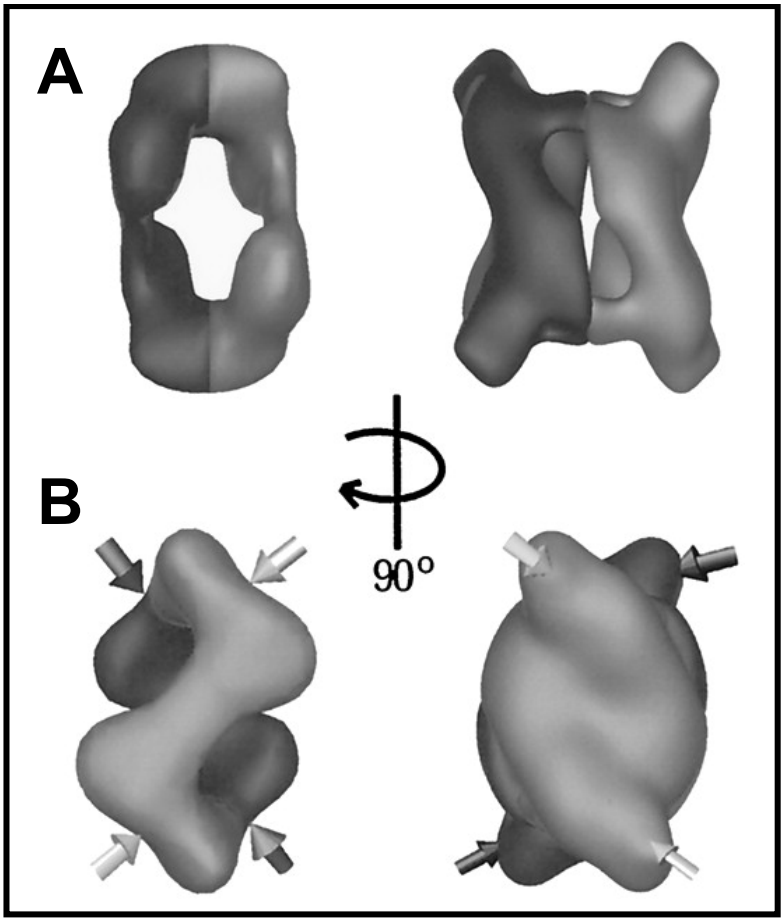

Figure 1.7. Global conformational change of Alpha2-Macroglobulin. The tetramer is shown as an electron microscopy reconstruction. The proteinase-entrapping mechanism appears to involve rotation and separation of the two strands at the top and the bottom of the unbound tetramer (left). The two Z-shaped protomers rotate 90 degrees clockwise when the unique thiol-ester bond, buried in the cavity is broken by the presence of a protease. The arrows indicate the approximate binding of Fab epitopes, representative of exposure of the receptor binding sites that is dependent on this conformational change (71).

lysine in close proximity, resulting in a covalent attachment of the protease. However, the covalent linkage of the protease is not required for α_2-Macroglobulin to trap and inhibit the protease. The α_2-Macroglobulin-protease complex is rapidly cleared from the circulation in a receptor-mediated manner, dependent on a receptor binding site that is exposed as a result of the conformational change.

Barstar: Electrostatic inhibition of the RNase, Barnase, prior to secretion

Barnase is a secreted RNase of the soil bacterium *Bacillus amyloliquefaciens*. Presumably, export of Barnase degrades environmental RNA to oligonucleotides which the bacterium salvages and metabolizes. Barnase-producing bacteria protect themselves from the toxic character of Barnase by expressing its protein inhibitor, Barstar. Barstar, an 89 amino acids intracellular inhibitor of Barnase (110 amino acids, mature), forms a 1:1 noncovalent protein inhibitor-enzyme complex with Barnase (Figure 1.8) (28). The affinity for Barnase-Barstar association is among the strongest of all known protein-protein interactions with an association rate of 10^{-8}-10^{-9} $M^{-1}s^{-1}$(80). Resolution of the crystal structure of the Barnase-Barstar complex reveals a complimentary binding surface. Electrostatic forces between oppositely charged residues (negatively charged surface of Barstar, positive surface of Barnase) steers and stabilizes the association of the protein inhibitor to the enzyme (36). The active site and recognition loop of Barnase form a prominent cleft, to which

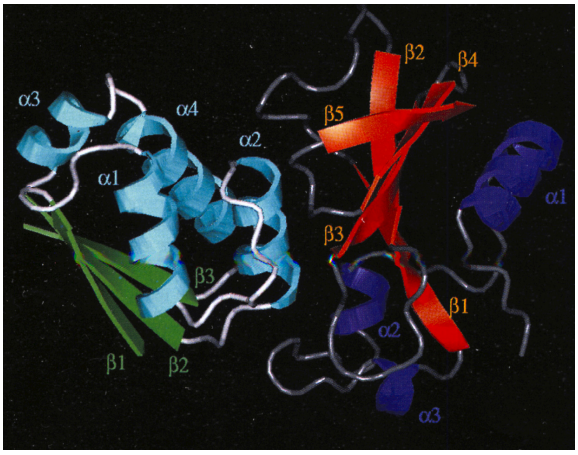

Figure 1.8. The inhibitory complex of Barnase and Barstar.
An overall view of the Barnase-Barstar complex. Barstar is located on the left (green β-sheets (β1-β3), cyan α-helices (α1- α4)) and Barnase on the right (red β-sheets (β1-β5) and blue α-helices (α1- α3)) (28).

Barstar occupies (28). The carboxylate group of Barstar D^{39} reaches into the phosphate- binding pocket of Barnase preventing association of the RNA substrate to the enzyme. Barnase is equipped with a signal peptide and is secreted from the cell. Despite the tight association *in vivo*, the inhibitory complex dissociates in the extracellular environment. The dissociation constant of Barnase-Barstar is on the order of 10^{-14} (37). The mechanism of dissociation of the complex is unknown.

T7 Lysozyme: Inhibition of Bacteriophage T7 RNA Polymerase

Bacteriophage T7 encodes its own DNA-dependent RNA polymerase (RNAP) that transcribes three classes of genes in the phage life cycle. Early in infection, class I and class II genes are transcribed, until RNAP is inhibited by a class II gene product, T7 lysozyme. Lysozyme regulates gene expression by binding to and locking RNAP in a non-processive conformation (Figure 1.9) (43). In complex with Lysozyme, RNAP is only able to initiate transcription of short RNA sequences from the promoter DNA of class I and class II viral genes, known as abortive transcription. Class III genes, however, have greater promoter strength and are transcribed by RNAP while bound by T7 Lysozyme, since T7 Lysozyme binds to RNAP far from its active site (87).

The RNAP-Lysozyme complex has been crystallized and the structure reveals that Lysozyme binds to RNAP far from the polymerase active site (Figure 1.9) (43). T7 RNAP has the characteristic fold of polymerases including

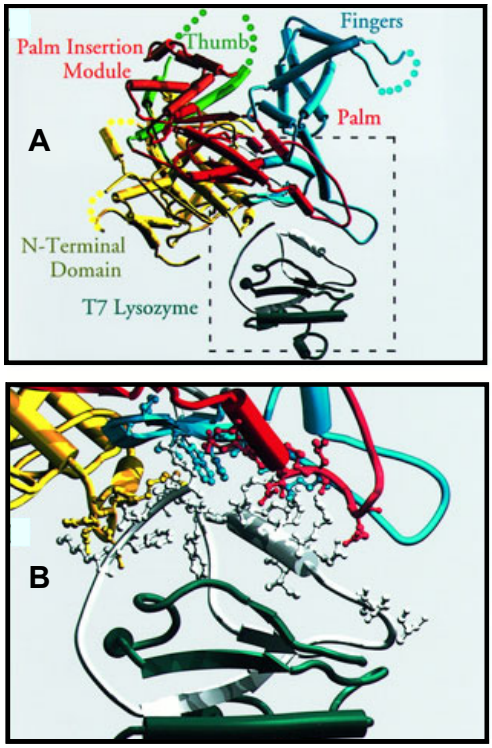

Figure 1.9. Indirect inhibition of T7 RNA Polymerase by T7 Lysozyme. (A) T7 RNA Polymerase (multicolored) is shown complexed with its inhibitor, T7 Lysozyme (green ribbon structure, boxed). The domains of T7 RNA Polymerase are labeled. (B) A zoomed in view of the protein-protein interface between T7 RNA Polymerase and T7 Lysozyme (dark green). Specific contact points are represented as ball and stick models. The domains of T7 RNA Polymerase are: N-terminal domain (yellow); Fingers (blue); Palm (red); Thumb (lime green) (43).

domains designated as the thumb and fingers and palm, as it resembles the general shape of a right hand. The polymerase active site is nestled between these domains, and although Lysozyme binds to parts of the palm and finger sub-domains, the active site is not occluded. Promoter DNA, ssRNA and nucleotides interact with RNAP as it is bound by Lysozyme, but RNAP is unable to transition into its processive conformation. While the details of the mechanism of inhibition are not fully understood, the remote binding of Lysozyme from the polymerase active site suggests indirect inhibition (110).

Inhibition of MurA by A_2

There are at least two potential forms of A_2 present in Qβ infected cells: A_2 assembled into phage particles and free, or unassembled, A_2. Bernhardt *et al*. (9) have shown that Qβ particles purified by CsCl gradient centrifugation are capable of inhibiting MurA present in cell extracts. Thus, while the amount of A_2 produced during a Qβ infection is not known with any certainty, it is plausible that only virion-associated A_2 is inhibitory. This would suggest that the lysis of Qβ infected cells occurs only after a sufficient number of progeny virions have been assembled to inhibit the requisite number of MurA molecules. In this case, once lysis has occurred, it is likely that the virions must dissociate from bound MurA in order to infect new hosts. Alternatively, free A_2 may be the effector of lysis and, thus, the total amount of A_2 would be greater than the number of phage particles assembled. In this case, either the affinity of A_2 for MurA or the

absolute amount of A_2 relative to cellular MurA must be such that the inhibition of MurA is not physiologically deleterious until a sufficient number of progeny virions have been assembled.

A single allele of *murA*, the *rat* allele, conferring resistance to A_2 was recovered in a selection designed to identify host mutants that would survive expression of the *A_2* gene from a plasmid. Sequence analysis of *murA^{rat}* mutant revealed the missense change, L138Q. By infecting *rat* mutants and selecting for compensatory Qβ mutants that plate on *rat* (por), several Qβ^{por} mutants were isolated. These were found to harbor missense mutations within the amino-terminus of A_2. The fact that compensatory changes in A_2 restored lysis of the *murA^{rat}* host suggests a physical interaction between the two proteins.

Questions to be addressed

At the start of the work presented in this dissertation, the mechanism by which the A_2 protein inhibits MurA was unknown. The primary goal of the research described in the following chapters is to define the interactions that occur between these two proteins. The approach taken was site-directed mutagenesis to assess the contribution of residues on the surface of MurA to the MurA-A_2 interaction. In related work, deletion analysis was used in an attempt to identify the domain of A_2 that is necessary and sufficient for host lysis.

It is tempting to speculate that a better understanding of the MurA-A_2 interaction might provide information useful in the design of low molecular weight

inhibitors of MurA that could serve as antibiotics. Because MurA and EPSPS are both induced-fit enolpyruvyl transferases, it is possible that they share enough similarity that a single compound might be inhibitory to both. The ability of a bacterial pathogen to develop resistance to such an inhibitor would be expected to be less likely than the appearance of resistance to antibiotics with a single target.

CHAPTER II

CHARACTERIZATION OF Qβ^{POR} MUTANTS

INTRODUCTION

Bacteriophage employ two general strategies to liberate their progeny from the confines of the host cell: (1) destruction of the existing cell wall or (2) inhibition of peptidoglycan synthesis. Small phages with single-stranded (ss) DNA or RNA genomes do not encode a muralytic enzyme (66) and so they use the latter mechanism to lyse their hosts. During Qβ infections, the cell's morphology is altered before cell lysis occurs. Rather than maintaining its normal rod shape, a bulge forms at the septal region. Eventually, the cell becomes spherical and ruptures leaving only a "ghost". Similar septal bulges are formed when growing cells are exposed β–lactam antibiotics (91). Moreover, only growing cells are susceptible to either β-lactam antibiotics or Qβ-mediated lysis (47). These observations support the notion that Qβ brings about cell lysis by interfering with cell wall synthesis.

Two laboratories independently reported that A_2, the maturation protein of Qβ, is necessary and sufficient for host lysis (101, 47). Although there is little sequence identity between the maturation proteins for group I (MS2-like, *Leviviridae*) and group III (Qβ-like, *Allolevivirida*e) phage, they perform many of the same functions. They bind to the 5' end of their ssRNA genome, assemble

to the capsid as a single molecule, and adsorb to bacterial F pili as a requirement for infection. It has been shown that following attachment to the F pilus, a fragment of the MS2 maturation protein accompanies the genome into the cytoplasm of the host cell (52). The fate of pili-adsorbed A_2 remains unknown. The one striking difference between the maturation proteins of these two classes of RNA phage is that only the *Allolevivirida*e maturation proteins fulfill an additional function, cell lysis.

Host mutants selected for resistance to A_2-mediated lysis and subsequently screened for Qβ-resistance ($Q\beta^r$) were mapped to *murA* (9). These *rat* (resistant to A_2) alleles of *murA* all had acquired a single missense mutation in *murA* that changed leucine 138 to glutamine. The MurA activity of in extracts from cells expressing only the wild type gene could be completely inhibited by Qβ virions. Under the same assay conditions, the MurA activity in extracts prepared from cells expressing the *rat* allele was unaffected by the addition of the virus. When large numbers of Qβ are plated on lawns of a $murA^{rat}$ host, a small number of plaques are observed. The phage ($Q\beta^{por}$ for plates on *rat*) contained within these plaques have mutations that result in amino acid substitutions in the amino-terminus of A_2, providing genetic evidence of a protein-protein interaction between A_2 and MurA. These findings lead to several predictions. First, since intact virions inhibit MurA, Qβ-infected cells only lyse when the number of progeny particles assembled are sufficient to inhibit a large fraction of the cellular MurA. This would ensure that host lysis only occurs after

a reasonable phage yield has accumulated. Second, the Qβ resistance of cells expressing *murA*^{rat} is due the reduced affinity of the MurA^{rat} protein for wild type A_2. Third, the *por* mutations result in an A_2 protein with an increased affinity for MurA^{rat}. In this chapter, these predictions are tested by determining the absolute amounts A_2 and MurA in the cell during Qβ and Qβ^{por} infections.

MATERIALS AND METHODS

Growth conditions

All cultures were grown in Luria-Bertani (LB) broth. Liquid cultures and LB agar plates were supplemented with ampicillin (100 μg/ml), kanamycin (40 μg/ml), chloramphenicol (10 μg/ml) or tetracycline (10 μg/ml) as indicated. Soft agar (76) was supplemented with 5 millimolar (mM) $CaCl_2$ and cooled to 42ºC before adding culture and pouring onto plates. For induction of pZE and pET plasmids, isopropyl-β-D-thiogalactopyranoside (IPTG) was added to log-phase culture to a final concentration of 1mM.

Bacterial strains, bacteriophage

All plasmids were propagated in *Escherichia coli* strain XL1Blue (*recA*1 *endA*1 *gyrA*96 *thi hsdR*17 *supE*44 *relA*1 *lac [*F'::Tn*10 proA+B+ laqI*^{q} *Δ(lacZ)*M15]). XL1Blue and XL1Blue^{rat} (*murA*^{L138Q} *recA*1 *endA*1 *gyrA*96 *thi hsdR*17 *supE*44 *relA*1 *lac [*F'::Tn*10 proA+B+ laqI*^{q} *Δ(lacZ)*M15]) (9) were used for liquid culture infections with bacteriophages Qβ and Qβ^{por} (A_2^{L28P}, A_2^{D52N}, or

A_2^{E125G}) (9). HfrH ((RY 15177)λ- *relA1 spoT1 thi-1 lacI*^{q1}*tonA::*Tn*10*) and HfrH ((RY 3095) λ- *relA1 spoT1 thi-1 lacI*^{q1} *lacZ::*Tn*5*) served as lawns for bacteriophage spot titering (Qβ, Qβ^{por} and MS2). The *murA*^{L138Q} (*rat*) allele was introduced to HfrH (RY 15177) by P1 transduction with XL1Blue^{rat} (9) serving as the donor strain and is referred to as HfrH^{rat}. Chromosomal *murA* was replaced with a kanamycin cassette (17), with *Bacillus subtilis murAA* (*murA*^{Bs}) encoded *in trans* in HfrH (RY 15177) to generate HfrH (RY 15177) *murA*<>*kan* pZE*murA*^{Bs}. Expression of A_2 from pET-A_2 was induced in BL21(DE3) pLysS (Novagen).

Molecular biology techniques

Standard DNA manipulation protocols were performed as described previously (76). PCR reactions and restriction enzyme digests were purified by using the PCR Purification Kit (Qiagen) or the Gel Extraction Kit (Qiagen) according to manufacturer's instructions. All enzymes including Taq polymerase, restriction endonucleases, Alkaline Phosphatase, and T4 DNA Ligase were purchased from New England Biolabs and used according to instructions. QuickChange PCR kit (Stratagene) was used to introduce nucleotide changes in a gene. Oligonucleotides were ordered from Integrated DNA Technologies (Coralville, IA) and were used without further purification. Automated fluorescent sequencing was performed by the Laboratory for Plant Genome Technology at the Texas Agriculture Experiment Station. Sequencing primers for A_2 are listed (Table 2.1). A minimum of two sequencing reactions

Table 2.1. Primers to amplify A_2, *murA* and incorporate *por* mutations to A_2.

Primer	Sequence
KpnI-NdeI-For	GTATAAGAGGTACCACATATGCCTAAATTACC
A_2Rev-BamHI	GCAGCCGGATCCAGTTTCA
KpnI-NdeI-BsMurA.2-For	ATATATGGTACCCATATGGAAAAAAT
BsMurA-Bam-Xba-Rev	GAGTGGTCTAGAGGATCCTTATGCAT
A_2^{L28P}	FOR: GGTTTCCAGACCCCTTTATGG REV: CGATAAAGGGGTCTGGAAACC
A_2^{D52N}	FOR: CCCACCTTGATAATCGTCTACC REV: GGTAGACGATTATCAAGGTGGG
A_2^{E125G}	FOR: AAAATCAAACCCCTTAGGTGC REV: GCACCTAAGGGGTTTGATTTT

were performed to read the entire length of A_2 (1,260 base pairs) and *murA* (1,257 base pairs).

Cloning and expression of A_2, $murA^{Bs}$ and murA

All plasmids constructs were verified by automated fluorescent DNA sequencing (Laboratory for Plant Genomics at the Texas Agricultural Experiment Station) and amplified in XL1Blue. The RNA genome was converted to cDNA by first performing reverse transcription using the M-MLV Reverse Transcriptase according to instructions (Ambion). The A_2 gene was then amplified by PCR using KpnI-NdeI-For and A_2Rev-BamHI primers (Table 2.1). The PCR product was digested either with KpnI and XbaI and ligated into similarly digested pZE12 to yield pZE12-A_2, or digested with NdeI and BamHI and ligated to similarly digested pET11a (Novagen). The vector pZE12 (59), is a medium copy number vector conferring ampicillin resistance where the cloned gene is under the control of the *Plac* promoter. The *por* mutations A_2^{L28P}(L28P), A_2^{D52N}(D52N), and A_2^{E125G}(E125G) were introduced to pZE12-A_2 by QuickChange PCR (Stratagene) with the primer pairs L28P-FOR and L28P-REV, D52N-FOR and D52N-REV, and E125G-FOR and E125G-REV (Table 2.1), respectively, to generate pZE12-A_2^{L28P}, pZE12-A_2^{D52N}, and pZE12-A_2^{E125G}. To regulate the basal level of expression of pZE12-A_2/A_2^{por}, the plasmids were expressed in HfrH (RY15177), which carries chromosomal *lacI*^{q1}. To generate an A_2 protein

standard, expression was induced with 1 mM IPTG from BL21(DE3) pLysS pET-A_2.

The *murAA* gene from *Bacillus subtilis* W23 (RY 7355) ($murA^{Bs}$) was amplified using the primers KpnI-NdeI-BsMurA.2-For and BsMurA-Bam-Xba-Rev (Table 2.1). The PCR product was digested with KpnI and XbaI and ligated to similarly digested pZE12 (59). In HfrH (RY 3095), a basal level of expression of the $murA^{Bs}$ gene from pZE12 is achieved without inducing agent. Higher levels of expression occur by inducing with IPTG. The *murA* gene of *E. coli* was cloned and expressed as described previously (9) from pZE12. A histidine epitope tag (GGHHHHHHGG) was added to the carboxy-terminus of *murA* with the primers by PCR. The PCR product was digested with KpnI and XbaI and ligated into similarly digested pZE12 to yield pZE12-$murA(his)_6$.

Determining phage titer

XL1Blue and XL1Blue^{rat} liquid cultures were grown to mid-late log phase in LB supplemented with tetracycline (XL1Blue) or kanamycin (XL1Blue^{rat}) and 5 mM $CaCl_2$ at 37ºC with aeration. An aliquot of culture was mixed with Qβ, QβA_2^{L28P}, QβA_2^{D52N}, or QβA_2^{E125G} diluted in LB supplemented with 5mM $CaCl_2$ then incubated at 37ºC without aeration for 5 minutes. The infected culture was mixed with soft agar (cooled to 42ºC) and immediately poured to an LB-agar plate supplemented with appropriate antibiotic. Once solidified, the plates were incubated for 12-16 hours at 37ºC. Plaques (cleared zones within the bacterial

lawn) were counted and titers calculated to plaque forming units per milliliter (pfu/ml).

Purification of A_2 and MurA proteins

A protein standard of A_2 was prepared by solubilizing the A_2 inclusion body with 10% SDS and determining the protein concentration with a detergent-compatible protein assay (DC Protein Assay, Bio-Rad Laboratories). A standard curve was generated with Bovine Serum Albumin (BSA) in 10% SDS. $MurAHis_6$ was purified by affinity chromatography (TALON Metal Affinity Resin, Clontech). The concentration of the purified $MurAHis_6$ was calculated from its absorbance at 280 nm using an extinction coefficient of (18500 $cm^{-1}M^{-1}$).

SDS-PAGE and quantitative Western blotting of A_2 and MurA

To analyze the amount of A_2 accumulated during Qβ infection, 1 milliliter of infected culture was precipitated with trichloracetic acid (TCA) at various times after infection. The TCA pellet was dissolved in sample loading buffer to an equivalent of OD_{550} 0.01 per µL (AU 0.01). AU 0.15 of each protein sample and prestained molecular mass standards (Invitrogen) were resolved by SDS-PAGE with a 4-20% Tris/Glycine gradient gel (Bio-Rad) or a 10% Tris/Glycine gel. Proteins were visualized either by staining with coomassie-brilliant blue or transferred to a 0.1-µm nitrocellulose membrane (Schleicher & Schuell) with a wet blotting apparatus for 14 hours at 200 mA. An antibody raised in rabbits

against a synthetic peptide (PKLPRGLRFGA) present in the A_2 primary sequence was obtained from Bethyl Laboratories, Inc., Montgomery, TX and was used as primary antibody at a dilution of 1:10,000. The secondary antibody (goat anti-rabbit immunoglobulin G conjugated to horseradish peroxidase, Pierce Biotechnology) and used at a dilution of 1:10,000. MurAHis was detected by immunoblot with a mouse anti-His antibody (Amersham Biosciences) used at a dilution of 1:10,000. The secondary antibody (goat anti-mouse immunoglobulin G conjugated to horseradish peroxidase) was purchased from Pierce and used at a dilution of 1:10,000. A_2 and MurA protein standards were prepared by mixing a known amount of the purified proteins with XL1Blue cell lysate and running these samples in lanes adjacent to the unknowns. The protein concentrations of standards were within the linear range of unknowns. Blots were developed by using the chromogenic substrate 4-chloro-1-naphthol (Sigma) or with SuperSignal West Femto Chemiluminescence (Pierce Biotechnology) according to manufacturer's instructions. Images of blots were digitized with an Epson Perfection 4990 photo scanner. Quantitative analysis of immunoblots was performed using the image analysis program Image J public domain software suit (W. Rasband, National Institutes of Health).

Stability of A_2 proteins during infection of Qβ/Qβ^{por}

XL1Blue was infected with Qβ or Qβ A_2^{L28P} at a multiplicity of 5 phage per cell (moi 5). Chloramphenicol (Cam) (300 μg/ml) was added to cultures 30

minutes after infection. Total culture samples were taken immediately before the addition of Cam, then 5, 10 and 20 minutes after and analyzed by Western blot. A_2 was visualized by SuperSignal development of the Western blot and A_2^{L28P} was developed colorimetrically.

RESULTS

A_2 is produced at levels in excess of what is needed for virion formation

Every infectious Qβ particle bears a single molecule of A_2, which enables adsorption to a new bacterial host's F pilus. While the amount of mature virions produced during a lytic cycle is known, the total amount of A_2 *in vivo* has never been determined. A protein band attributable to A_2 is not observed when infected cells are examined by SDS-PAGE stained with Coomassie blue. Therefore, we raised an antibody to a peptide contained within the A_2 primary sequence for use in Western blotting. Using this antibody, we first detect the A_2 protein approximately 30 minutes after infection and the amount of A_2 increased throughout the infection cycle until host lysis occurred (Figure 2.1, 2.2). The absolute amount of A_2 present at 30 and 60 minutes after infection was determined by comparison to A_2 protein standards present on the same blot (Table 2.2). At 30 and 60 minutes after infection, there were $5.4x10^3$ and $8.8x10^3$ molecules of A_2 per cell, respectively. This value is in great excess to the number of phage particles which is 50/cell and 170/cell at these two time points. Interestingly, when Qβ infects strains carrying the carrying *$murA^{L138Q}$ rat*

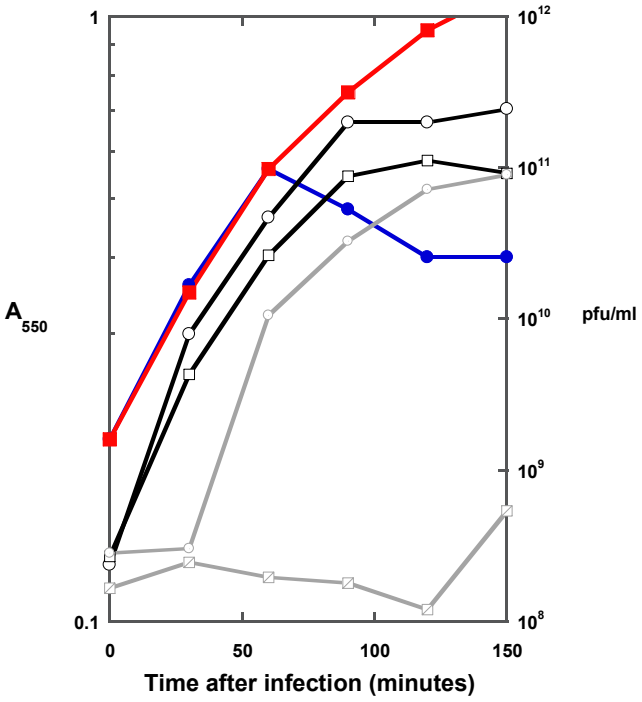

Figure 2.1. Accumulation of Qβ particles during infection.
XL1Blue (Blue line with (•)) or XL1Blue^{rat} (*murA*^{L138Q}) (Red line with (•)) cultures were infected with Qβ. The turbidity of the culture was measured as a function of time. Total (black line with (•)) and released (gray line with (•)) Qβ plaque forming units per ml (pfu/ml) were measured with time after infection of XL1Blue. Total (black line with (•)) and released (gray line with (•)) Qβ plaque forming units per ml (pfu/ml) resulting from XL1Blue^{rat} infection is shown for comparison.

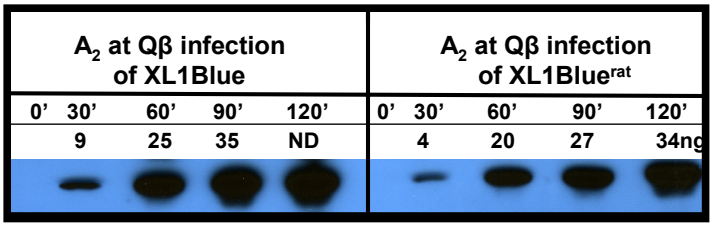

Figure 2.2. Quantification of A_2 during Qβ infection.
Western blot comparing the amount of A_2 produced during infection. Aliquots of XL1Blue/XL1Blue^{rat} infected with Qβ were taken at 30 minute intervals after infection. The amount of A_2 in each band of A_2 is given in nanograms (ng). ND, protein concentration not determined.

allele on its chromosome, the total A_2 and the number of infectious progeny are the same as seen upon infection of a wild type strain (Figure 2.1, 2.2, and Table 2.2). Thus, the only difference between Qβ infections of wild type and *rat* hosts is the failure of the latter to undergo lysis.

Overproduction of MurA protects cells from A_2-mediated lysis

Although A_2 is produced in 50-100 fold excess to what is required for virion assembly, it was not known if this "free" A_2 could inhibit MurA. To address this issue, we introduced pZE12-*murA(his)$_6$* into a HfrH derivative (RY 3095) that was phenotypically *lacY*$^-$ due to the polar effects of a Tn*5* insertion in the *lacZ* gene. This arrangement allows gradient inductions of the epitope tagged *murA* gene with IPTG (Figure 2.3, Table 2.3). Lawns of the test strain were prepared on a series of plates containing increasing concentrations of the inducing agent. Each lawn was tested for Qβ sensitivity by spotting different dilutions of a Qβ lysate on its surface. At 0, 12.5, and 25 μM IPTG, the cells remained sensitive to Qβ-induced lysis. However at 50 μM IPTG, and above, the cells were protected from lysis. Since there are approximately 1.2×10^4 molecules of MurA/cell at 25 μM IPTG, and this value roughly equal the number of A_2 molecules present at the time of lysis (9×10^3/cell, see Table 2.2.), it is clear that the A_2 protein need not be incorporated into a phage particle for it to inhibit the activity of MurA.

Table 2.2. The amount of A_2 accumulated during Qβ infection of XL1Blue and XL1Blue^{rat}.

Time after infection (minutes)	Pfu/ml	Total cells	Qβ/ cell	Total ng A_2	Total cells/lane	A_2 Molecules/cell
XL1Blue						
0'	$2.4x10^8$	10^8	2.4	nd		
30'	$8x10^9$	$1.7x10^8$	47	8.7	$2x10^7$	$5.4x10^3$
60'	$4.7x10^{10}$	$2.8x10^8$	167	25	$3.5X10^7$	$8.8x10^3$
90'	$2x10^{11}$			35	lysis	
120'	$2x10^{11}$			nd*		
XL1Blue^{rat}						
0'	$2.7x10^8$	10^8	2.7	nd		
30'	$4.3x10^9$	$1.7x10^8$	25	4.4	$2X10^7$	$2.7x10^3$
60'	$2.6x10^{10}$	$2.8x10^8$	92	20	$3.5X10^7$	$7.1x10^3$
90'	$9x10^{10}$	$3.7x10^8$	243	26.5	$4.5X10^7$	$7.3x10^3$
120'	$1.2x10^{11}$	$4.7x10^8$	255	34	$5.5X10^7$	$7.7x10^3$

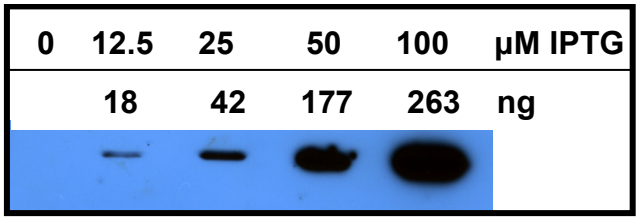

Figure 2.3. Quantification of the amount of MurA with level of induction. Western blot of the amount of MurAHis$_6$ accumulated after induction of HfrH (RY 3095) pZE12-*murAhis*$_6$ with IPTG (0-100 µM). The amount of MurA accumulated at each level of induction is labelled above the band in nanograms (ng).

Table 2.3. Amount of MurA accumulated per cell with increasing expression from plasmid.

Level of induction (μM IPTG)	Total MurA per lane (ng)	MurA molecules/cell
0	nd	nd
12.5	18	4.7×10^3
25	43	1.2×10^4
50	180	4.5×10^4
100	260	7.1×10^4
1000	1800	4.8×10^5

Qβ^{por} mutants display a rapid lysis phenotype in MurA^{wt} hosts

When Qβ phage are plated on a *murA^{rat}* host, plaques appear with a frequency of approximately 10^{-4} per phage. The size of these plaques is small compared to those formed on a wild type host. After purification, the phage recovered from these plaques have a high plating efficiency on both wild type and *rat* strains, forming large plaques on the former and small plaques on the latter (Figure 2.4). These Qβ variants all harbor mutations in the *A_2* gene leading to the amino acid L28P, D52N or E125G and the phage carrying these mutations are termed Qβ^{por} (plates on *rat*). Unexpectedly, hosts expressing the wild type *murA* gene lyse considerably sooner after infection with any of the Qβ^{por} mutants than with Qβ^{wt} (Figure 2.5). The earlier lysis time for the Qβ^{por} mutants is accompanied with a lower burst size when compared to Qβ (Figure 2.5). Hosts expressing the *rat* allele of *murA* (MurA^{L138Q}) cease to grow logarithmically after infection with the Qβ^{por} mutants (Figure 2.6). *Qβ^{por} mutations result in overexpression of the A_2 protein*

To provide an explanation for the rapid-lysis phenotype of the Qβ^{por} mutants, we first measured the amount of A_2 protein produced during infections with the Qβ^{por} phage. To our complete surprise, *por* mutations appeared to decrease the time needed for the A_2 protein to accumulate to lytic concentrations (Figure 2.7, Table 2.2). For example, the L28P mutant is present at nearly 60,000 molecules per cell 30 minutes after infection, which is more than 10 times the level seen with wildtype A_2 (A_2^{wt}) (Figure 2.7, Table 2.2). This

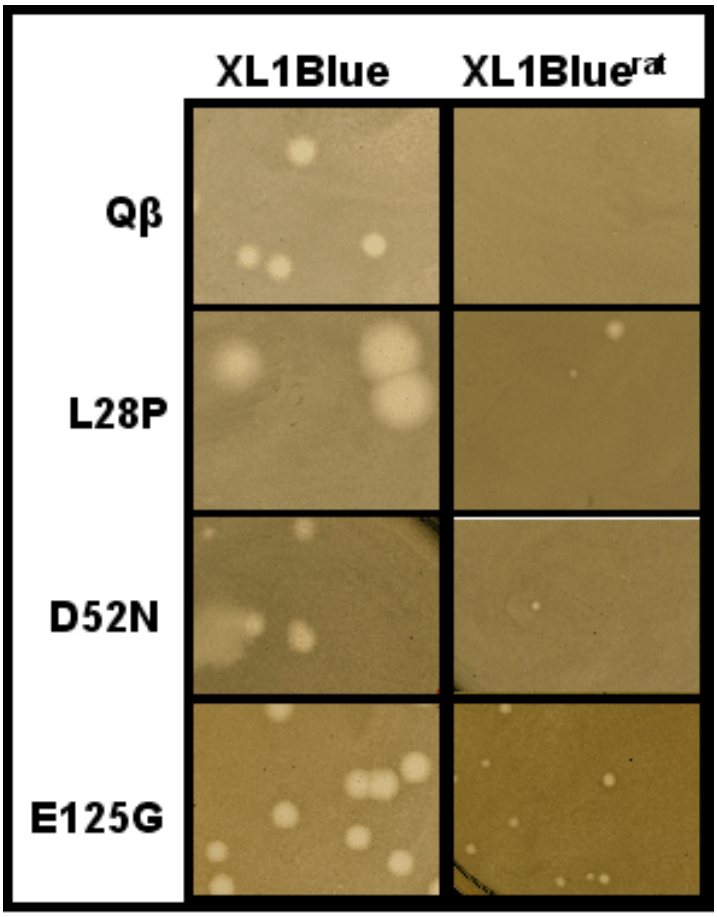

Figure 2.4. Comparison of Qβ and Qβ^{por} plaque morphologies on XL1Blue and XL1Blue^{rat} lawns. Cultures of XL1Blue and XL1Blue^{rat} were infected with Qβ and Qβ^{por} (Qβ A_2^{L28P}(L28P), Qβ A_2^{D52N}(D52N), Qβ A_2^{E125G}(E125G)), respectively.

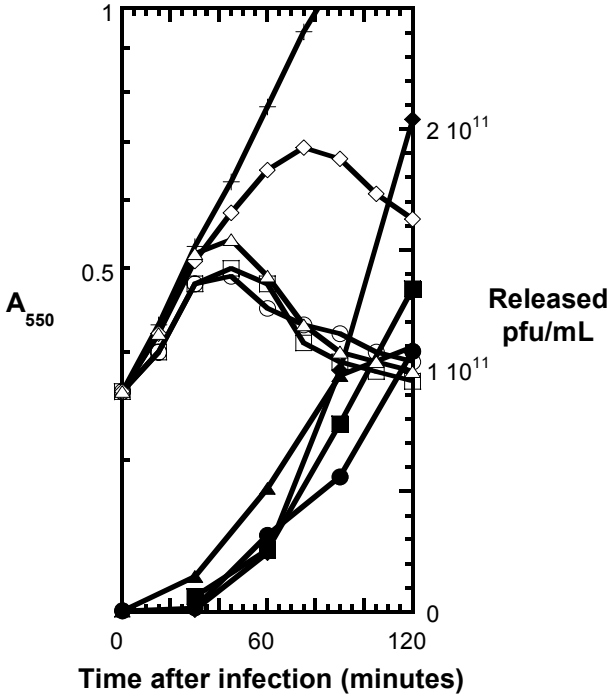

Figure 2.5. Lysis of XL1Blue infected with Qβ or $Q\beta^{por}$.
Cultures of XL1Blue were infected with with Qβ (◊), $Q\beta^{por}A_2^{L28P}$ (L28P) (•), $Q\beta^{por}A_2^{D52N}$ (D52N) (•) or $Q\beta^{por}A_2^{E125G}$ (E125G) (∆). Uninfected culture is represented by (+). Culture growth was measured as a function of time. The amount of released phage with time is plotted with filled symbols.

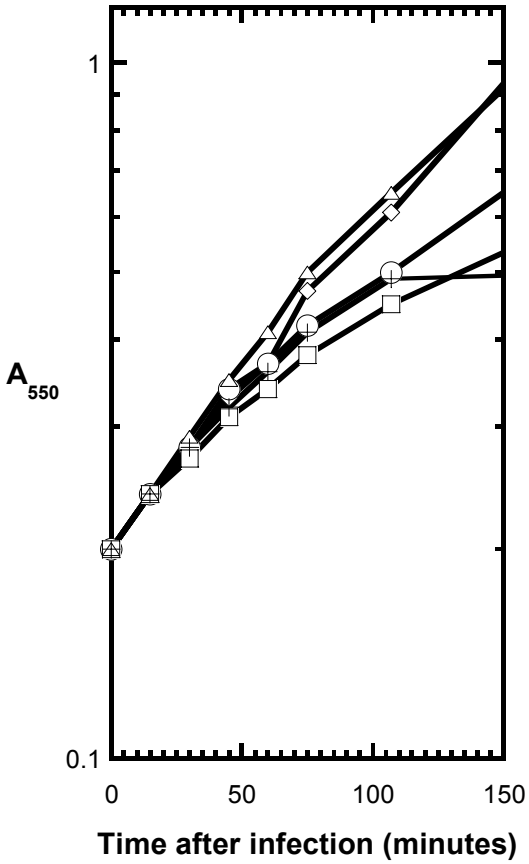

Figure 2.6. Infection of XL1Blue^{rat} with Qβ and Qβ^{por} mutants.
XL1Blue^{rat} was infected with Qβ (•), Qβ$^{por}A_2^{L28P}$ (L28P) (•), Qβ$^{por}A_2^{D52N}$ (D52N) (Δ) or Qβ$^{por}A_2^{E125G}$ (E125G) (+). Uninfected culture is represented by (◊). Culture turbidity was monitored as a function of time.

raises the possibility that the ability of $Q\beta^{por}$ phage to lyse *rat* hosts lies not in an increased affinity of the variant A_2 proteins for $MurA^{rat}$, but is due solely to a dramatic increase in the rate and extent of A_2 accumulation in the infected cell.

Mechanism by which por mutations enhance A_2 production

The increased amount of A_2 present during $Q\beta^{por}$ infections may be due to enhanced translation of the Qβ message or to the increased stability of the mutant A_2 proteins. To differentiate between these two possibilities, we first examined the stability of the A_2 protein in cells treated with chloramphenicol 30 minutes after infection. As can be seen in Figure 2.8, the por mutations have little effect on the stability of A_2.

Because the genome of Qβ adopts a complex secondary structure that serves to regulate its translation, it is possible that the por mutations disrupt this structure resulting in the upregulation of A_2 translation. If so, the effect of the *por* mutations might only be exerted in full length Qβ RNA and might not be observed with the cloned A_2 gene sequence. When the por mutations were moved into the plasmid pZE12-*A_2*, only the D52N protein was able to cause host lysis and did so with the kinetics of wild type A_2 expressed from the parental plasmid (Figure 2.9A). Neither A_2^{L28P} nor A_2E125G proteins mediated cell lysis when the mutant alleles were expressed from the plasmid. Moreover, unlike the situation with the phage, the *por* mutations had no significant effect on the levels

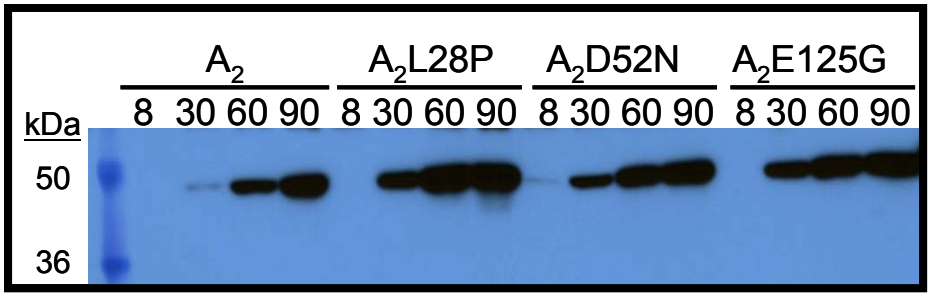

Figure 2.7. A_2^{por} mutants accumulate greater amount of protein than A_2. Protein samples of XL1Blue infected with Qβ/Qβ^{por} (A_2^{L28P}, A_2^{D52N} and A_2^{E125}) were analyzed by Western blot as a function of time after infection. The first lane is a molecular weight marker in kilodaltons (kDa).

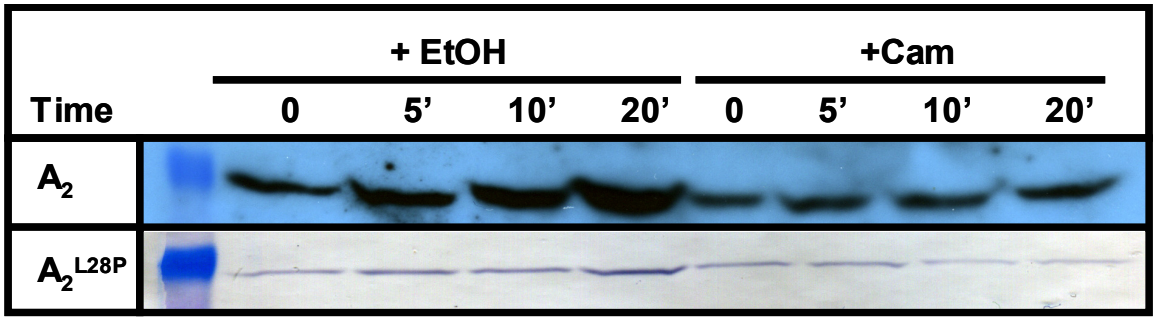

Figure 2.8. A_2 and A_2^{por} are stable proteins during infection.
Western blots showing the stability of A_2 and A_2^{L28P}. XL1Blue was infected with Qβ/Qβ$^{por}A_2^{L28P}$ and the amount of A_2 was monitored as a function of time after inhibition of translation with chloramphenicol (Cam). As a control, ethanol (EtOH) was added to cultures at time zero. Western blots were developed by chemiluminescence (A_2) or colorimetrically (A_2^{L28P}). The first lane of each blot is a 50 kDa molecular weight marker.

of A_2 produced when the various alleles were expressed from the plasmid (Figure 2.9B).

The E125G variant of A_2 inhibits the MurAA enzyme from Bacillus subtilis

Due to the high sequence divergence between the *E. coli* and *B. subtilis* *murA* genes, it was not surprising to find that Qβ has a low plating efficiency on *E. coli* hosts expressing $murA^{Bs}$ (Figure 2.10), suggesting that only one or a few mutations in the A_2 gene might be sufficient to generate an A_2 protein that can efficiently inhibit $MurA^{Bs}$. In fact, the *por* allele, A_2^{E125G} appears to be one such mutant since it has the same efficiency of plating on cells expressing $murA^{Bs}$ as on wild type hosts (Figure 2.10).

DISCUSSION

During phage infections, A_2, the maturation protein of Qβ is synthesized in amounts far greater than what are necessary for phage morphogenesis. Thus, although A_2 can inhibit the enzymatic activity of MurA after its incorporation into Qβ particles (9), it appears that free A_2 is responsible for host lysis during infection. This observation eliminates the simplest model for lysis timing by Qβ where host lysis would only occur after the number of progeny assembled was sufficient to inhibit the cellular pool of MurA to the extent necessary for lysis to occur. Instead, the rate of A_2 synthesis and its affinity for

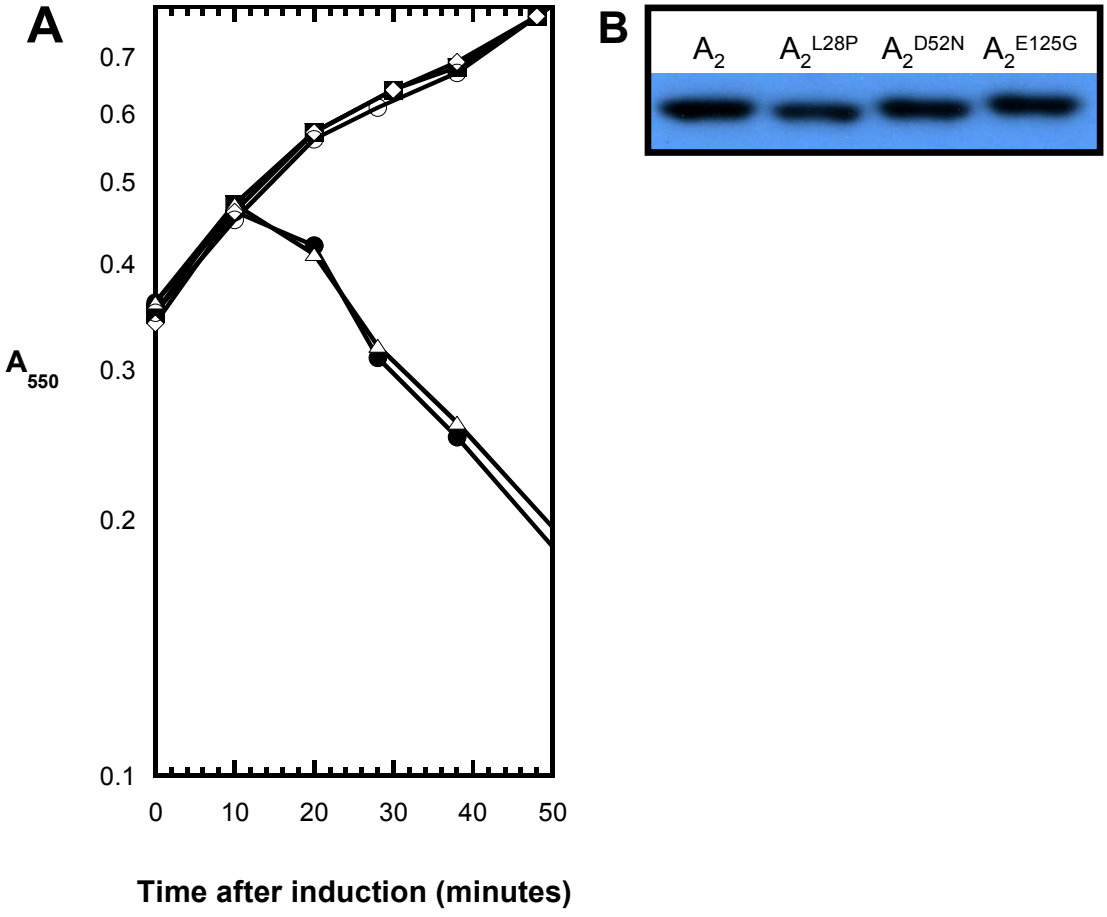

Figure 2.9. Expression of cloned A_2^{por} does not induce faster lysis. (A) Cultures of HfrH (15177) carrying the plasmids: pZE-*A_2* (•),pZE-*A_2^{L28P}*(•), pZE-*A_2^{D52N}*(Δ), pZE-*A_2^{E125G}*(◊) were induced at time zero. The growth of the culture was monitored as a function of time. Uninduced culture (•). (B) Protein samples of A_2, A_2^{L28P}, A_2^{D52N}, and A_2^{E125G} were analyzed by Western blot.

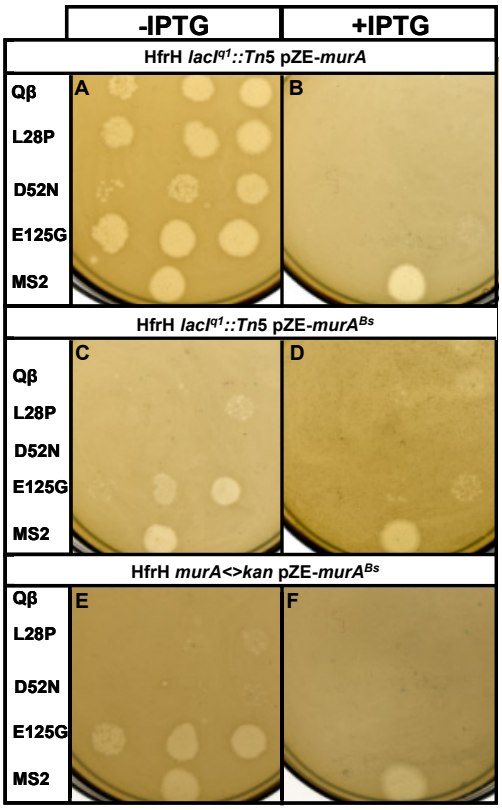

Figure 2.10. Qβ and Qβ^{por} plaque formation on MurA^{Bs} lawns.
Qβ and Qβ^{por} dilutions were spotted onto lawns of HfrH (RY3095) pZE-*murA*(Panels A and B), HfrH (RY3095) pZE-*murA*^{Bs} (Panels C and D) and HfrH (RY15177) *murA*<>*kan* pZE-*murA*^{Bs} (Panels E and F) with and without inducing agent (+IPTG, -IPTG). Qβ^{por}A$_2^{L28P}$ (L28P), Qβ^{por}A$_2^{D52N}$ (D52N), Qβ^{por}A$_2^{E125G}$ (E125G) and MS2 were spotted to each bacterial lawn. MS2 is a *Levivirus* that infects F+ *E. coli* but does not target MurA to elicit host cell lysis.

MurA must be such that an “acceptable” number of progeny are assembled before the block in peptidoglycan synthesis results in lysis. This mechanism for lysis timing is potentially catastrophic since increasing the rate of A_2 synthesis or its binding constant for MurA might lead to host lysis during the eclipse period.

Except for their ability to plate on *murA*^{rat} hosts, the Qβ^{por} mutants described by Bernhardt, *et al*. (9) were uncharacterized at the molecular level. It was hoped that identifying a number of different *murA*^{rat} alleles and their allele-specific *A*$_2^{por}$ suppressors would allow the interacting surfaces of MurA and A_2 to be delineated. However, in this study, we have found that the existing por mutants appear to act globally by significantly increasing the rate of A_2 translation. Thus, not only are these mutations not allele-specific, but they may not identify residues on the surface of A_2 that directly contact the surface of MurA. The fact that these mutants lyse *murA*^{wt} hosts more rapidly that Qβ^{wt} but with a lower burst size is consistent with our conclusion that A_2 need not be assembled into a phage particle to be an effective inhibitor of MurA.

Over three decades ago, Lodish found that the amount of the maturation, or A protein, obtained by the translation of f2 phage RNA *in vitro* was highly dependent upon temperature (57). He concluded that the stimulatory effect was due to the loss of RNA secondary structure at high temperature. More recently, it was shown that the translation of *L*, the lysis gene for MS2, is controlled by an RNA secondary structure called the L-hairpin. Disruption of the hairpin dramatically decreases phage yield presumably due to overproduction of L and

premature lysis (49). Thus, it is not unreasonable to expect that mutations in Qβ might affect the synthesis of A_2 by altering the secondary structure of the viral RNA. In fact, it is possible that $Q\beta^{por}$ isolates may have mutations that lie outside of the A_2 reading frame and were overlooked in the initial analysis.

Finally, one surprising finding that may have practical application is the ability of Qβ to rapidly "evolve" to lyse cells expressing the *murA* gene from the Gram-positive organism, *B. subtilis*. Fortuitously, one of the initial $Q\beta^{por}$ mutants encoded an A_2 protein, the E125G variant, was capable of inhibiting $MurA^{Bs}$. This property was not solely due to the overproduction of the A_2 protein since hosts expressing the *Bacillus* enzyme were not sensitive to $Q\beta^{por}A_2^{L28P}$ or $Q\beta^{por}A_2^{D52N}$ phage, which also overproduce A_2. Thus, a better understanding of how A_2 interacts with MurA might assist in the design of novel compounds that inhibit peptidoglycan synthesis in both Gram-negative and Gram-positive bacteria.

CHAPTER III

IDENTIFICATION OF THE LYTIC DOMAIN OF A_2

INTRODUCTION

In an attempt to identify the elusive lysis-mediator of bacteriophage Qβ, fragments of the ssRNA genome DNA complement were cloned into expression vectors. Two laboratories identified that expression of the maturation (*A_2*) gene fragment encoded protein with lytic function (101, 47). Each group attempted to isolate a lytic fragment of A_2 to no avail. Lysis activity was abolished with each carboxy-terminal truncation, amino-terminal truncation, and internal deletion tested. Since the discovery that A_2 is necessary and sufficient for host lysis, Qβ mutants able to overcome a host strain resistant to A_2-mediated lysis have been isolated (9). The phenotype has been attributed to mutations in the A_2 coding sequence: A_2^{L28P}, A_2^{D52N} and A_2^{E125G}. Because these mutations map to the amino-terminal third of A_2, we decided to reinvestigate the possibility that the lysis function is retained in a fragment of A_2. We decided to study the lytic function of manipulated A_2 proteins in a plasmid based system where the lytic function is scored by the drop in turbidity of a culture.

MATERIALS AND METHODS

Bacterial strains and culture growth

Plasmids were propagated in *E.coli* strain XL1Blue (*recA*1 *endA*1 *gyrA*96 *thi hsdR*17 *supE*44 *relA*1 *lac [*F'::Tn*10 proA+B+ laqI*^{q} *Δ(lacZ)*M15]). Lysis profiles were obtained with BL21(DE3) (Novagen) or BL21(DE3)^{rat} . BL21(DE3)^{rat} was constructed by introducing the *rat* allele *murA*^{L138Q} into BL21(DE3) by P1 transduction with the donor strain, XL1Blue^{rat} (9).

Cultures were grown in Luria-Bertani (LB) medium, supplemented with chloramphenicol (10 μg/ml), ampicillin (100 μg/ml), and kanamycin (40 μg/ml) as necessary. For inductions, a final concentration of 100 ng/ml anhydrotetracycline and/or 1mM isopropyl-β-D-thiogalactopyranoside (IPTG) (Research Products International Corp.) was added to cultures as indicated. Standard conditions for growth and monitoring of lysis kinetics by measuring the turbidity of the culture at A_{550} have been described (83).

Molecular biology techniques

Standard DNA manipulation protocols were performed as described previously (76). PCR reactions and restriction enzyme digests were purified by using the PCR Purification Kit (Qiagen) or the Gel Extraction Kit (Qiagen) according to manufacturer's instructions. All enzymes including Taq polymerase, restriction endonucleases, Alkaline Phosphatase, and T4 DNA Ligase were purchased from New England Biolabs and used according to

instructions. QuickChange PCR kit (Stratagene) was used to introduce nucleotide changes in a gene. Oligonucleotides were ordered from Integrated DNA Technologies (Coralville, IA) and were used without further purification. Automated fluorescent sequencing was performed by the Laboratory of Plant Genomics at the Texas Agriculture Experiment Station. Sequencing primers for A_2 are listed (Table 3.1). A minimum of two sequencing reactions were performed to read the entire length of *A_2* (1,260 base pairs) and *murA* (1,257 base pairs).

Cloning and expression of A_2 and $murA^{Bs}$

A_2 was amplified and cloned into pET11a as described in chapter II, materials and methods section. Derivatives of the *A_2* gene cloned into pET-A_2 will be referred to as pET-*A_2**. The vector pET11a is a medium copy number vector conferring ampicillin resistance where the cloned gene is under the control of the T7 promoter. Expression of pET-*A_2** in BL21(DE3) pLysS was induced by the addition of 1mM IPTG in mid-log phase. pLysS constitutively expresses low levels of T7 Lysozyme and confers chloramphenicol resistance. The *murAA* (*$murA^{Bs}$*) gene from *Bacillus subtilis* W23 (RY 7355) was amplified using the primers KpnI-NdeI-BsMurA.2-For and BsMurA-Bam-Xba-Rev (Table 3.1). The PCR product was digested with KpnI and XbaI and ligated to similarly digested pZA31, a medium copy number vector conferring chloramphenicol resistance. In the resulting plasmid, pZA31-*$murA^{Bs}$,* expression of *$murA^{Bs}$* is

under control of the $P_{LtetO-1}$ promoter of the vector. Expression of the *murA*^{Bs} gene is achieved by inducing with (100 ng/ml) anhydrotetracycline and was co-transformed with pET-*A*$_2$* into BL21(DE3).

Generating derivatives of pET-A$_2$ encoding truncations/ internal deletions of A$_2$

An amber codon was introduced to the carboxy-terminal half of *A*$_2$ by QuickChange PCR (Stratagene). Oligonucleotides are listed in Table 3.1. Amino-terminal truncations of *A*$_2$ were generated by exclusion PCR with pET-*A*$_2$ or pET11a-*A*$_2$-*190* serving as the template. To exclude a segment of gene sequence, each primer incorporates a terminal NdeI site and anneals at the boundary of the region to be excluded. The primers extend away from each other, amplifying the entire plasmid except for the excluded sequence. For each truncation, a common reverse primer complimentary upstream and including the NdeI site of pET11a was used. The forward primer incorporated a new NdeI site and amplified downstream from the site of truncation in *A*$_2$. The combination of these two primers excludes an amino-terminal fragment of A_2. The linear PCR product was purified, digested with NdeI and ligated to recircularize the vector. Internal deletions in the amino-terminal domain of A_2 were engineered by Splicing by Overlapping Extension (SOE) PCR (38) with pET11a-*A*$_2$ serving as the template. The SOE PCR primers have two purposes: (1) to anneal to the boundary of the sequence to be deleted, and (2) to contain overlapping sequence with each other. Each gene fragment was amplified independently

Table 3.1. Primers used to study fragments of A_2.

Primer name	Primer
KpnI-NdeI-A_2-FOR	TAAGA**GGTACCCATATG**CATCACCATCATCACCACGGC
RV-Xba-Bam-A_2-REV	TGGTAA**GGATCC**TCTAGAGATATCTTATCAACGCTTTACGCGTTGGG
His-A_2-FOR	TGATTAGGTACCCATATGCATCACCATCATCACCACGGCGGCCCTAAAT TACCGCGTTCC
A_2-311-FOR	TTCAGTATGATCCCGCAGCAC
A_2-611-FOR	GTAGGGTTATCCAGTCCTACC
A_2-388- REV	TCGCACTATCGCCATTACCGA
KpnI-NdeI-BsM-For	ATATAT**GGTACCCATATG**GAAAAAATCATCG
BsM-Bam-Xba-Rev	GAGTGGTCTAGA**GGATCC**TTATGCATTTAAGTCAGAAACG
Internal deletion	
Δ45-153	FOR: TACACACTGAAGGGTCGTGAAGGGCTCGAGACTATA REV: TATAGTCTCGAGCCCTTCACGACCCTTCAGTGTGTA
Δ45-98	FOR: TACACACTGAAGGGTCGTGTTGACTGGGATTTCGGTAAT REV: ATTACCGAAATCCCAGTCAACACGACCCTTCAGTGTGTA
Δ45-118	FOR: TACACACTGAAGGGTCGTACCTTTGCACCTAAGGAG REV: CTCCTTAGGTGCAAAGGTGCGACGACCCTTCAGTGTGTA
Δ80-99	FOR: GCCTCTTCAGGCCTTCGTGTTGACTGGGATTTCGGT REV: ACCGAAATCCCAGTCAACACGAAGGCCTGAAGAGGC
Δ71-83	FOR: ACTCCACATCGCGTCACCGTTCAGTATGATCCCGCA REV: TGCGGGATCATACTGAACGGTGACGCGATG
Δ129-140	FOR: CCTAAGGAGTTTGATTTTTCCGCGTTTAATGCCAAG REV: CTTGGCATTAAACGCGGAAAAATCAAACTCCTTAGG
Truncation	
Δ1-32	NdeI FOR: ATTGGG**CATATG**TCCGACACGCATCCG
Δ1-54	NdeI FOR: CCAGACCTCTTTATC**CATATG**GGTCGCC
Δ1–89	NdeI FOR: GTTCAGTATGAT**CATATG**GCACTATCGTTC
Δ125–140	REV: CATTAACCTAGGGGATCCTCACTCCT
Δ135-420	REV: CATTAACCTAGGGGATCCTCAACGAG

Table 3.1. Primers used to study fragments of A_2 continued.

Truncation	Primer
Δ147-420	FOR: AATGCCAAG**TAG**GGCACTATG
	REV: CATAGTGCC**CTA**CTTGGCATT
Δ160-420	FOR: ACTATAAAA**TAG**CTCGGGCTT
	REV: AAGCCCGAG**CTA**TTTTATAGT
Δ172-420	FOR: CGTGAGGGT**TAG**CGCGCTGTT
	REV: AACAGCGCG**CTA**ACCCTCACG
Δ180-420	BamHI REV:TGGTAA**GGATCC**TTATTAATCGCCACGCTTAACAGC
Δ186-420	BamHI REV:TGGTAA**GGATCC**TTATTACCTACGAAGAGCACG
Δ190-420	FOR: ATCCAGTCC**TAG**CATAATGGT
	REV: ACCATTATG**CTA**GGACTGGAT
Δ200-420	BamHI REV: TGGTAA**GGATCC**TTATTAAGTAGCCGG
Δ205-420	BamHI REV: TGGTAA**GGATCC**TTATTACCAGAGATTACC
Δ209-420	FOR: GAATTTCGT**TAG**GGCCTTATG
	REV: CATAAGGCC**CTA**ACGAAATTC
Δ246-420	FOR: GGCGAGGAT**TAG**GTTGTCGAA
	REV: TTCGACAAC**CTA**ATCCTCGCC
Δ284-420	FOR: CGCGAAGGA**TAG**GCTGTTTTC
	REV: GAAAACAGC**CTA**TCCTTCGCG
Δ339-420	FOR: GGTCAGCTA**TAG**CATAATATC
	REV: GATATTATG**CTA**TAGCTGACC
Δ1-417	FOR: CGCGTAAAGCGTTGA**CATATG**
Δ18-420	REV: ACGCGGTAATTTAGG**CATATG**

Amber codons and restriction endonuclease sequences are highlighted by bold font.

and then mixed together for a second round of PCR. In this second reaction, the denatured strands anneal to one another within the complimentary region and serve as primers that splice the two gene fragments together, yielding a single PCR product. The final PCR product was flanked by NdeI and BamHI restriction sites. After restriction endonuclease digests, the PCR product was purified and ligated into pET11a similarly cut with NdeI and BamHI. As indicated, a histidine$_6$ epitope tag (HHHHHHGG) was fused to the amino terminus of *A_2* by PCR with HisA_2-For and RevpET (Table 3.1) and cloned into pET11a in the same manner that pET-*A_2* was constructed to render pET-*his_6A_2*.

Alignment of lytic maturation proteins

The protein sequences of ssRNA bacteriophages Qβ, SP, NL95, MX1, M11 and F1 were obtained at the NCBI website (www.ncbi.nlm.nih.gov) and aligned using CLC Workbench software (www.clcbio.com).

RESULTS AND DISCUSSION

Choosing sites for truncating the A_2 gene

When performing a deletion/truncation analysis of a protein, it is useful to have structural information to avoid disruption of important secondary structure elements. Unfortunately, no structural information is available for A_2. Moreover, A_2 does not bear any similarity in primary sequence to any protein whose structure is known and could be used as a scaffold to predict the three

dimensional conformation of A_2 using existing software. Multiple sequence alignment of *Alloleviviridae* maturation proteins reveals a very conserved sequence, with the exception of three unconserved regions (amino acids 28-63, 90-140 and 357-386, numbered according to the Qβ sequence) (Figure 3.1). SP, NL95 and F1 have an additional 20-30 amino acids inserted between residues 190 and 191 (numbered according to Qβ sequence), and by manual inspection, this sequence is conserved. Interestingly, two of the A_2^{por} mutations, L28P and D52N are not conserved amino acids. Although E at residue 125 is not strictly conserved, each maturation protein in the alignment has either an E or a G at this position. Without an obvious rational starting point, amber codons were introduced at select glutamine, tyrosine, and serine residues within the sequence of *A2*.

Cloning and expression of the A_2 gene

Due to the toxic nature of A_2 upon expression, it was necessary to express A_2 from a tightly regulated plasmid. Although typically used for protein overexpression, the T7 expression system is tightly regulated in the presence of T7 lysozyme. T7 lysozyme (encoded from the pLysS plasmid) is a bi-functional protein that inhibits the transcriptional activity of T7 RNA polymerase. Thus, we used pET11a for A_2 expression in a BL21(DE3) derivative that also contained pLysS. Cells carrying pET-*A2* began to undergo lysis beginning about 30 minutes after induction. Using a host expressing the *murA*^{rat} allele, culture lysis is not observed indicating that it results from the inhibition of MurA and is not a

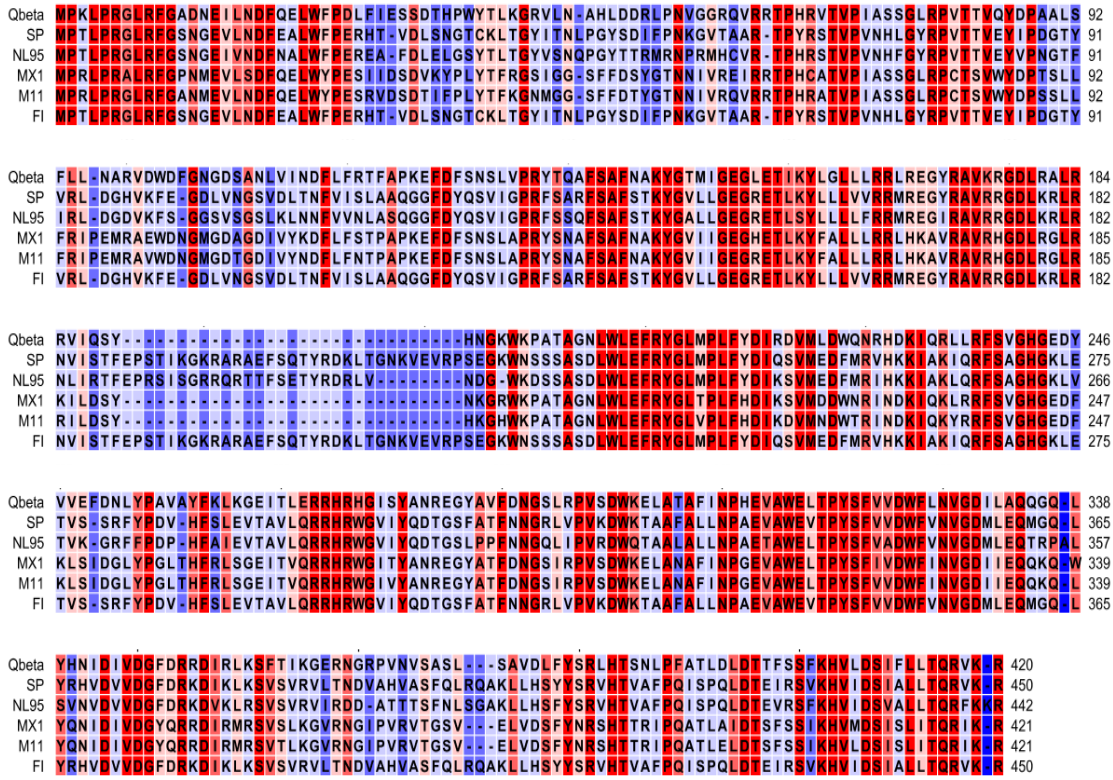

Figure 3.1. Multiple alignment of *Allolevivirus* maturation proteins. ssRNA bacteriophages Qβ, SP, NL95, MX1, M11 and F1 maturation protein primary structure is shown. The amino acids are represented as single letter abbreviations. Conserved residues are indicated by red background with highest conserved identity in dark red. Residues that are not conserved are coded by blue background with dark blue representing the most dissimilar residues.

non-specific toxic affect due to the overproduction of A_2. Essentially all of the A_2 produced during this induction is found as an insoluble aggregate after the cells are broken open, which can be solubilized with 6M guanidine HCl. Attempts to remove the guanidine by dialysis results in the precipitation of the protein. Even though soluble A_2 was not obtained with this system the fact that lysis occurs and is prevented by co-expressing *murA*^{rat} indicates that this expression system can be used for the deletion/truncation analysis of A_2.

Truncation and deletion analysis indicates that the lytic function of A_2 lies within the N-terminal domain

A series of amino- and carboxy-terminal truncations and internal deletions of A_2 were engineered (Figure 3.2) and cloned into pET11a. For each derivative, the accumulation of an A_2 of the expected size was confirmed by SDS-PAGE and either Coomassie blue staining or Western blotting with an A_2-specific antibody (Figure 3.4, Figure 3.6).

A_2 derivatives with amino-terminal internal deletions of codons 45-153, 45-118, 45-98, 71-83, 129-140, or 80-93 were unable to elicit cell lysis (Figure 3.3), although the protein accumulates (Figure 3.4). Serial truncations from the carboxy-terminus of A_2 resulting in expression fragments consisting of the first 339 and 284 residues results in the loss of lysis phenotype upon expression (Figure 3.5, Figure 3.6). Surprisingly, some lytic activity was restored when the carboxy-terminal truncation was extended to

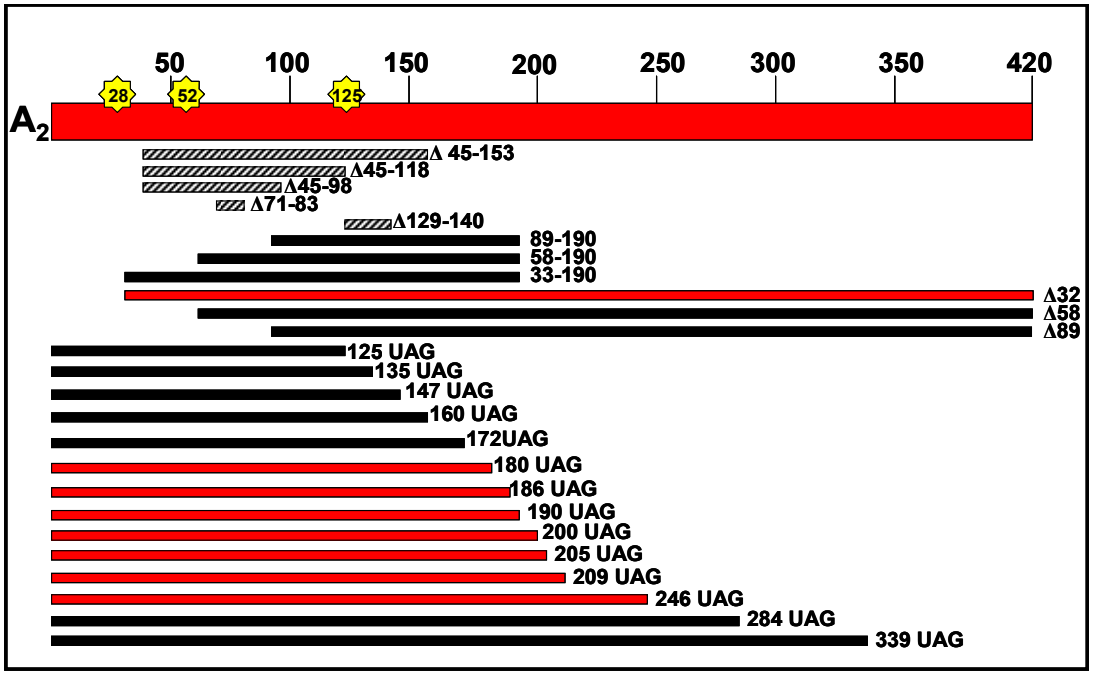

Figure 3.2. Internal deletion and truncation constructs of A_2.
The rectangle is a linear representation of the 420 residue A_2 protein. The yellow bursts represent the locations of A_2^{por} mutants L28P, D52N and E125G, respectively. The hatched boxes indicate deleted regions (Δ) and solid boxes represent the length of truncated A_2. Functional (lytic) fragments of A_2 are indicated with red boxes.

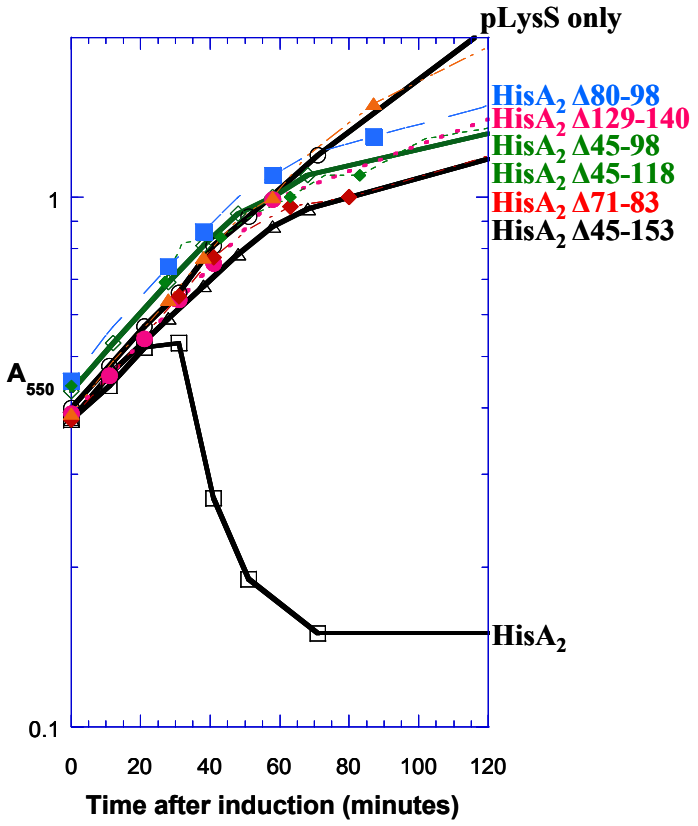

Figure 3.3. A_2 lytic function is lost with N-terminal internal deletions. The lysis profile of BL21(DE3)pLysS expressing internal deletion mutants from pET11a-His_6A_2(•) derivatives. Internal deletions include: His_6A_2 Δ 45-98 (◊), His_6A_2 Δ 45-118 (-♦-, green), His_6A_2 Δ 45-153 (Δ), His_6A_2 Δ71-83 (-♦-, red), His_6A_2Δ80-98 (•), and His_6A_2Δ129-140 (-•-). Also shown is BL21(DE3) pLysS (•). Culture turbidity was monitored as a function of time.

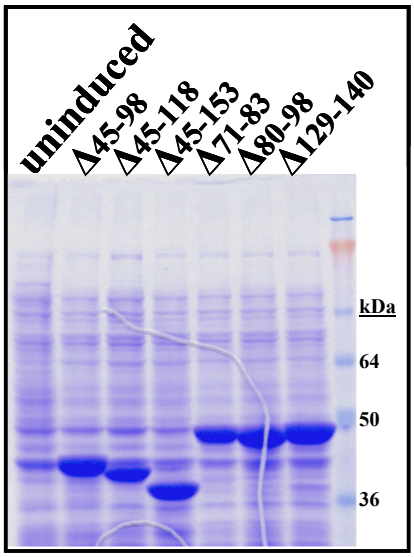

Figure 3.4. Accumulation of internal deletion mutants of A_2.
Coomassie brilliant blue stained SDS-PAGE of BL21(DE3) pLysS expressing internal deletion mutants of A_2 from pET11a: Δ45-98, Δ45-118, Δ45-153, Δ71-83, Δ80-98, and Δ129-140. The region deleted (Δ) from A_2 is indicated above each lane. The last lane contains a molecular size marker in kilodaltons (kDa).

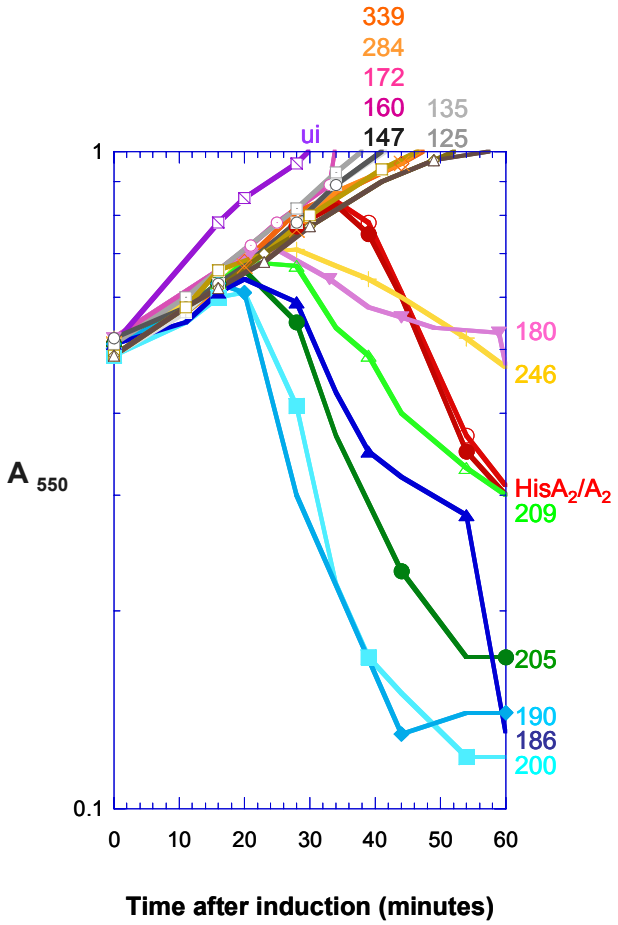

Figure 3.5. The amino terminus of A_2 is sufficient for plasmid-induced lysis. Growth profiles of N-terminal fragments of *A_2* (A_2*) as expressed in BL21(DE3) pLysS pET11a-(His)A_2*. His_6A_2 (maroon), A_2 (red), A_2-339 (dark orange), A_2-284 (orange), A_2-246 (yellow), A_2-209 (lime green), A_2-205 (dark green), A_2-200 (cyan), A_2-190 (light blue), A_2-186 (dark blue), A_2-180 (light purple), A_2-172 (light pink), A_2-160 (dark pink), A_2-147 (light gray), A_2-135 (medium gray), A_2-125 (dark gray). Culture turbidity was monitored as a function of time.

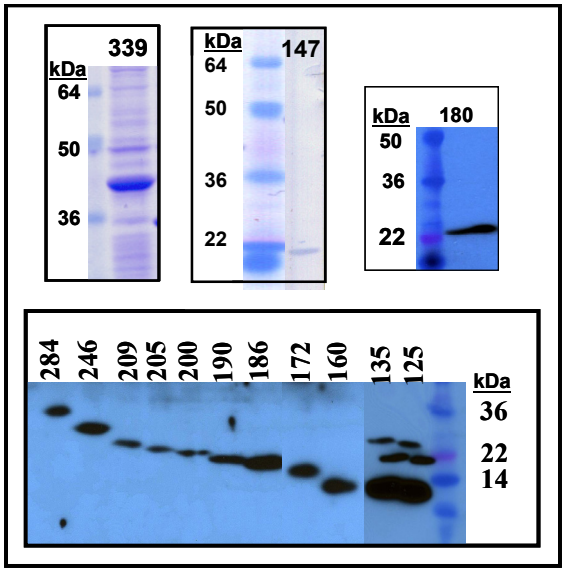

Figure 3.6. Accumulation of A_2 C-terminal truncations.
Whole cell samples were collected after induction of A_2 carboxy-terminal truncations from pET11a in BL21(DE3) pLysS. A_2-339 accumulates to be visible with coomassie-brilliant blue staining of SDS-PAGE. The remaining carboxy-terminal truncations of A_2 were detected by western blot. The site of truncation is indicated above each lane. Included is a molecular weight marker in kilodalton (kDa) units.

residue 246 (Figure 3.5). Lysis mediated by A_2-246 begins about 28 minutes after induction, 11 minutes earlier than the onset of A_2-mediated lysis. Further truncation to 209 maintains the same lysis time as 246, however a greater portion of the population undergoes lysis by A_2-209. Removal of 4 more residues (A_2-205) results in faster lytic activity with lysis 13 minutes faster than wildtype A_2. Lytic activity is maintained with further carboxy-terminal truncations to 200, 190 and 186, with lysis times of 22 minutes. Although lysis begins at 22 minutes for the truncations in the region of residues 200-186, A_2-200 and A_2-190 exhibit sharper lysis kinetics than 186. Lytic activity is lost with carboxy-terminal truncations beyond residue 172. A_2 fragments 180, 186, 190, 200, 205, 209 and 246 are lytic, suggesting that its amino-terminal domain is the lysis mediator.

We next truncated both A_2 and A_2-190 from the N-terminus to determine whether even smaller lytic fragments could be generated. Alignment analysis of other *Alloleviviridae* bacteriophage maturation proteins shows clusters of identical, and very similar sequences throughout the length of the protein (Figure 3.1). Relevant to the identification of the lytic domain are highly conserved regions of the amino-terminus: residues 1-27, 64-75 and 78-88. With the exception of Δ32-A_2, each of the amino-terminal truncations abolished the lytic function of A_2 and A_2-190 (Figure 3.7). Although lysis is not as rapid or complete as with A_2 or A_2-190, the growth of cells expressing Δ32-A_2 slows about 35 minutes after induction, and then the culture turbidity begins to decline after 60 minutes. Microscopic observation of cells undergoing lysis by Δ32-A_2 revealed a

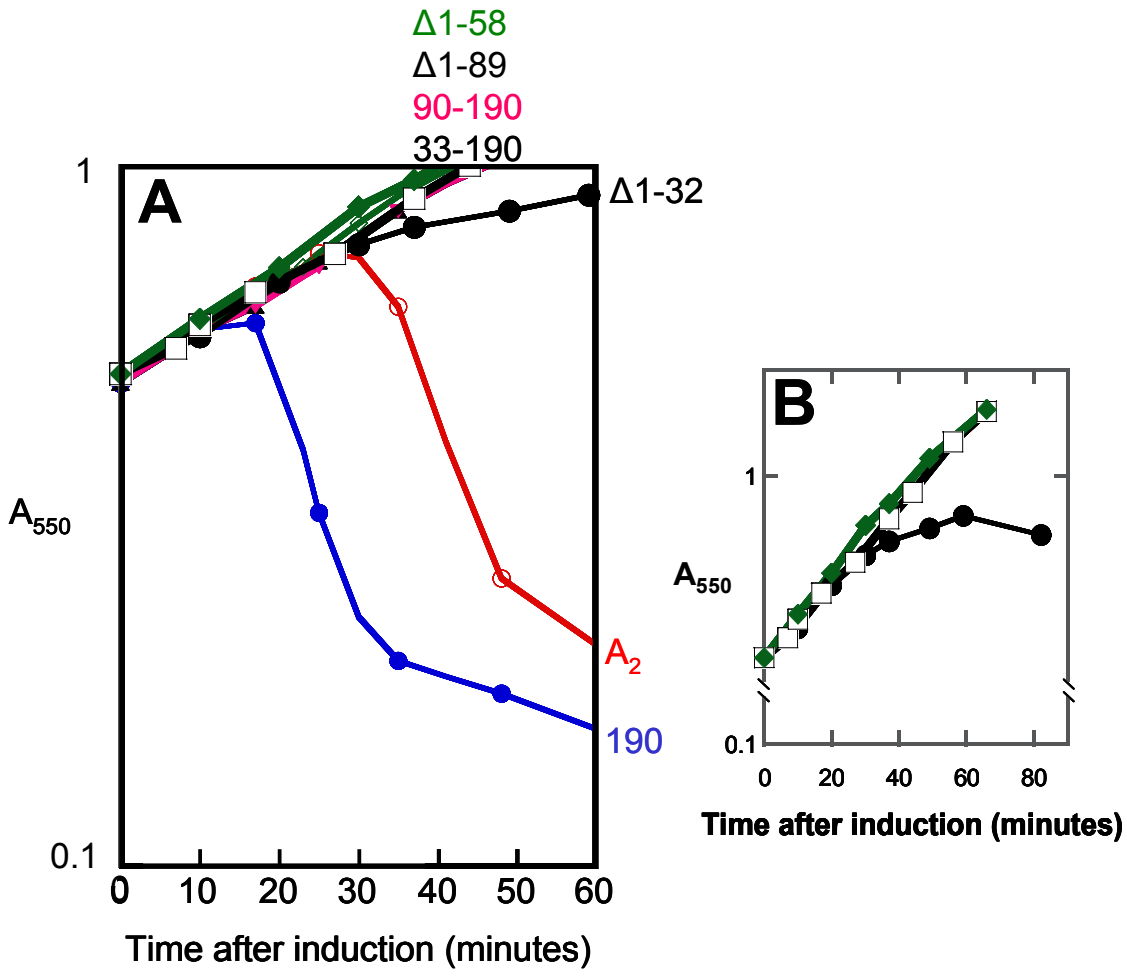

Figure 3.7. Lytic activity of amino-terminal truncations of A_2 and A_2-190. (A) BL21(DE3)^{rat} pLysS carrying the indicated plasmids were induced at time zero, and culture turbidity was monitored as a function of time for 60 minutes: pET11a-A_2(•),pET11a-A_2-190 (•, blue), pET11a-Δ32-A_2 (•, black), pET11a-Δ58A_2 (♦), pET11a-Δ89A_2 (Q), pET11a-A_2 90-190 (▼), pET11a-$A_2$33-190 (▲). (B) An 80 minute lysis profile of BL21(DE3) pLysS expressing pET11a-A_2Δ1-32 (•) and A_2 33-190 (•). Uninduced culture (♦). Culture growth was monitored as a function of time.

unique morphology. Rather than bulging exclusively from the septal region of a dividing cell, as is seen when A_2 induces lysis, bulges are sometimes observed at both poles, and other times the entire cell appears to be swelling. In each case, the cells become increasingly translucent, similar to what is observed when the cell contents spill into the environment due to lysis.

A_2 fragments that cause lysis of cells expressing murA^{rat}

Since A_2 is unable to alter the growth rate of the *rat* hosts even 100 minutes after induction, we expected the same to be true for its lytic fragments. However, as is shown in Figure 3.8, this was not the case. This raises the question as to whether the lytic activity of the fragments is due to MurA inhibition or some other mechanism. To address this issue, we next tested the ability of the A_2 fragments to lyse cells expressing *murA^{Bs}*. While lysis was prevented in these cultures, cell growth ceased shortly after induction, a situation that is also seen after induction of the full-length *A_2* gene in this host. From this, we conclude that the lytic fragments of A_2 function by inhibiting MurA.

CONCLUSION

Considering that mutations in the maturation gene of Qβ enable the phage to plate on an A_2-resistant host strain map to the amino terminus, we decided to investigate whether lysis function is confined to a segment of A_2. Analysis of truncated A_2 proteins expressed from a plasmid revealed that

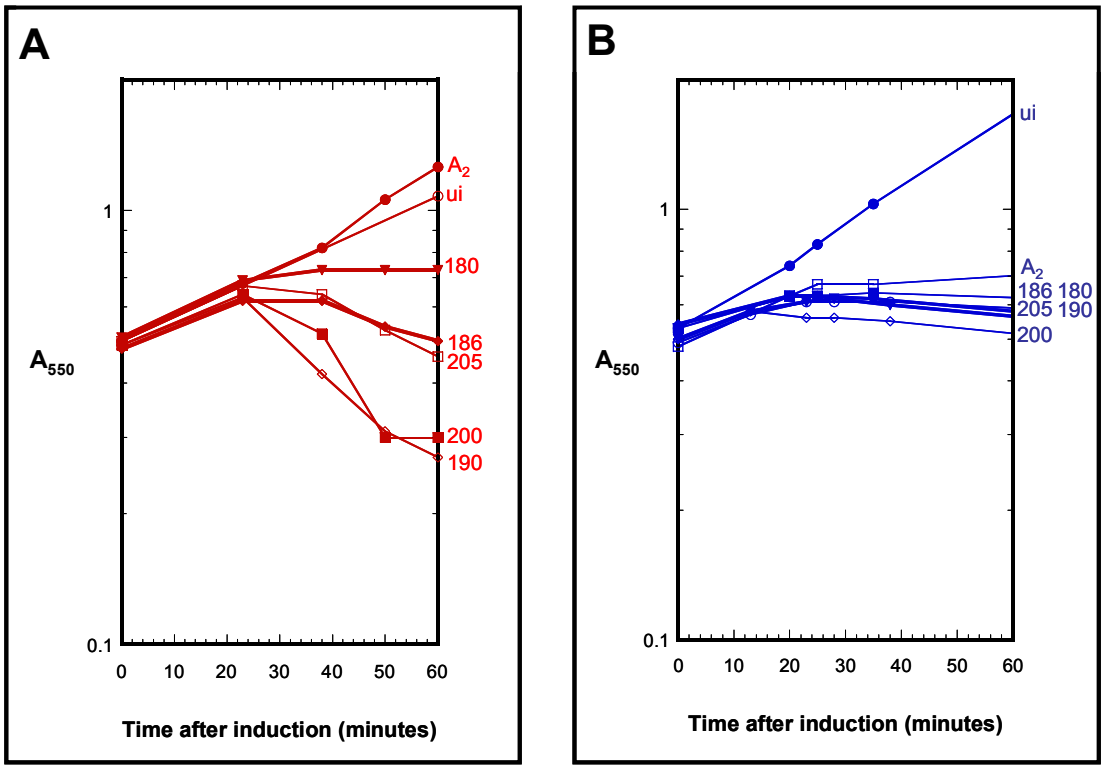

Figure 3.8. Lytic fragments of A_2 lyse MurA^{rat} strain and target MurA. (A) BL21(DE3)^{rat} pLysS carrying the indicated plasmids were induced at time zero, and culture turbidity was monitored as a function of time: pET11a-*A_2* (!), pET11a-*A_2*-205 (Q), pET11a-*A_2*-200 (#), pET11a-*A_2*-190 (◊), pET11a-*A_2*-186 (♦), pET11a-*A_2*-180 (▼), uninduced pET11a-*A_2* (ui, "). (B) BL21(DE3) pZA31*murA*^{Bs} carrying the indicated plasmids were induced at time zero, and culture turbidity was monitored as a function of time: pET11a-*A_2* (!), pET11a-*A_2*-205 (Q), pET11a-*A_2*-200 (#), pET11a-*A_2*-190 (◊), pET11a-*A_2*-186 (♦), pET11a-*A_2*-180 (▼), uninduced pET11a-*A_2* (ui, ") were supplemented with anhydrotetracycline to constitutively express MurA^{Bs}. Expression of A_2 was induced at at time zero. Culture density was monitored as a function of time.

the lytic function of A_2 lies within the amino-terminal half of the protein. Lysis is mediated earlier than A_2^{wt} with truncations within residues 246-180. Within this group of truncated proteins, the onset of lysis varies by a few minutes. Still within this group, truncations exhibiting the same time of lysis display different lysis kinetics. A_2-246, A_2-209 and A_2-180 begin to lyse their culture 26 minutes after induction, but unlike A_2-246 and A_2-180, A_2-209 lyses a greater population of cells 30 minutes after the onset of lysis. If we set aside the stretch of amino acids unique to SP, NL95 and F1, the alignment of *Alloleviviridae* maturation proteins shows a 100 residue conserved domain from 140 to 240. Each of the lytic fragments are truncated within this domain, but if the truncated A_2 includes this entire conserved domain, lysis function is lost. A 10 amino acid stretch less conserved within the conserved domain lies between residues 164-174. Interestingly, no lytic function is associated with A_2-172, suggesting that the amino acids between 180 and 240 are important for A_2 lytic function. It may turn out that the charged residues within this 60 amino acid stretch play a role in lysis; there are 15 conserved charged residues, 10 positively charged and 5 negatively charged. We cannot rule this domain as sufficient for lysis because lytic activity was lost when even short stretches of sequence were deleted from A_2. Additionally, the observation that Δ32-A_2 retains some lytic function suggests that the extreme N-terminus is also needed. Unlike A_2^{wt}, each of the lytic carboxy-terminal truncations of A_2 also elicits lysis in a strain expressing $MurA^{L138Q}$. However, lysis was curbed upon co-expression of *Bacillus subtilis*

MurA with A_2 and the lytic fragments, indicating that the lytic fragments of A_2 function by inhibiting MurA.

CHAPTER IV

MAPPING THE INTERACTING DOMAIN OF A_2 ON MURA BY SCANNING MUTAGENESIS

INTRODUCTION

The terminal event of the bacteriophage lytic life cycle is induction of host cell lysis, caused by inhibition of cell wall synthesis in bacteriophage Qβ infections. The lysis protein of Qβ, A_2, mediates cell wall inhibition, presumably by complex formation with MurA. How complex formation leads to inhibition is not known. It was previously shown that Qβ virions, possessing a single molecule of A_2 attached to its capsid, abolish the activity of MurA *in vitro* (9). A mutant host strain, resistant to lysis by Qβ, was found to have a single mutation in *murA*. Consequently, Qβ mutants that were selected to overcome resistance had acquired mutations in *A_2*, providing genetic evidence for a protein-protein interaction between MurA and A_2. The original *murA* allele resistant to $\underline{A_2}$ (rat) is L138Q, a solvent exposed residue in the catalytic domain of MurA.

The cell wall is the shape determinant of bacteria and it protects the cell from osmotic rupture. During normal cell growth, the bacterium is actively synthesizing cell wall components. Inhibition of cell wall synthesis causes the cell to lyse. At least two bacteriophage are known to encode proteins that target cell wall synthetic enzymes to induce lysis: (1) the E protein of ΦX174 inhibits

MraY, the enzyme catalyzing the lipid-linked intermediate (8), and (2) the A_2 protein of Qβ inhibits MurA, the first and committed step of cell wall biosynthesis (9).

MurA is a 419 amino acid protein that folds into two globular domains known as the C-terminal and catalytic domains, respectively. The globular domains are connected by a double stranded hinge, and a flexible loop projects from the catalytic domain opposite the hinge (Figure 4.1). MurA transfers the enolpyruvyl moiety of phosphoenolpyruvate (PEP) to UDP-*N*-acetylglucosamine (UDP-NAG) (Figure 1.2). In the reaction, the C-O bond of PEP is cleaved, rather than the high energy P-O bond more commonly observed. Release of an inorganic phosphate (Pi) is a by-product of the reaction (32). MurA is an induced fit enzyme, existing in an unliganded, open conformation and a liganded, closed state. The transition from open to closed state is accompanied by a substantial conformational change of the flexible loop (Figure 4.2). In the open conformation, the flexible loop is extended away from the globular domains and solvent exposed. The most prominent conformational change occurs upon binding of UDP-NAG, causing movement of the flexible loop toward the interglobular space. A similar closed conformation of MurA is observed when a nonhydrolyzable derivative of PEP or fosfomycin binds to the enzyme in combination with UDP-NAG, generating a stable tetrahedral intermediate. Isothermal calorimetry studies demonstrated that the binding of PEP does not significantly perturb the conformation of MurA (74). MurA does not appear to

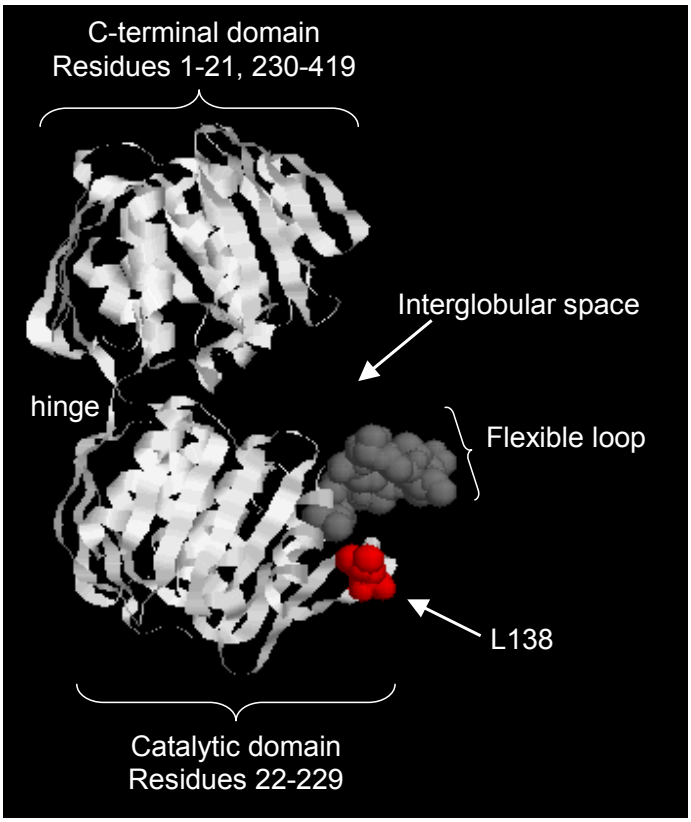

Figure 4.1. The structural features of MurA.
A ribbon diagram of the open conformation of *Enterobacter cloacae* MurA (PDB accession no. 1DLG) (78) was generated using the RasMol molecular graphics visualization tool (version 2.7.3). Highlighted are the two globular domains connected by a double-stranded hinge. The catalytic loop (gray) and L138 (red) are depicted as spacefill molecules. The interglobular space is also identified.

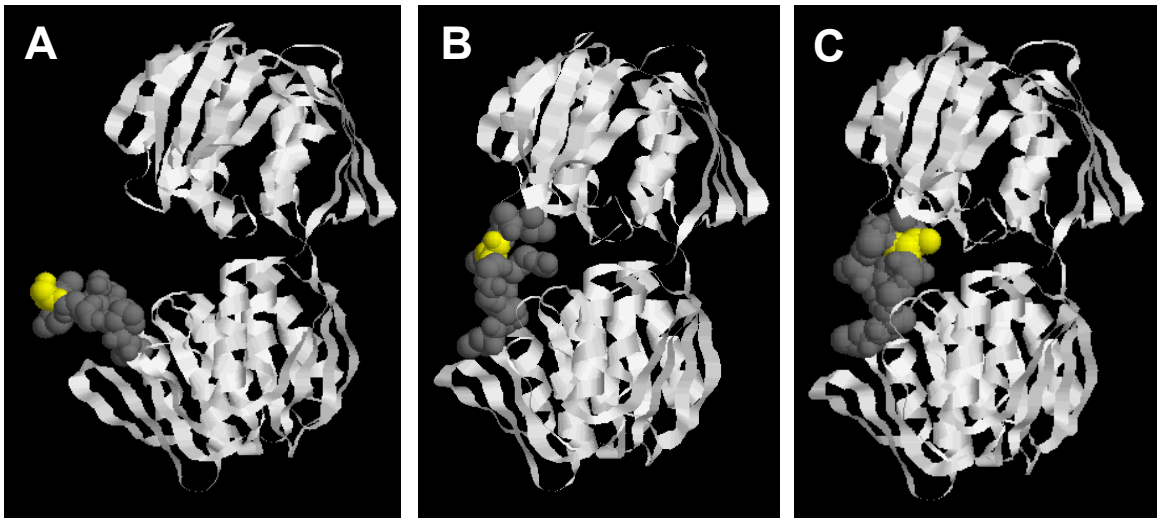

Figure 4.2. The conformational changes of MurA upon ligand binding. (A) A ribbon diagram of the open conformation of *Enterobacter cloacae* MurA (PDB accession no. 1DLG) (78). MurA is composed of two globular domains connected by a double stranded hinge. The flexible loop is represented as gray spacefill model with residue 115 of the flexible loop labeled yellow. (B) *E. coli* MurA (PDB accession no. 1UAE) (81) with UDP-NAG bound (not shown) shows the flexible loop in the interglobular space. (C) The structure of *E. coli* MurA (PDB accession no. 1A2N) (82) in the fluoro-tetrahedral intermediate state shows the flexible loop changes conformation upon transition from the singly-liganded state (B) to the tetrahedral intermediate (C). Ribbon diagrams were generated using the RasMol molecular graphics visualization tool (version 2.7.3).

bind its substrate in an ordered manner, but when both ligands are bound, the conformation of MurA shifts from open to closed (Figure 4.2).

The altered residue in the *rat* mutant, $MurA^{L138Q}$, is located on the surface of the catalytic domain in a β-sheet near the flexible loop when MurA is in its open conformation (Figure 4.1). Inspection of MurA crystal structures in the open, UDP-NAG bound and tetrahedral intermediate closed states does not reveal significant structural changes in the catalytic domain, with the exception of the rearrangement of the flexible loop (77, 78, 81, 82, 97).

To understand how A_2 inhibits MurA, we need to determine if MurA and A_2 require other proteins to associate. It would also be advantageous to identify the protein-protein interaction sites on each partner. To address these questions, we used a yeast two-hybrid system to determine if MurA and A_2 interact in the absence of other bacterial proteins. We then determined if other *rat* alleles exist in the catalytic domain of MurA. To identify new *rat* alleles and to map the interface between MurA and A_2, we carried out arginine-scanning mutagenesis of MurA. Mutations were made, and cells carrying them were characterized for Qβ-resistance.

MATERIALS AND METHODS

Bacterial and yeast strains, bacteriophage and growth conditions

XL1-Blue (*recA1 endA1 gyrA96 thi hsdR17 supE44 relA1 lac* [F'::Tn*10 proA*$^+$*B*$^+$ *lacI*^{q} *Δ(lacZ)*M15]) was used for all plasmid constructions. HfrH ((RY

15177)λ- *relA1 spoT1 thi-1 lacI^{q1}tonA::*Tn*10*) and HfrH ((RY 3095) λ- *relA1 spoT1 thi-1 lacI^{q1} lacZ::*Tn*5*) served as lawns for bacteriophage spot titering (Qβ, Qβ^{por} and MS2). Yeast strain AH109 (*MATa, trp 1-901, leu2-3, 112, ura3-52, his3-200, gal4Δ, gal80Δ, LYS2::GAL1$_{UAS}$-GAL1$_{TATA}$-HIS3, GAL2$_{UAS}$-GAL2$_{TATA}$-ADE2, URA3::MEL1$_{UAS}$-MEL1$_{TATA}$-lacZ*). All *E.coli* strains were grown in LB medium supplemented with ampicillin (100 μg/ml), or kanamycin (30 μg/ml) as indicated, at 37ºC with aeration. Yeast strain AH109 (*Saccharomyces cerevisiae)* (Clontech) was grown in supplemented drop out medium (yeast two-hybrid manual, Clontech) at 30ºC.

DNA manipulations

All molecular biology techniques were performed according to previously established protocols (76). Plasmid stocks were purified from saturated cultures using QiaQuick miniprep spin columns (Qiagen) according to manufacturer's instructions. PCR products, enzyme digests, and agarose gel extractions of DNA fragments were purified following manufacturer's protocol for QiaQuick PCR purification and QiaQuick Gel extraction kits (Qiagen), respectively. All restriction enzymes and T4 DNA Ligase and Taq polymerase were purchased from New England Biolabs and used according to the accompanying instructions. Pfu polymerase, either purchased from Stratagene or produced and purified in-house, was used according to Stratagene published instructions. Quick-change PCR (Stratagene) was performed according to manufacturer's

instructions. The primers used for site-directed mutagenesis are listed in table 4.1.

Plasmid construction

Expression of a gene cloned into the plasmid pZE12 (59) is regulated by the *Plac* promoter. pZE12 is a medium copy plasmid selectable with ampicillin. To construct pZE12-*murA*, pZE12-*luc* (59) was digested with KpnI and XbaI and the vector backbone was separated from *luc* by size on a 0.7% agarose gel. The excised backbone was purified using Qiagen's gel extraction kit. *murA* was amplified from the *E.coli* chromosome by PCR with the primers KpnI-NdeI-murA-FOR (AGAACAGGTACCATATGGATAAAT) and murA-XbaI-REV (GAGTGGTCTAGAGGTAGCCCC). The PCR fragment, digested with KpnI and XbaI, was ligated to similarly digested pZE12 vector backbone to render pZE12-*murA*.

Plasmids pGBKT7-*A2* and pGADT7-*murA* were amplified in XL1Blue and expressed in the yeast strain AH109. To clone A_2 into pGBKT7, an NdeI restriction site was first introduced upstream of the *cmyc* epitope tag encoded in pGBKT7 by Quick-change PCR (Stratagene) (pGBKT7-NdeI-up-FOR (GGGCGAGCCGCCCATATGGAGGAGC) and pGBKT7-NdeI-up-Rev (CTGCTCCTCCATATGGGCGGCTCGCC)). The plasmid results with the *cmyc* tag coding sequence flanked by NdeI sites. The plasmid was digested with NdeI and BamHI, removing the *cmyc* coding region and enabling similarly digested A_2

TABLE 4.1 Primers used in this study

Allele	Sequence
L138Q	FOR: ACCATCAAACTGGAAGAAGGT
	REV: ACCTTCTTCCAGTTTGATGGT
L138M	FOR: ACCATCAAAATGGAAGAAGGT
	REV: ACCTCCTTCCATTTTGATGGT
L138P	FOR: ACCATCAAACCGGAAGAAGGT
	REV: ACCTCCTTCCGGTTTGATGGT
L138R	FOR: ACCATCAAACGGGAAGAAGGT
	REV: ACCTTCTTGCCGTTTGATGGT
A119R	FOR: GTACGATCGGTCGTCGTCCGGTTG
	REV: CAACCGGACGACGACCGATCGTAC
P121R	FOR: CGGTGCGCGTCGTGTTGATCTAC
	REV: GTAGATCAACACGACGCGCACCG
V122R	FOR: GTGCGCGTCCGCGTGATCTACACATT
	REV: AATGTGTAGATCACGCGGACGCGCAC
D123R	FOR: GCGCGTCCGGTTCGTCTACACATTTC
	REV: GAAATGTGTAGACGAACCGGACGCGC
I126R	FOR: GATCTACACCGTTCTGGCCTCGAAC
	REV: GTTCGAGGCCAGAACGGTGTAGATC
S127R	FOR: GATCTACACATTCGTGGCCTCGAAC
	REV: GTTCGAGGCCACGAATGTGTAGATC
E130A	FOR: TCTGGCCTCGCACAATTAGGC
	REV: GCCTAATTGTGCGAGGCCAGA
E130R	FOR: CTGGCCTCCGTCAATTAGGCGCG
	REV: CGCGCCTAATTGACGGAGGCCAG
Q131R	FOR: CTGGCCTCGAACGTTTAGGCGCGAC
	REV: GTCGCGCCTAAACGTTCGAGGCCAG
G133R	FOR: CCTCGAACAATTACGTGCGACCATCAA
	REV: TTGATGGTCGCACGTAATTGTTCGAGG
A134R	FOR: AACAATTAGGCCGTACCATCAAAC
	REV: GTTTGATGGTACGGCCTAATTGTT
T135R	FOR: AATTAGGCGCGCGTATCAAACTGGA
	REV: TCCAGTTTGATACGCGCGCCTAATT
I136R	FOR: TAGGCGCGACCCGTAAACTGGAAGA
	REV: TCTTCCAGTTTACGGGTCGCGCCTA
E139A	FOR: ATCAAACTGGCAGAAGGTTAC
	REV: GTAACCTTCTGCCAGTTTGAT
E139R	FOR: GCGACCATCAAACTGCGTGAAGGTTA
	REV: CGTAACCTTCACCGAGTTTGATGGTC
K137D	FOR: GCGACCATCGATCTGGAAGAAGG
	REV: CCTTCTTCCAGATCGATGGTCGC
G141R	FOR: AACTGGAAGAACGTTACGTTAAA
	REV: TTTAACGTAACGTTCTTCCAGTT

TABLE 4.1 Primers used in this study continued.

Allele	Sequence
V143R	FOR: GAAGAAGGTTACCGTAAAGCTTCCG
	REV: CGGAAGCTTTACGGTAACCTTCTTC
K152R	FOR: GATGGTCGTTTGCGTGGTGCACATATC
	REV: GATATGTGCACCACGCAAACGACCATC
H155R	FOR: GAAAGGTGCACGTATCGTGATGG
	REV: CCATCACGATACGTGCACCTTTC
D159R	FOR: ATCGTGATGCGTAAAGTCAGCG
	REV: CGCTGACTTTACGCATCAC
K160E	FOR: GTGATGGATGAAGTCAGCGTT
	REV: AACGCTGACTTCATCCATCAC
D305A	FOR: GCATTCCCGACCGCTATGCAGGCC
	REV: GGCCTGCATAGCGGTCGGGAATGC
E329R	FOR: GAAACGGTCTTTCGTAACCGCTTTATGC
	REV: GCATAAAGCGGTTACGAAAGACCGTTTC
N330R	FOR: CGGTCTTTGAACGTCGCTTTATGC
	REV: GCATAAAGCGACGTTCAAAGACCG
E332R	FOR: CTTTGAAAACCGCCGTATGCATGTGCC
	REV: GGCACATGCATACGGCGGTTTTCAAAG
M333R	FOR: GAAAACCGCTTTCGTCATGTGCCAGAG
	REV: CTCTGGCACATGACGAAAGCGGTTTTC
V335R	FOR: CGCTTTATGCATCGTCCAGAGCTG
	REV: CAGCTCTGGACGATGCATAAAGCG
P336R	FOR: GCTTTATGCATGTGCGTGAGCTGAGCC
	REV: GGCTCAGCTCACGCACATGCATAAAGC
E337R	FOR: GCATGTGCCACGTCTGAGCCGTATGGC
	REV: GCCATACGGCTCAGACGTGGCACATGC
R340E	FOR: GAGCTGAGCGAAATGGGCGCGCACGCC
	REV: GGCGTGCGCGCCCATTTCGCTCAGCTC
M366R	FOR: CGCACAGGTTCGTGCAACCGATCTGCG
	REV: CGCAGATCGGTTGCACGAACCTGTGCG
T368R	FOR: GGTTATGGCACGTGATCTGCGTGC
	REV: GCACGCAGATCACGTGCCATAACC
R391E	FOR: CGGTGGTTGATGAAATTTATCACATCG
	REV: CGATGTGATAAATTTCATCAACCACCG
H394R	FOR: GATCGTATTTATCGTATCGATCGTGGC
	REV: GCCACGATCGATACGATAAATACGATC

to be ligated. The source of A_2 was described previously (Chapter II, Methods and Materials). pGADT7 was digested with NcoI and BamHI and ligated with similarly digested *murA* PCR product. pZE12-*murA/murA*^{L138Q} served as the template to flank *murA/murA*^{L138Q} by NcoI and BamHI sites by PCR with the primers NcoI-murA-FOR (TTGGTTCCATGGATAAATTTCGTG) and BamHI-murA-REV (TATTATTCTAGAGGATCCGCTCTCAGACGATTAACCAC).

Site-directed mutagenesis

MurA mutations were engineered by QuickChange site-directed mutagenesis kit (Stratagene) according to the manufacturer's instructions. The primer pairs used to generate mutants are listed in table 4.1. All mutations were verified by automated fluorescent DNA sequencing performed by the Laboratory of Plant Genomics and Technology at the Texas Agriculture Experiment Station.

Controlling the expression level of MurA alleles

Mutant alleles of MurA were expressed from a plasmid in the *E.coli* strain HfrH (RY 3095), where a basal level of expression of *murA** gene from pZE12 is achieved without inducing agent. Higher levels of expression occur by inducing with IPTG. This allows for the titration of MurA activity by controlling the expression level. HfrH (RY3095) pZE12-*murA* mutants (pZE12-murA*) were grown in LB supplemented with ampicillin at 37ºC with aeration to mid-log phase (approximately OD_{550} 0.4) and induced with 0, 12.5 µM, 25 µM, 50 µM, 100 µM

or 1 mM IPTG. To ensure an increase of protein accumulation with increasing inducing agent, whole cell samples were prepared for SDS-PAGE analysis one hour after induction. The level of protein samples were resolved by 10% SDS-PAGE followed by coomassie-brilliant blue staining. A bioassay was used to screen MurA alleles for sensitivity to A_2.

Bioassay to identify MurA alleles resistant to A_2

Bacterial lawns of HfrH (RY3095) pZE12-*murA** expressing different levels of MurA* were generated by mixing 200µL of culture grown to OD_{550} 0.4 at 37ºC, with aeration in LB supplemented with 5 mM $CaCl_2$, kanamycin and ampicillin, with 3mL of 42ºC soft agar supplemented with 5 mM $CaCl_2$ and immediately poured to an LB-Kan-Amp agar plate. The plates contained 0, 12.5 µM, 25 µM, 50 µM, 100 µM, or 1 mM IPTG and were incubated at 37ºC for 30 minutes to allow induction of pZE12-*murA**. Ten-fold serial dilutions of Qβ cell-free lysate were spotted to the lawn (see *Spot titering* section) and were further incubated at 37ºC for 12-16 hours. Following incubation, the plates were screened for plaque formation (Figure 4.3). In the presence of a low level of induction, wildtype MurA is sensitive to Qβ, but at the level of MurA accumulated when induced with 50 µM IPTG, Qβ plaque formation is blocked. Thus, the MurA alleles screened for resistance to Qβ are required to demonstrate resistance at lower levels of induction than wildtype MurA to be scored as a *rat* allele.

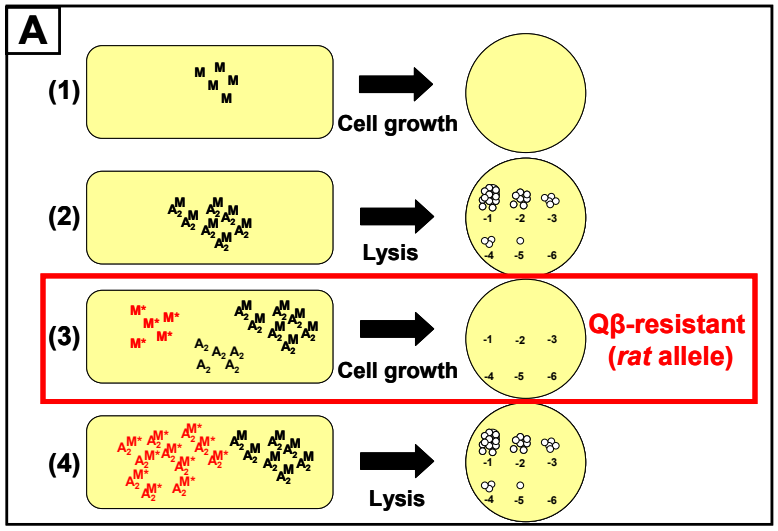

B

	MurA allele				
μM IPTG	WT	L138Q	L111R	P121R	S127R
100	$Q\beta^R$	$Q\beta^R$	$Q\beta^R$	$Q\beta^R$	$Q\beta^S$
50	$Q\beta^R$	$Q\beta^R$	$Q\beta^R$	$Q\beta^R$	$Q\beta^S$
25	$Q\beta^S$	$Q\beta^R$	$Q\beta^R$	$Q\beta^R$	$Q\beta^S$
12.5	$Q\beta^S$	$Q\beta^R$	$Q\beta^R$	$Q\beta^S$	$Q\beta^S$
0	$Q\beta^S$	$Q\beta^R$	$Q\beta^S$	$Q\beta^S$	$Q\beta^S$

Figure 4.3. Qβ bioassay to identify new *rat* mutants.
(A) Lawns of HfrH (RY 3095) pZE12-*murA** (mutant allele of *murA*, *) were spotted with Qβ lysate to determine if the MurA allele expressed *in trans* renders resistance to A_2 (rat), as assayed by Qβ-resistance ($Q\beta^R$). The rectangles on the left represent single cells with either the physiological amount of MurA (M, black), or additional copies of MurA or MurA mutant alleles (*) expressed *in trans* (M*, red). A_2 is expressed during Qβ infection. MA_2 and M^*A_2 indicates protein-protein interaction and inhibition of MurA(*) activity. The large circles on the right represent lawns of bacteria on agar plates. Numbers are serial dilutions of Qβ lysate at the site of application. Small white circles represent plaques. (1) Uninfected lawn of bacteria. (2) Localized Qβ infection of HfrH (RY 3095) lawn. (3) MurA* is not inhibited by A_2 enabling the cell to be $Q\beta^R$. This MurA* is scored as a *rat* allele. (4) MurA* is inhibited by A_2, resulting in cell lysis and plaque formation. (B) Lawns of HfrH (RY3095) pZE12-*murA** (*, mutant allele) were induced with 0, 12.5, 25, 50, 100 μM IPTG to express different levels of MurA, and screened for Qβ-resistance at each level of expression. The criteria to be a *rat* allele is to block Qβ plaque formation with lower levels than $MurA^{wt}$. Blue bars are alleles that protect the cell from lysis equivalently to $MurA^{wt}$. Colored bars indicate strength of the *rat* allele with red>orange>yellow. Black bars are alleles that are sensitive to Qβ plaque formation at 100 μM or greater.

Spot titering Qβ

Using sterile filter tips, 5 µl of each Qβ/Qβ^{por} serial dilution is applied onto a solidified soft-agar lawn of piliated *E.coli*. Here we spot titered onto lawns of HfrH (RY 3095) pZE12murA/murA*. Plates were incubated for 12-16 hours at 37ºC. If cells are sensitive to Qβ/Qβ^{por} lysis, clearing zones in the lawn (plaque forming units (pfu)) are visible. If the lawn is uniformly dense (no plaques) the strain is scored as Qβ-resistant. To verify the lawns were composed of piliated bacterium, the *Levivirus* MS2 was spotted to each lawn. MS2 requires pili for infection but does not target MurA to elicit host-cell lysis.

Deletion-insertion replacement of chromosomal murA *gene and complementation of* Bacillus subtilis murAA *gene* in trans

The transducing bacteriophage P1 was used to lift *ΔmurA::kan* from ZK1745 (W3110 *tna2 ΔlacU169 Δara ΔmurZ::kan* (pBAD30-Z)) (17) and delivered it to HfrH (RY 15177) pZE12-*murA^{Bs}*. Transductants were selected for by plating onto LB-Kan-Amp agar plates. Resultant transductants were screened for sensitivity to P1 and T4 bacteriophages, respectively to ensure that the candidate was not lysogenized by P1 during transduction. PCR was employed to confirm chromosomal replacement of *murA* with *kan*, requiring three primers and two reactions. In one PCR reaction, primers that annealed up and downstream of chromosomal *murA* rendered a 1,488 bp product if *murA* was not replaced. In the other PCR reaction, a primer annealed to the 3’ region

of the *kan* cassette that, in combination with the up and downstream primers, generated a 564 bp product if the *kan* cassette had replaced *murA*.

Yeast-two hybrid experiments

The Matchmaker GAL4 Two-Hybrid System 3 (Clontech, Palo Alto, CA) was used according to manufacturer's standard protocols to screen for an interaction between A_2 and MurA. In this system, yeast strain AH109 is equipped with the GAL upstream activating sequence and the GAL promoter fused to a reporter gene, thus regulating its expression. Here, nutritional reporter genes *HIS3* and *ADE2* are used. The yeast GAL4 transcriptional activator is encoded as two modular fragments; the activation domain (AD) and the DNA binding domain (BD) and is dependent on re-association to promote transcription of the reporter gene. The GAL4 fragments are encoded by two different plasmids, pGADT7 and pGBKT7, respectively. Each plasmid is compatible for amplification and expression in both *Escherichia coli* and *Saccharomyces cerevisiae.* pGADT7 confers ampicillin resistance in bacteria and *LEU2* to yeast for selection. pGBKT7 confers kanamycin resistance in bacteria and *TRP1* in yeast for selection. Each plasmid is suited for gene fusions and were engineered to carry either A_2 (pGBKT7-A_2) *or murA/murA*^{L138Q} (pGADT7- *murA* and pGADT7-*murA*^{L138Q}, respectively) (see *plasmid construction* section of Methods and Materials for details). In this system, if the two fusion proteins interact, the GAL4 AD and BD are brought into close

proximity, and establish transcriptional activation of the reporter genes. Protein-protein interactions are detected by the ability of co-transformed yeast cells to grow in selective media lacking leucine, tryptophan, histidine and adenine.

Yeast strain AH109 was co-transformed with pBKT7-A_2 and pGADT7-*murA/murA*^{L138Q} by the lithium acetate method and selected on solid media deficient of tryptophan and leucine, respectively to select for plasmids. Colonies emerged after incubation for 4 days at 30ºC. Individual colonies were streaked on more stringent media, deficient of leucine, tryptophan, histidine and adenine to select for the plasmids and interaction of fusion proteins. As controls, yeast were co-transformed with pGBKT7-53 (BD fused to murine p53) and pGADT7-T (AD fused to SV40 large T-antigen) or pGBKT7-Lam (DB fused to human lamin C) and pGADT7-T. In yeast two-hybrid assay, p53 and T interact, whereas Lam and T do not.

MurA activity assay

Cultures of HfrH (RY 3095) pZE12-*murA/murA** (30 mL) were induced with 1 mM IPTG for one hour. The culture was harvested at 8K rpm in a Sorvall SS-34 rotor. The pellet was resuspended in 0.1 M Tris, pH 8 and lysed in a SLM-Aminco French Pressure cell at 16,000 psi. The lysates were cleared of cellular debris by a second centrifugation step. The supernatant was brought to 70% ammonium sulfate and stored as a precipitant at 4ºC. An aliquot of precipitated MurA/MurA* was pelleted at max speed in a microcentrifuge,

resuspended in 0.1M Tris, pH 8, 2.5mM DTT and assayed for activity. The activity of MurA was assayed colorimetrically by monitoring the amount of inorganic phosphate byproduct released during catalysis (60).

RESULTS AND DISCUSSION

Yeast two-hybrid analysis of the interaction of MurA and A_2

To screen for a protein-protein interaction between A_2 and MurA, and A_2 and $MurA^{L138Q}$ in the absence of other bacterial proteins, we used a yeast two-hybrid system. In this system, A_2 was fused to the DNA Binding Domain (DB) of GAL4 and MurA or $MurA^{L138Q}$ was fused to the GAL4 activating domain (AD). The yeast cells AH109 require transcriptional activation of a nutritional reporter gene when grown in media deficient of the nutrient. Transcriptional activation is dependent on re-association of GAL4 AD and BD. If the fused proteins, in this case A_2 and MurA or A_2 and $MurA^{L138Q}$, interact then the modular domains of GAL4 are brought into close proximity and transcription of the reporter gene is activated, the yeast cells grow in nutrient-deficient media. As seen in Figure 4.4, plasmid maintenance is sufficient to provide plasmid encoded *TRP1* and *LEU2* and all tested strains grow. However, if the colonies are transferred to media additionally lacking histidine and adenine, the cells can only grow if the fusion proteins interact. As seen with Lam and T, two proteins known not to interact, no yeast colonies grow. However, yeast colony growth is supported by the

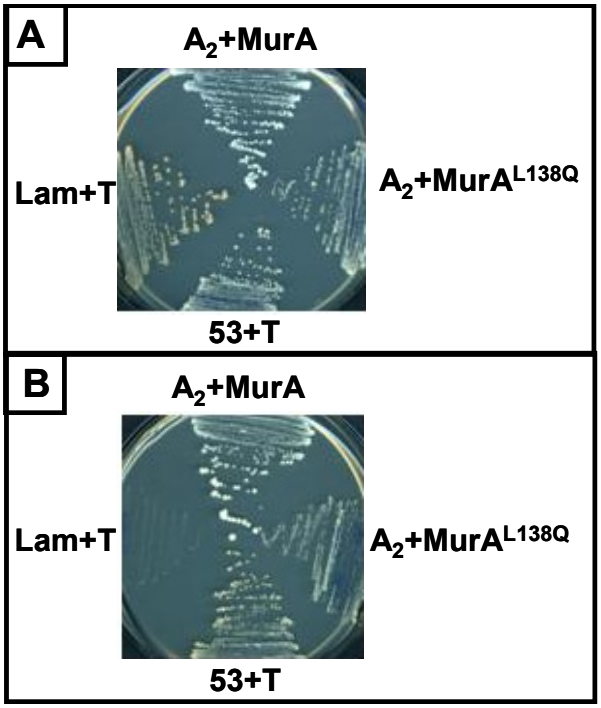

Figure 4.4. Yeast two-hybrid to detect the physical interaction of A_2-MurA. Yeast strain AH109 carrying plasmids expressing Gal4 DBDΦA_2 and Gal4 ADΦMurA/MurA^{L138Q} permit growth in nutrient-deficient media (See materials and methods). (A) Growth is supported by constitutive plasmid-encoded proteins. (B) Growth requires a physical interaction of fusion proteins.

interaction of both A_2-MurA and A_2-MurA^{L138Q} fusion proteins, providing evidence of a protein-protein interaction in the absence of other bacterial or phage proteins.

The finding that A_2 and MurA^{L138Q} interact was unexpected. Previous studies showed that MurA^{L138Q} rendered *E. coli* resistant to A_2, and that virion-associated A_2 was unable to inhibit the catalytic activity of MurA^{L138Q} (9). By yeast two-hybrid analysis, A_2 interacts with MurA^{L138Q} however, compared to the positive control p53-T, as well as A_2-MurA expressing cells, the A_2-MurA^{L138Q} colonies are small. The small colony size may reflect a slower growth rate due to a weak interaction between A_2 and the mutant MurA^{L138Q}. In this case, despite a protein-protein interaction between an enzyme and its protein inhibitor, the enzymatic activity of MurA^{L138Q} is preserved while the inhibitory function of A_2 is abolished.

Resistance to A_2 is not limited to the MurA^{L138Q} allele

Originally, selection for A_2/Qβ resistance yielded multiple clones with a single mutation in the *murA* gene (*murA*^{L138Q}). By developing a "protection assay" (described in Chapter II), we screened alleles of *murA* for their ability to confer resistance to Qβ. Mutations introduced to plasmid-borne *murA* (pZE12-*murA**) by site-directed mutagenesis were first verified to accumulate by SDS-PAGE after expression (Figure 4.5). Then, pZE12-*murA** was introduced into a male host that is phenotypically *lacY*$^-$ due to a Tn*5* insertion into the *lacZ* gene.

Using this system, basal expression of pZE12-*murA*^{L138Q} blocks Qβ plaque formation while the same Qβ-resistant phenotype is obtained with pZE12-*murA*^{wt} only after induction with 50 μM IPTG. Thus, any *murA* allele providing Qβ resistance in the presence of less than 50 μM IPTG is classified as a *rat* allele. By this criterion, the three other *murA* alleles (L138P, L138R, L138M) that result from single base changes in codon 138 are all *rat* alleles with *murA*^{L138R} being indistinguishable from *murA*^{L138Q}.

Next, to better understand the interaction between A_2 and MurA, we decided to introduce mutations into the *murA* gene at positions that altered either residues neighboring L138 on the surface of the MurA protein or on the same face of MurA but in the C-terminal domain based on the available crystal structures of the enzyme. Basal level of expression of alleles encoding the A119R, I126R**,** V143R, and T368R proteins (Figure 4.6) also behaved as *rat*, providing resistance to Qβ equivalent to the *murA*^{L138Q} allele. I126, L138 and V143 reside on the surface of the catalytic domain, on the same face as the flexible loop, while A119 is part of the flexible loop, itself. T368 resides in the C-terminal domain above the flexible loop in the closed conformation of MurA. Several mutants required low level induction to display a Qβ resistant phenotype. Strains harboring MurA alleles encoding the L111R, V122R, E139A, G141R, and M333R proteins provide Qβ resistance when induced with 12.5 μM IPTG. L111 is located within the flexible loop, and V122, E139 and G141 are within the catalytic domain near L138. M333 is located in the C-terminal

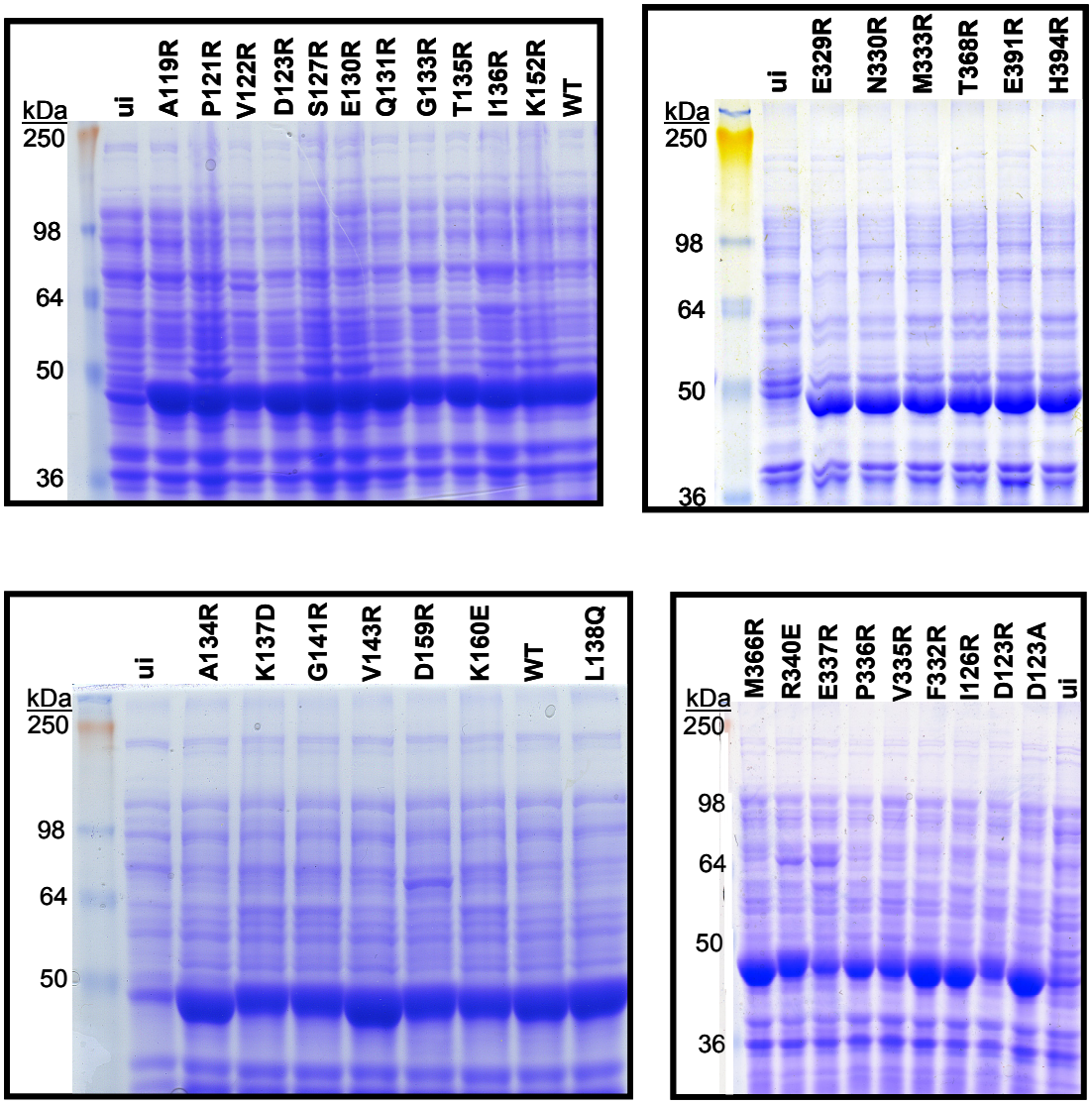

Figure 4.5. Qualitative accumulation of MurA mutant alleles.
Coomassie blue-stained SDS-PAGE of HfrH (RY 15177) pZE12-*murA** cultures expressing MurA alleles(*murA**). At the left of each panel is the molecular size marker in kilodaltons (kDa). Above each lane is the allele of MurA expressed *in trans*. For comparison, cells expressing wildtype MurA (WT) and cells not expressing any plasmid-borne protein (uninduced, ui) are included.

domain, spatially adjacent to T368. Strains expressing MurA mutants P121R, E130A, E130R, and Q131R, become Qβ resistant when induced with 25 μM IPTG. P121, E130 and Q131 reside in the catalytic domain near L138.

The interpretation of Qβ-resistance is that A_2 binds to the catalytic domain of MurA, and residues L111, A119, P121, V122, I126, E130, Q131, G141 and V143 are important to establish the A_2-MurA protein-protein interaction, in addition to L138. Two residues in the C-terminal globular domain of MurA also appear to interact with A_2: M333 and T368. Together, this data suggests that A_2 binds to the face of MurA opposite the double stranded hinge. Of the fourteen new *rat* alleles, ten residues important for interaction with A_2 map to the catalytic domain, with two residues in the flexible loop, and two additional residues in the C-terminal domain of MurA.

Several other mutations screened included: S127R, A134R, E329R, N330R, F332R, V335R, P336R, E337R, R340E, M366R, R391E and H394R. Expression of each of these alleles, even at 1 mM IPTG ($4.8x10^5$molecules/cell), remained sensitive to Qβ plaque formation (Figure 4.6). These alleles were assayed for activity and found to be inactive either by direct loss of activity or due to insolubility. It is possible that these inactive alleles are misfolded and thus, it is not known if A_2 interacts with these residues. A subset of engineered MurA alleles were as susceptible to Qβ as $MurA^{wt}$, requiring induction of expression with 50 μM IPTG before Qβ could no longer lyse the cells. These alleles include G133R, T135R, I136R, K137D, E139R, E140R, K152D, D159R,

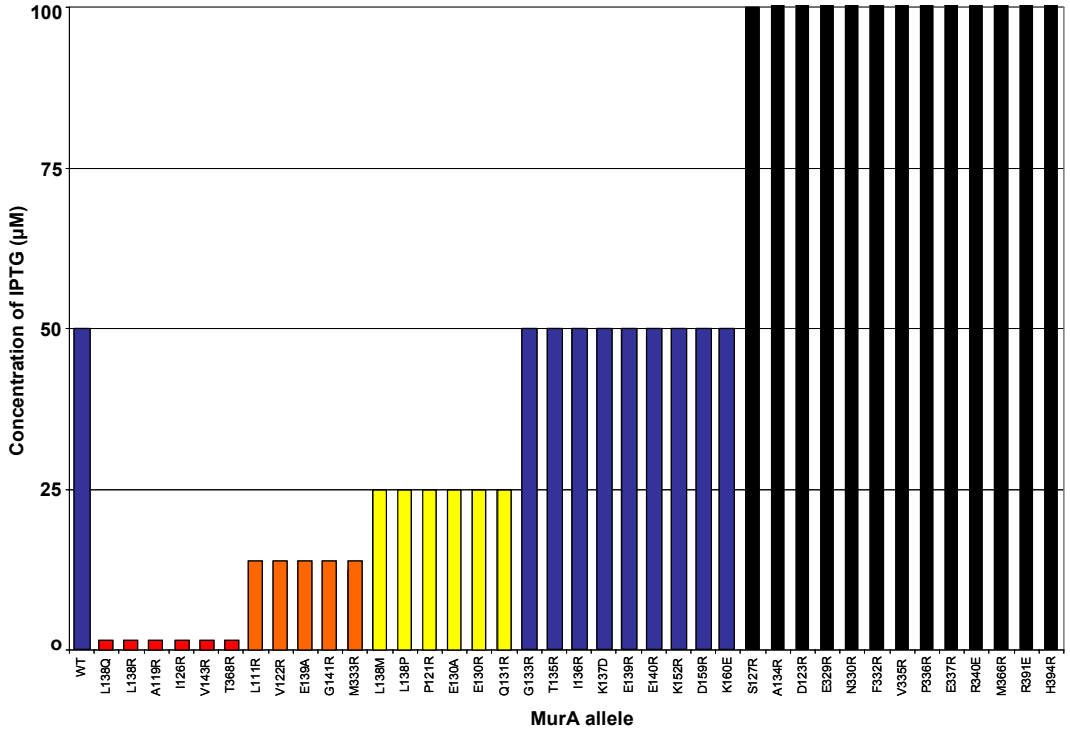

Figure 4.6. MurA^{rat} alleles block Qβ plaque-formation at lower levels of induction than wildtype MurA. Lawns of HfrH (RY3095) pZE12-*murA** (MurA mutant allele, (*)) were induced with 0, 12.5, 25, 50, 100 μM IPTG to express different levels of MurA, and screened for Qβ-resistance at each level of expression. Each bar indicates the minimum level of IPTG that blocks Qβ plaque formation. The criterion to be a *rat* allele is to block Qβ plaque formation with lower levels of MurA than wildtype. Blue bars indicate alleles that protect the cell from lysis equivalently to MurA^{wt}. Alleles that block Qβ plaque-formation below 50μM IPTG are scored a *rat* allele. Colored bars indicate strength of the *rat* allele with red>orange>yellow. Black bars are alleles that are sensitive to Qβ plaque formation at 100 μM or greater. For simplicity, the graph stops at 100μM IPTG, however A134R, D123R, E329R, N330R, F332R, V335R, P336R, E337R, R340E, M366R, R391E and H394R do not block Qβ plaque-formation with MurA levels induced with 1 mM IPTG.

and K160R. To determine if these variants bind with A_2, we introduced the second mutation D305A that renders the enzyme inactive (75) and screened for Qβ resistance. If A_2 binds to these inactivated alleles, then the cells are afforded protection from lysis by titrating out A_2. As expected, conversion of $MurA^{wt}$ to $MurA^{D305A}$ protects the cell from A_2-mediated lysis when expression is induced with IPTG, whereas $MurA^{L138Q\ D305A}$ does not. As inactivated enzymes, G133R, T135R, I136R, K137D, E139R, E140R, K152D, D159R, and K160R protect the cells from lysis, suggesting that these residues are not important for the interaction between A_2 and MurA. This group of alleles may define a boundary of the MurA-A_2 interface at the catalytic domain (Figure 4.7). The strong *rat* alleles L138Q, L138R, A119R, I126R, V143R, and T368R do not afford protection to the cells when inactivated by the D305A mutation even when induced at high level, suggesting that these residues are important contact sites for A_2. Interestingly, L138P, although a *rat* allele, protects the cell when it is expressed at high levels as an inactive protein. This suggests that unlike a glutamine, arginine or methionine, a proline at position 138 does not abolish the interaction with A_2. Instead L138P may weaken the interaction. The same phenotype is observed upon expression of $MurA^{E139A\ D305A}$, which resides adjacent to L138 in a short, solvent exposed β-sheet of MurA (Figure 4.1). $MurA^{E139R}$ as an active allele is equivalent to wildtype MurA, and protects the cells from lysis as an inactive enzyme, suggesting contact with this β-sheet.

The mode of A_2 inhibition of MurA

In order to interpret the meaning of the contact surface of A_2 on MurA, it is necessary to discuss the position of the flexible loop in the open and closed conformations (Figure 4.8). In the closed conformation, the flexible loop is parallel to the globular domains, acting as a door to the interglobular space (81, 82). In the open conformation, the loop is perpendicular to the catalytic domain, extending into solution (78). *Rat* alleles most affected by the dynamics of the flexible loop are L111 and A119. These residues are at the junction between the loop and the catalytic domain. The accessibility of L111, A119, and residues spatially nearby is substantially different when the flexible loop is open versus closed (Figure 4.8). In the open conformation, the loop may restrict A_2 from contacting L111, A119, P121 and V122. On the other hand, in the closed conformation these residues are part of a flat, solvent exposed surface. While it seems that binding to a flat surface would be energetically more favorable, we cannot rule out the possibility that A_2 interacts with the surface of MurA in a manner that would prevent the loop from closing. M333R and T368R are *rat* alleles residing in the C-terminal domain, peripheral to the flexible loop in the closed conformation, suggesting that A_2 binds to both globular domains of MurA. Together with the other seven *rat* alleles identified in the catalytic domain, it appears that A_2 binds to the surface of MurA, likely restricting the dynamics of the flexible loop. This type of uncompetitive inhibition may be similar to the strategy exhibited by T7 Lysozyme on T7 RNA polymerase (110).

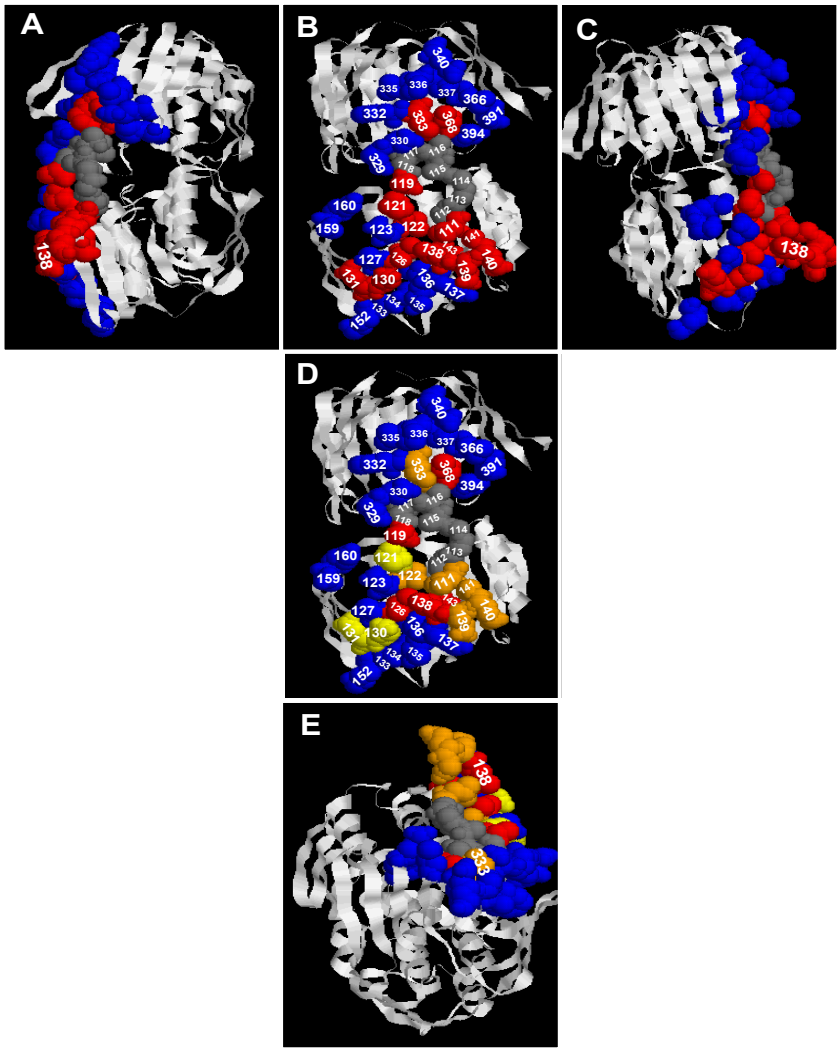

Figure 4.7. Map of MurA residues important for A_2 binding. Structure of *E.coli* MurA (PDB accession no. 1A2N) (82) in the closed conformation, highlighting the residues screened for A_2 binding. Panels A-D: The top globular region is the C-terminal domain and the bottom globular region is the catalytic domain. Panels A, B, C: Blue residues are not resistant to A_2 (*rat*), red residues are *rat*, gray residues define the dynamic catalytic loop (not subjected to mutagenesis). Panels D and E: The strength of the *rat* phenotype is color coded with red>orange>yellow. Panel A is a right side view. Panel B and D are front views. Panel C is a left side view. Panel E is a top view (from C-terminal domain down to the catalytic domain). Numbers identify the amino acid residue. The ribbon diagram was generated using the RasMol molecular graphics visualization tool (version 2.7.3).

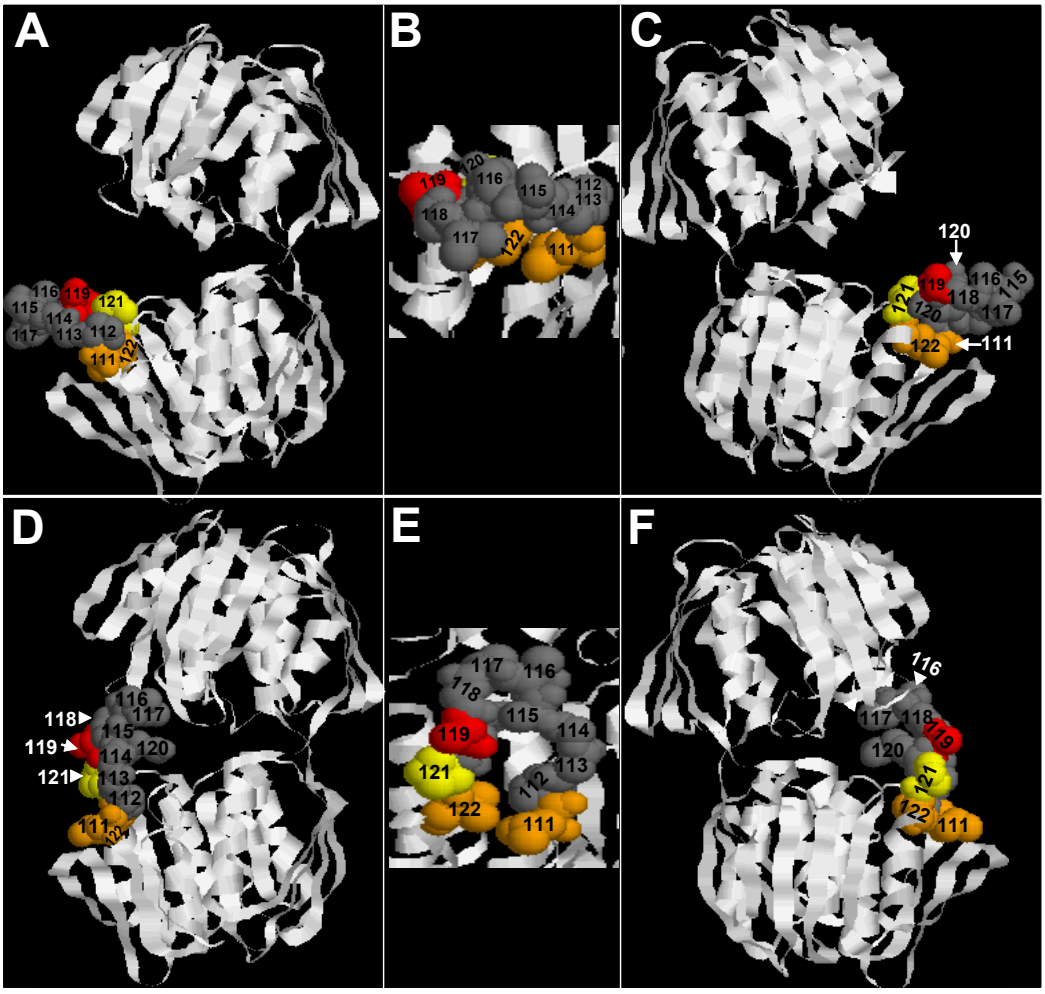

Figure 4.8. Accessibility of possible A_2 contact sites affected by the flexible loop of MurA. The position of the flexible loop in the open versus closed conformation may alter the accessibility of residues at the interface with A_2, and therefore may dictate the state of MurA in the inhibitory complex. Panels A-C show *Enterobacter cloacae* MurA in the open conformation (PDB accession no. 1DLG) (78). Panels D-F show the structure of *E. coli* MurA (PDB accession no. 1A2N) (82) in the fluoro-tetrahedral intermediate state. MurA is viewed from the right (A,D) and the left (C, F) of the flexible loop surface (front view, B and E). The flexible loop is composed of residues 111-120, represented by spacefilled gray areas. Residues important for A_2 binding spatially near, or as part of the flexible loop include L111, A119, P121 and V122 are spacefilled and colored according to strength of binding as determined by the plating assay (See Materials and Methods, Figure 4.3). Numbers identify the structural location of amino acids. Ribbon diagrams were generated using the RasMol molecular graphics visualization tool (version 2.7.3).

CONCLUSION

To gain a better understanding of the inhibitory action of A_2 on MurA, we first determined if the binary complex could form in the absence of other bacterial proteins with a yeast two-hybrid system. We found that A_2 and MurA form a protein-protein complex. While yeast growth was supported, the small colony size suggests a weaker interaction between A_2 and the *rat* mutant $MurA^{L138Q}$. In the bacterial protection assay, a low level of $MurA^{L138Q}$ is sufficient to block A_2-mediated lysis, while the inactive L138Q does not protect the cell from lysis. Together these results suggest that A_2 and $MurA^{L138Q}$ may form a weak, noninhibitory complex.

To expand upon the A_2 binding surface of MurA, we employed site-directed mutagenesis and scanned the surface of MurA in the vicinity of the original *rat* allele, $MurA^{L138Q}$. Sixteen new *rat* alleles have been identified that localize to thirteen sites on the flexible loop face of MurA, including regions of the catalytic domain, the flexible loop, and the C-terminal domain. Each *rat* allele, except $MurA^{L138P}$ and $MurA^{E139A}$ appear not to bind A_2 as assayed with the inactive form of each allele. L138P and E139A may represent a class of *rat* alleles with a weakened binding affinity for A_2. As mapped onto the closed structure of MurA, residues that may be important for A_2 binding form a contiguous surface on the flexible loop face of the catalytic and C-terminal globular domains of MurA. While we cannot rule out that A_2 may preferentially interact with the open or closed form of MurA at this time, it is possible that A_2

associates with MurA and locks the enzyme in its closed conformation. In this case, A_2 inhibits ligand-bound MurA by binding to its surface, away from the active site, suggesting an uncompetitive mode of inhibition.

CHAPTER V

CONCLUSION AND FUTURE DIRECTIONS

CONCLUSION

The question, “How do phage get out?” has been a matter of discussion and the focus of research for many years. Previous work identified inhibition of cell wall synthesis as the lysis strategy of small bacteriophages ΦX174 and Qβ. ΦX174 lysis protein E inhibits the MraY-catalyzed step whereas A_2 of Qβ targets MurA. Genetic and biochemical analysis of A_2 and MurA suggests a protein-protein interaction. Although it was previously established that Qβ virions inhibit MurA activity *in vitro*, it was not known if MurA and A_2 required other proteins to form an inhibitory complex *in vivo*. It was also unknown how single mutations in A_2 overcome a resistant allele of MurA to re-establish lysis, and how A_2 and MurA may contact each other in the event of protein-protein complex formation. The work in this dissertation has provided evidence for the following conclusions: (1) A_2 and MurA interact independently of other bacterial proteins; (2) free A_2, not mature Qβ particles, mediate lysis; (3) the lytic function of A_2 lies within the amino-terminal domain; (4) the ability of A_2 mutants to overcome a resistant allele of MurA is due to an increased rate of synthesis; (5) the A_2^{E125G} allele inhibits *Bacillus subtilis* MurAA, and (6) important contact sites for A_2 map

to the flexible loop surface of MurA including the catalytic and C-terminal globular domains.

FUTURE DIRECTIONS

A_2-MurA complex

The kinetics of binding and inhibition of A_2 and MurA are not known, due to the insoluble nature of overexpressed A_2. It is worth continuing to search for conditions that keep A_2 soluble. Attempts to obtain and purify soluble A_2 are currently underway. In the meantime, the solubility of the lytic fragments of A_2 is worth investigation. It is possible that the faster lysis time exhibited by the fragments compared to full length A_2 is due to increased solubility *in vivo.* Due to the toxic nature of the lytic fragments soon after induction, it is necessary to develop an overexpression system. Co-expression with *Bacillus subtilis* MurAA may serve as a starting point. It has already been demonstrated in this system that culture growth ceases after induction of the lytic fragments; however, an appreciable amount of protein may accumulate. If the lytic fragments of A_2 have improved solubility properties, it may be possible to affinity purify with an amino-terminal histidine tag. Inhibition and binding assays with MurA and the *rat* alleles of MurA, including assays in which MurA is held in either the open or closed conformation would then be feasible. It may also be possible to obtain structural information of the inhibitory complex by crystallography or NMR methods.

Characterize pob *mutants*

The Qβ^{por} mutant A_2^{E125G} is able to plate on host lawns expressing *Bacillus subtilis* MurAA (MurA^{Bs}) (plates on *B. subtilis* MurAA, *pob*), in a manner unique to this allele of A_2. Initial identification of Qβ^{por} mutations within *A_2* did not include analysis of the rest of the genome. It is necessary to determine if other mutations exist. If the only mutation attributable to plating is A_2^{E125G}, then Qβ that plate on MurA^{Bs} should be characterized. It is also possible to engineer and screen for MurA^{Bs} that are resistant to A_2 by the protection assay introduced in this dissertation to better our understanding of the interaction between A_2 and MurA^{Bs}. Characterization of this interaction may facilitate the design of lead compounds with broad-spectrum antibacterial effects.

REFERENCES

1. **Atkins, J.F., Steitz, J.A., Anderson, C.W., Model, P.** 1979. Binding of mammalian ribosomes to MS2 phage RNA reveals an overlapping gene encoding a lysis function. Cell **18:**247-256.

2. **Baum, E.Z., Montenegro, D.A., Licata, L., Turchi, I., Webb, G.C., Foleno, B.D., Bush, K.** 2001. Identification and characterization of new inhibitors of *Escherichia coli* MurA enzyme. Antimicrob. Agents Chemother. **66:**697-706.

3. **Barrell, B.G., Air, G.M., Hutchison, I.C.A.** 1976. Overlapping genes in bacteriophage ØX174. Nature **264:**34-41.

4. **Bayles, K.W.** 2000. The bactericidal action of penicillin: new clues to an unsolved mystery. Trends Microbiol. **8:**274-278.

5. **Beekwilder, J., Nieuwenhuizen, R., Poot, R., van Duin, J.** 1996. secondary structure model of the first three domains of Qβ RNA. Control of A-protein synthesis. J. Mol. Biol. **256:**8-19.

6. **Beremand, M. N., Blumenthal, T.** 1979. Overlapping genes in RNA phage, a new protein implicated in lysis. Cell **18:**257-266.

7. **Bernhardt, T.G., Roof, W.D., Young, R.** 2000(a). Genetic evidence that the bacteriophage ØX174 lysis protein inhibits cell wall synthesis. Proc. Natl. Acad. Sci. USA **97:**4297-4302.

8. **Bernhardt, T.G., Struck, D.K., Young, R.** 2000(b). The lysis protein E of ØX174 is a specific inhibitor of the MraY-catalyzed step in peptidoglycan synthesis. J. Biol. Chem. **276:**6093-6097.

9. **Bernhardt, T.G., Wang, I., Struck, D.K., Young, R.** 2001. A protein antibiotic in the phage Qβ virion: Diversity in lysis targets. Science **292:**2326-2329.

10. **Bernhardt, T.G., Wang, I.N., Struck, D.K., Young, R.** 2002. Breaking free: "protein antibiotics" and phage lysis. Res. Microbiol. **153:**493-501.

11. **Bläsi, U., Nam, K., Hartz, D., Gold, L., Young, R.** 1989. Dual translational initiation sites control function of the lambda S gene. EMBO **8:**3501-3510.

12. **Bläsi, U., Chang, C.-Y., Zagotta, M.T., Nam, K., Young, R.** 1990. The lethal λ *S* gene encodes its own inihibitor. EMBO J. **9:**981-989.

13. **Bläsi, U., Young, R.** 1996. Two beginnings for a single purpose: the dual-start holins in regulation of phage lysis. Mol. Microbiol. **21:**675-682.

14. **Boocock, M.R. and Coggins, J.R.** 1983. Kinetics of 5-enolpyruvylshikimate-3-phosphate synthase inhibition by glyphosate. FEBS Lett. **154:**127-133.

15. **Borth, W.** 1992. α-2 Macroglobulin, a multifunctional binding protein with targeting characteristics. *FASEB J.* **6:**3345-3353.

16. **Bowen, M.E., Gettins, P.G.W.** 1998. Bait region involvement in the dimer-dimer interface of human α-2 macroglobulin and in mediating gross conformational change. JBC **273:**1825-1831.

17. **Brown, E.D., Vivas, E.I., Walsh, C.T., Kolter, R.** 1995. MurA (MurZ), the enzyme that catalyzes the first committed step in peptidoglycan synthesis, is essential in *Escherichia coli*. J. Bacteriol. **177:**4194-4197.

18. **Burley, S.K., Petsko, G.A.** 1986. Amino-aromatic interactions in proteins. FEBS Lett. **203:**139-143.

19. **Chang, C.-Y., Nam, K., Young, R.** 1995. S gene expression and the timing of lysis by bacteriophage lambda. J. Bacteriol. **177:**3283-3294.

20. **Chen, M., Nagarajan, V.** 1993. The roles of signal peptide and mature protein in RNase (barnase) export from *Bacillus subtilis*. Mol. Gen. Genet. **239:**409-415.

21. **Dajkovic, A., Lutkenhaus, J.** 2006. Z ring as executor of bacterial cell division. J. Mol. Microbiol. Biotechnol. **11:**140-151.

22. **De Smet, K.A.L., Kempsell, K.E., Gallagher, A., Duncan, K., Young, D.B.** 1999. Alteration of a single amino acid residue reverses fosfomycin resistance of recombinant MurA from *Mycobacterium tuberculosis*. Microbiology. **45:**3177-3184.

23. **El Zoiby, A., Sanschagrin, F., Levesque, R.C.** 2003. Structure and function of the Mur enzymes: development of novel inhibitors. Mol. Microbiol. **47:**1-12.

24. **Eschenburg, S., Kabsch, W., Healy, M.L., Schonbrunn, E.** 2003. A new view of the mechanisms of UDP-N-acetylglucosamine enolpyruvyl transferase (MurA) and 5-enolpyruvylshikimate-3-phosphate synthase (AroA)

derived from X-ray structures of their tetrahedral reaction intermediate states. J. Biol. Chem. **278:**49215-49222.

25. **Eschenburg, S., Priestmann, M.A., Abdul-Latif, F.A., Delachaume, C., Fassy, F., Schonnbrun, E.** 2005. A novel inhibitor that suspends the induced fit mechanism of UDP-N-acetylglucosamine enolpyruvyl transferase (MurA). J. Biol. Chem. **280:**14070-14075.

26. **Fiers, W., Contreras, R., Duerinck, F., Haegeman, G., Iserentant, D., Merregaert, J., Jou, W.M., Molemans, F., Raeymaekers, A., Van den Berghe, A., Volckaert, G., Ysebert, M.** 1976. Complete nucleotide sequence of of bacteriophage MS2 RNA primary and secondary structure of the replicase gene. Nature. **260:**500-507.

27. **Gardner, A.D.** 1940. Morphological effects of penicillin on bacteria. Nature **146:**837-838.

28. **Guillet, V., Lapthorn, A., Hartley, R.W., Mauguen, Y.** 1993. Recognition between a bacterial ribonuclease, Barnase, and its natural inhibitor, Barstar. Structure **1:**165-177.

29. **Gründling, A., Smith, D.L., Bläsi, U., Young, R.** 2000(a). Dimerization between the holin and holin inhibitor of phage Lambda. J. Bacteriol. **182:**6075-6081.

30. **Gründling, A., Bläsi, U., Young, R.** 2000(b). Biochemical and genetic evidence for three transmembrane domains in the class I holin, λS. J. Biol. Chem. **275:**769-776.

31. **Gründling, A., Manson, M.D., Young, R.** 2001. Holins kill without warning. Proc. Natl. Acad. Sci. USA **98:**9348-9352.

32. **Guntileke, K.G. and Anwar, R.A.** 1968. Biosynthesis of uridine diphospho-*N*-acetylmuramic acid. J. Biol. Chem. **243:**5770-5778.

33. **Hahn, F.E., Ciak, J.** 1957. Penicillin-induced lysis of *Escherichia coli*. Science **125:**119-120.

34. **Hartley, R.W., Smeaton, J.R.** 1973. On the reaction between the extracellular ribonuclease of *Bacillus amyloliquefaciens* (Barnase) and its intracellular inhibitor (Barstar). J. Biol. Chem. **248:**5624-5626.

35. **Hartley, R.W.** 1977. Complementation of peptides of Barnase, extracellular ribonuclease of *Bacillus amyloliquefaciens*. J. Biol. Chem. **252:**3252-3254.

36. **Hartley, R.W.** 1989. Barnase and Barstar: two small proteins to fold and fit together. TIBS **14:**450-454.

37. **Hartley, R.W.** 1993. Directed mutagenesis and Barnase-Barstar recognition. Biochemistry **32:**5978-5984.

38. **Ho, S.N., Hunt, H.D., Horton, R.M., Pullen, J.K., Pease, L.R.** 1989. Site-directed mutagenesis by overlap extension using the polymerase chain reaction. Gene **77:**51-59.

39. **Höltje, J.-V.** 1998. Growth of the stress bearing and shape maintaining murein sacculus of *Escherichia coli.* Micobiol. Mol. Biol. Rev. **62:**181-203.

40. **Horiuchi, K, Webster, R.E., Matsuhashi, S.** 1971. Gene products of bacteriophage Qβ. Virology **45:**429-439.

41. **Huntington, J.A., Read, R.J., Carrell, R.W.** 2000. Structure of a serpin-protease complex shows inhibition by deformation. Nature **407:**923-926.

42. **Jeppesen, P.C., Argetsinger-Steitz, J., Gasteland, R.F., Spahr, P.F.** 1970. Gene order in the bacteriophage R17 RNA. 5'-A protein-coat protein-synthetase-3'. Nature **226:**230-237.

43. **Jeruzalmi, D., Steitz, T.A.** 1998 Structure of T7 RNA polymerase complexed to the transcriptional inhibitor T7 lysozyme. EMBO **17:**4101-4113.

44. **Josslin, R.** 1971. Physiological studies on the t gene defect in T4-infected *Escherichia coli*. Virology **44:**101-107.

45. **Jucovic, M., Hartley, R.W.** 1996 Protein-protein interaction: A genetic selection for compensating mutations in the Barnase-Barstar interface. Biochemistry **93:**2343-2347.

46. **Kahan, F.M., Kahan, J.S., Cassidy, P.J., Kropp, H.** 1974 The mechanism of action of fosfomycin (phosphonomycin). An. NY Acad. Sci. **235:**364-385.

47. **Karnik, S., Billeter, M.** 1983. The lysis function of bacteriophage Qβ is mediated by the maturation (A2) protein. EMBO J. **2:**1521-1526.

48. **Kastelein, R.A., Remaut, E., Fiers,W., and vanDuin, J.** 1982. Lysis gene expression of RNA phage MS2 depends on a frameshift during translation of the overlapping coat protein gene. Nature **295:**35-41.

49. **Klovins, J., vanDuin, J., Olsthoom, R.C.** 1997. Rapid evolution of translational control mechanisms in RNA genomes. J. Mol. Biol. **265:**372-384.

50. **Krekel, F., Oecking, C., Amrhein, N., Macheroux, P.** 1999. Substrate and inhibitor-induced conformational changes in the structurally related enzymes UDP-N-acetylglucosamine enolpyruvyl transferase (MurA) and 5-enolpyruvylshikimate 3-phosphate synthase (EPSPS). Biochemistry **28:**8864-8878.

51. **Kock, H., Gerth, U., Hecker, M.** 2004. MurAA, catalyzing the first committed step in peptidoglycan biosynthesis, is the target of Clp-dependent proteolysis in *Bacillus subtilis*. Mol. Microbiol. **51:**1087-1102.

52. **Kozak, M., Nathans, D.** 1971. Fate of the maturation protein during infection by colihage MS2. Nat. New Biol. **234:**209-211.

53. **Kumar, A., Studier, F.W.** 1997. Inhibition of T7 RNA polymerase: transcription initiation and transition from initiation to elongation are inhibited by T7 lysozyme via a ternary complex with RNA polymerase and promoter DNA. Biochemistry **36:**13954-13962.

54. **Lleo, M.M., Canepari, P., Satta, G.** 1990. Bacterial cell shape regulation: testing of additional predictions unique to the two-competing-sites- model for peptidoglycan assembly and isolation of conditional rod-shaped mutants from wild-type cocci. J Bacteriol. **172:**3758-3771.

55. **Lodish, H.F., Horiuchi, K., Zinder, N.D.** 1965. Mutants of the bacteriophage f2. V. On the production of noninfectious phage particles. Virology **27:**139-155.

56. **Lodish, H.F.** 1970. Secondary structure of bacteriophage f2 RNA and initiation of *in vitro* protein synthesis. J. Mol. Biol. **50:**689.

57. **Lodish, H.F.** 1971. Thermal melting of bacteriophage f2 RNA and initiation of synthesis of the maturation protein. J. Mol. Biol. **56:**627-628.

58. **Lomas, D.A., Carrell, R.W.** 1993. A protein structural approach to the solution of biological problems: α_1-antitrypsin as a recent example. Am. J. Physiol. **265:**211-219.

59. **Lutz, R., Bujard, H.** 1997. Independent and tight regulation of transcriptional units in *Escherichia coli* via the LacR/O, the TetR/O and AraC/I1-I2 regulatory elements. Nucl. Acids Res. **25:**1203-1210.

60. **Marquardt, J.L., Siegele, D.A., Kolter, R., Walsh, C.T.** 1992. Cloning and sequencing of *Escherichia coli murZ* and purification of its product, a UDP-*N*-acetylglucosamine enolpyruvyl transferase. J. Bacteriol. **174:**5748-5752.

61. **Meinhardt, H., de Boer, P.A.** 2001 Pattern formation in *Escherichia coli*: a model for the pole-to-pole oscillations of Min proteins and the localization of the division site. Proc. Natl. Acad. Sci. USA **98:**14202-14207.

62. **Mengin-Lecreulx, D. and van Heijenoort, J.** 1985. Effect of growth conditions on peptidoglycan content and cytoplasmic steps of its biosynthesis in *Escherichia coli*. J. Bacteriol. **163:**208-212.

63. **T. Maniatis, E.F. Fritsch and J. Sambrook.** 1986. *Molecular cloning: a laboratory manual*, Cold Spring Harbor Laboratory Press, Cold Spring Harbor, NY.

64. **Miller, J.H.** 1972. *Experiments in molecular genetics* Miller, J.H. (ed). Cold Spring Harbor, NY: Cold Spring Harbor Laboratory.

65. **Miller, J.H.** 1992. *A short course in bacterial genetics: A laboratory manual and handbook for Escherichia coli and related bacteria* Cold Spring Harbor, NY: Cold Spring Harbor Laboratory Press.

66. **Model, P., Webster, R.E., Zinder, N.D.** 1979. Characterization of Op3, a lysis defective mutant of bacteriophage f2. Cell **18:**235-246.

67. **Mullis, K., Faloona, F., Scharf, S., Saiki, R., Horn,G., Erlich, H.** 1986. Specific enzymatic amplification of DNA in vitro: the polymerase chain reaction. Cold Spring Harb. Symp. Quant. Biol. **51:**263-273.

68. **Nanninga, N.** 1998. Morphogenesis in *Escherichia coli*. Microbiol. Mol. Biol. Rev. **62:**110-129.

69. **Ozaki, K., Valentine, R.C.** 1973. Inhibition of bacterial cell wall mucopeptide synthesis: a new function of RNA bacteriophage Qβ. Biochemica Biophysica Acta **304:**707-714.

70. **Paranchych, W.** 1975. Attachment, ejection, and penetration stages of the RNA phage infection process. In *RNA phages*. Zinder, N.D. (ed). Cold Spring Harbor, NY: Cold Spring Harbor Laboratory, pp.85-111.

71. **Qazi, U., Gettins, P.G.W., Strickland, D.K., Stoops, J.K.** 1999. Structural details of proteinase entrapment by human α-2 macroglobulin emerge from three-dimensional reconstructions of Fab labeled native, half-transformed, and transformed molecules. JBC **274:**8137-8142.

72. **Raab, R., Neal, G., Garrett, J., Grimaila, R., Fusselman, R., Young, R.** 1986. Mutational analysis of bacteriophage lambda lysis gene S. *J* Bacteriology **167:**1035-1042.

73. **Reader, R.W., Siminovitch,L.** 1971. Lysis defective mutants of bacteriophage lambda: genetics and physiology of S cistron mutants. Virology **43:**607-622.

74. **Samland, A.K., Jelesarov, I., Kuhn, R., Amrhein, N., Macheroux, P.** 2001. Thermodynamic characterization of ligand-induced conformational changes in UDP-N-acetylglucosamine enolpyruvyl transferase. Biochemistry **40:**9950-9956.

75. **Samland, ,A.K., Etezady-Esfarjani, T., Amrhein, N., Macheroux, P.** 2001. Asparagine 23 and aspartate 305 are essential residues in the active site of UDP-N-acetylglucosamine enolpyruvyl transferase from *Enterobacter cloacae*. Biochemistry **40:**1550-1559.

76. **Sambrook, J., Fritsch, E.F., Maniatis, T.** 1989. *Molecular cloning: a laboratory manual* Sambrook, J., Fritsch, E.F., Maniatis, T. (eds). Cold Spring Harbor, NY: Cold Spring Harbor Press.

77. **Schönbrunn, E., Svergun, D.I., Amrhein, N., Koch, M.H.** 1998. Studies on the conformational changes in the bacterial cell wall biosynthetic enzyme UDP-*N*-acetylglucosamine enolpruvyl transferase (MurA). Eur. J. Biochem. **253**: 406-412.

78. **Schönbrunn, E., Eschenburg, S., Krekel, F., Luger, K., Amrhein, N.** 2000. Role of the loop containing residue 115 in the induced-fit mechanism of the bacterial cell wall biosynthetic enzyme MurA. Biochemistry **39:**2164-2173.

79. **Schreiber, G., Fersht, A.R.** 1993. Interaction of Barnase with its polypeptide inhibitor Barstar studied by protein engineering. Biochemistry **32:**5145-5150.

80. **Schreiber, G., Fersht, A.R.** 1995. Energetics of protein-protein interactions: Analysis of the Barnase-Barstar interface by single mutations and double mutant cycles. JMB **248:**478-486.

81. **Skarzynski, T., Mistry, A., Wonacott, A., Hutchinson, S.E., Kelly, V.A., Duncan, K.** 1996. Structure of UDP-*N*-acetylglucosamine enolpyruvyltransferase, an enzyme essential for the synthesis of bacterial peptidoglycan, complexed with substrate UDP-*N*-acetylglucosamine and the drug fosfomycin. Structure **4:**1465-1474.

82. **Skarzynski, T., Kim, D.H., Lees, W.J., Walsh, C.T., Duncan, K.** 1998. Stereochemical course of enzymatic enolpyruvyl transfer and catalytic conformation of the active site revealed by the crystal structure of the fluorinated analogue of the reaction tetrahedral intermediate bound to the active site of he C115A mutant of MurA. Biochemistry **37:**2572-2577.

83. **Smith, D. L., Struck, D. K., Scholtz, J. M., Young, R.** 1998. Purification and biochemical characterization of the lambda holin. J. Bacteriol. **180:**2531-2540.

84. **Spratt, B.G.** 1975. Distinct penicillin binding proteins involved with the division, elongation, and shape of *Escherichia coli* K12. Proc. Natl. Acad. Sci. USA **72:**2999-3003.

85. **Stallings, W.C., Abdel-Meguid, S.S., Lim, L.W., Shieh, H., Dayringer, H.E., Leimgruber, N.K., Stegeman, R.A., Anderson, K.S., Sikorski, J.A., Padgette, S.R., Kishore, G.M.** 1991. Structure and topological symmetry of the glyphosate target 5-*enol*pyruvylshikimate-3-phosphate synthase: A distinctive protein fold. Proc. Natl. Acad. Sci. USA **88:**5046-5050.

86. **Steinrucken, H.C. and Amrhein, N.** 1980. The herbicide glyphosate is a potent inhibitor of 5-enolpyruvylshikimic acid 3-phosphate synthase. Biochem. Biophys. Res. Comm. **94:** 1207-1212.

87. **Stano, N.M., Patel, S.S.** 2004. T7 lysozyme represses T7 RNA polymerase transcription by destabilizing the open complex during initiation. JBC **279:**16136-16143.

88. **Staples, D.H., Hindley, J., Billeter, M.A., Weismann, C** 1971. Localization of Qβ maturation cistron ribosome binding site. New Nat. Biol. **234:**202-204.

89. **Stroud, R.M., Kossiakoff, A.A., Chambers J.L.** 1977. Mechanisms of zymogen activation. Ann. Rev. Bioeng. **6:**177-193.

90. **Stultz, C.M., White, J.V., Smith, T.F.** 1993. Structural analysis based on state-space modeling. Protein Science **2:**305-314.

91. **Tomasz, A.** 1979. The mechanism of irreversible antimicrobial effects of penicillins: how the beta-lactam antibiotics kill and lyse bacteria. Annu. Rev. Microbiol. **33:**113-137.

92. **Van Duin, J.** 1988. *Single-stranded RNA bacteriophages*. Calendar, R. (ed). NY: Plenum Press, pp. 117-167.

93. Virtual laboratory. <http://virtuallaboratory.net/Biofundamentals/lectureNotes/Topic3-4_Proteins.htm>

94. **Volmer, W., Höltje, J.V.** 2001. Morphogenesis of *Escherichia coli*. Current opinion in Microbiology **4:**625-633.

95. **von Heijenoort, J.** 1998. Assembly of the monomer unit of bacterial peptidoglycan. CMLS **54:**300-304.

96. **von Heijenoort, J.** 2001. Formation of the glycan chains in the synthesis of bacterial peptidoglycan. Glycobiology **11:**25-36.

97. **Wanke, C., Amrhein, N.** 1993. Evidence that the reaction of the UDP-N-acetylglucosamine 1-carboxyvinyltransferase proceeds through the O-phosphothioketal of pyruvic acid bound to Cys115 of the enzyme. Eur. J. Biochem. **218:**861-870.

98. **Weber, K. And Konigsberg, W.** 1975. Proteins of the RNA phages. In RNA Phages, N.D. Zinder, ed. (Cold Spring Harbor, New York: Cold Spring Harbor Laboratory), pp.69-71.

99. **Weiner, A.M. and Weber, K.** 1971. Natural read-through at the UGA termination signal of Qβ coat protein cistron. Nature New Biol. **234:**206-209.

100. **White, J.V., Stultz, C.M., Smith, T.F.** 1994. Protein classification by stochastic modeling and optimal filtering of amino-acid sequences. Mathematical Biosciences **119:**35-75.

101. **Winter, R.B. and Gold, L.,** 1983. Overproduction of bacteriophage Qβ maturation (A_2) protein leads to cell lysis. Cell **33:**877-885.

102. **Xu, M., Arulandu, A., Struck, D.K., Swanson, S., Sacchettini, J.C., Young, R.** 2005. Disulfide isomerization after membrane release of its SAR domain activates P1 lysozyme. Science **307:**113-117.

103. **Xu, M., Struck, D.K., Deaton, J., Wang, IN., Young, R.** 2004. A signal-arrest-release sequence mediates export and control of the phage Pi endolysin. Proc. Natl. Acad. Sci. USA **101:**6415-6120.

104. **Young, K.D., Young, R.** 1982. Lytic action of cloned ØX174 gene E. J. Virol. **44:**993-1002.

105. **Young, R., Way, J., Way, S., Yin, J., Sayvanen, M.** 1979. Transposition mutagenesis of bacteriophage lambda: a new gene affecting cell lysis. J. Mol. Biol. **132:**307-322.

106. **Young, R.** 1992. Bacteriophage lysis: mechanism and regulation. Microbiol. Rev. **56:**430-481.

107. **Young, R., Wang, I.-N., Roof, W.D.** 2000. Phages will out: strategies of host cell lysis. Trends Microbiol. **8:**120-128.

108. **Young, R., Wang, I.-N.** 2006. Phage lysis. In The bacteriophages, Oxford University Press.

109. **Zhang, N., Young, R.** 1999. Complementation and characterization of the nested Rz and Rz1 reading frames in the genome of bacteriophage lambda. Mol. Genetics **262:**659-667.

110. **Zhang, X., Studier, F.W.** 1997. Mechanism of inhibition of bacteriophage T7 RNA polymerase by T7 lysozyme. J. Mol. Biol. **269:**10-27.

111. **Zinder, N.D. and Cooper, S.** 1964. Host-dependent mutants of the bacteriophage f2. I. Isolation and preliminary characterization.Virology **23:**152-158.

112. **Zinder, N.D.,** 1975. *RNA phages,* Cold Spring Harbor Laboratory Press, NY.

VITA

Name: Carrie-Lynn Langlais

Address: Texas A&M University Department of Biochemistry & Biophysics, Bio/Bio Building, MS 2128, College Station, TX 77843-2128

Email Address: carrielanglais@tamu.edu

Education: B.S., Biology, University of Great Falls, 2000
Ph.D., Biochemistry, Texas A&M University, 2007